DOCTOR THESIS

SHIBAURA INSTITUTE OF TECHNOLOGY

CHARACTERIZATION AND APLICATION OF

HOLLOW CATHODE OXYGEN PLASMA

MARCH 2016

ERSYZARIO EDO YUNATA

CHARACTERIZATION AND APLICATION

OF HOLLOW CATHODE OXYGEN PLASMA

A Dissertation

Submitted to the Graduate Faculty of the

Shibaura Institute of Technology (SIT)

Regional Environment System Department

in partial fulfilment of the requirements for the degree of

Doctor of Engineering

by

Ersyzario Edo Yunata

S. Si., Brawijaya University, Indonesia, 2009

M. Si., Brawijaya University, Indonesia, 2011

March 2016

ABSTRACT

Diamond like carbon (DLC) films and CVD diamond films have been widely utilized as protective coatings for tools and other materials. The attractive properties of this novel structure include high values of hardness, transparency in the infrared range, chemical inertness, low coefficient of friction and high wear resistance. By this properties diamond like carbon (DLC) films and CVD diamond films have applied in several important applications in the fields of mechanical manufacturing, solar energy devices, electric devices, and nano technology. In the present study, CVD diamond films have applied in several applications in manufacturing field. First, CVD diamond films with thickness 20μm have coated in the WC (Co) disk specimen with the purpose to make micro-texture in the disk specimen. Second, the CVD-diamond coatings have coated in the cutting tools with the purpose to extend the tool life by recoating after ashing process.

There are many ways to make micro-texture and to remove coating materials from the substrates. Wet chemical etching, micro-EDM, photolithography, and plasma process are kind of method can be used to achieve this point. The advantage and disadvantage factors are resulted from each method. In the present study, hollow cathode oxygen plasma has been developed to make dry etching and ashing for each application. Hollow cathode plasma is proposed to generate high ion and electron density in the chamber. High ion and electron density are utilized to make micro-texture in the substrate and to remove coating materials from the sample.

Firstly, characterization of hollow cathode plasma system has done by varying pressure, RF-voltage, and DC-bias voltage. Langmuir probe and

optical emission spectroscopy have utilized to measure ion, electron density and spectrum of hollow cathode plasma. The measurement result indicates hollow cathode plasma system has high ion density seven times higher in the order 10^{17}-10^{18} m^{-3} than without using hollow cathode system. The optical emission spectroscopy indicates hollow cathode plasma system produce high intensity of oxygen atomic peak and it is effective for etching and ashing process.

Secondly, hollow cathode oxygen plasma has developed to make ashing for CVD-diamond coated end milling tools. The end milling tools have coated with CVD-diamond coating with thickness 15μm. The only oxygen gas has utilized to generate plasma inside the hollow cathode. The variations of pressure, RF-voltage, and DC-bias have done to describe the optimum condition for ashing process. The low damage of cutting tools after ashing process has achieved in the low RF- voltage and one hour ashing process. The SEM and optical microscope have utilized to identify surface profile of end milling tool after and before ashing processing. Raman spectroscopy has utilized to prove diamond coating has removed from the end milling tools surface.

Thirdly, hollow cathode plasma system has utilized to make micro texturing in the CVD diamond coating with the thickness 20 μm. The metal mask and only oxygen gas have utilized to cover diamond coating area and to generate plasma. After the present etching for 7.2 ks, the micro-texture has imprint in the diamond coating. The etching rate by using hollow cathode plasma system reaches to 10 μm/H. The SEM and surface profilometer have indicated the anisotropic etching result after etching process.

TABLE OF CONTENTS

1. INTRODUCTION

1.1 PLASMA

Plasma is often referred to as the fourth state of matter [1]. As temperature increases, molecule become more energetic and transform in the sequence: solid, liquid, gas, and plasma. The figure 1.1 presents schematically the range of temperature, or particle energy, in which each of the four forms of matter occur in nature.
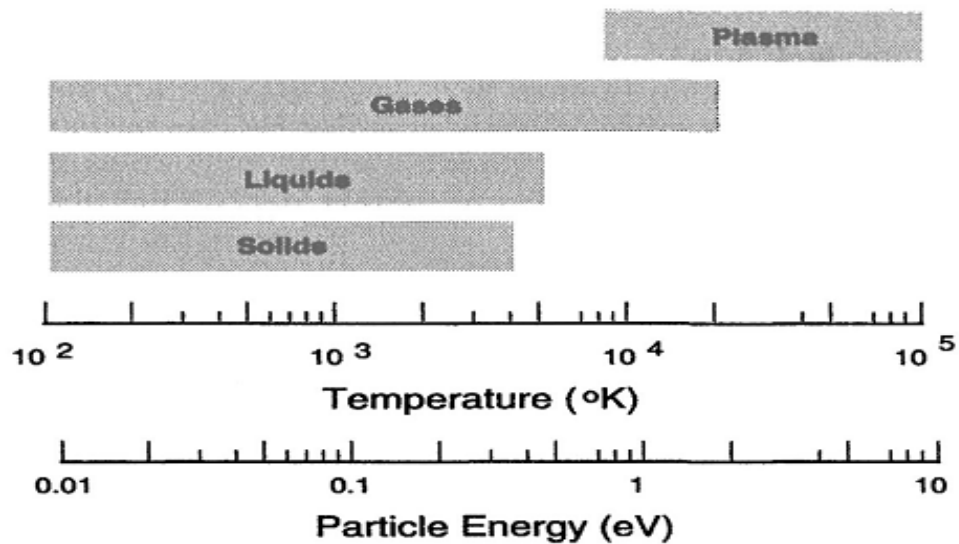
Figure 1.1 State of matter versus temperature

In the latter stages, molecule in the gas dissociate to form a gas of atoms and then a gas of freely moving charged particles, electrons and positive ions. This state is called the plasma state, a term attributed to Langmuir to describe the region of a discharge not influenced by wall or electrodes. It is characterized by a mixture of electron, ions, and neutral particles moving in random direction that, on average, is electrically neutral. In addition plasma are electrically conducting due to the presence of these free-charge carriers and can attain electrical conductivities larger than those of metal such as gold and copper [2].

Plasma occurs naturally, but also can manmade. Although somewhat rare on earth, plasma occurs naturally and comprises the majority of the universe, encompassing among other phenomena, the solar corona, solar wind, and earth ionosphere [3]. In the earth atmosphere, plasma is often observed as a transient event in the phenomenon of lightning strokes. Because air is normally non-conducting, large potential differences can be generated between clouds and earth during storms. Lightning discharges that occur to neutralize the accumulated charge in the clouds take place in two phases. First, an initial leader stroke progresses in steps across the potential gap between clouds or earth. This leader stroke creates a low degree of ionization in the path and provides condition for the second phase, the return stoker, to occur. The return stroke creates a high conducting plasma path for the large current to flow and neutralize the charge accumulation in the clouds [4]. Aurora is also other types of natural plasma in the earth and easily to be found in the north and south poles of the earth.
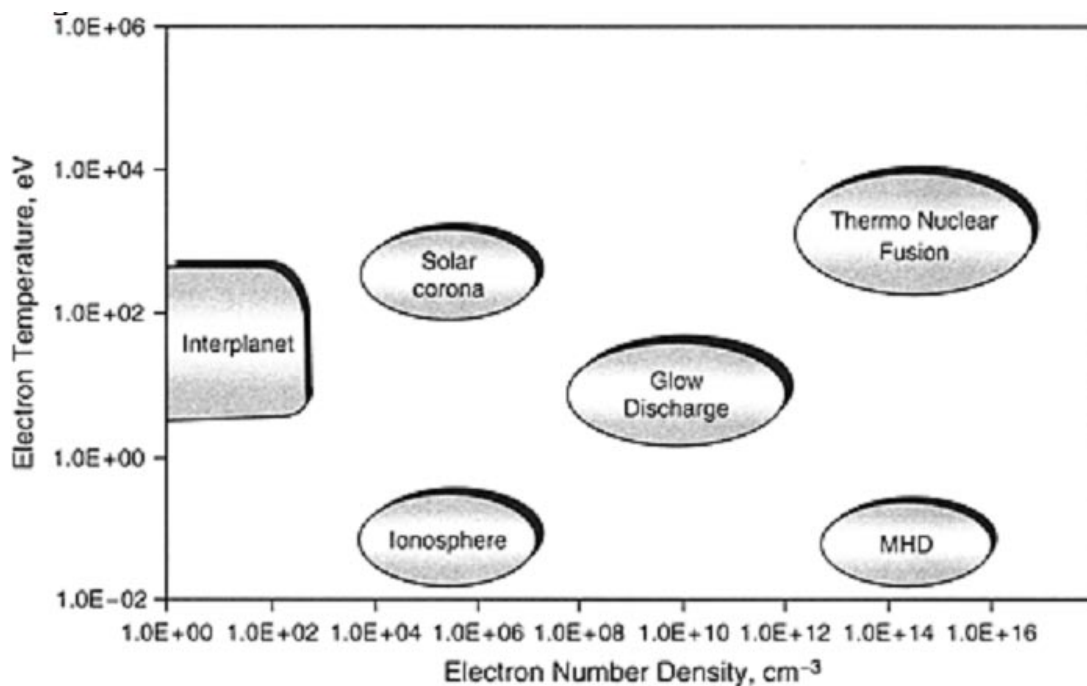
Figure 1.2 Operating regions of natural and manmade plasma

Figure 1.2 shows the classification of plasma in term of electron density and electron temperature. This figure provides a representation of the electron temperature in electron volt and electron densities (cm^{-3}) typical of natural and manmade plasmas. Electron temperature is expressed in electron volt (eV; 1 eV is equal to approximately 11600K. Manmade plasma ranges from slightly above room temperature to temperatures comparable to the interior of stars. Electron densities span over 15 orders of magnitude. However, most plasmas of practical significance have electron temperature of 1 to 20 eV with electron densities in the range 10^6 to $10^{18} cm^{-3}$ [5].

Plasma generation and stabilization in the laboratory and in industrial devices are not easy, but very promising for many modern applications, including thermonuclear synthesis, electronic, laser, and many others. Most of computer hardware is made based on plasma technologies, as well as the very large and thin TV plasma screen [6]. Plasma offers two main characteristic for practical applications. They can have temperatures and energy densities greater than those produced by ordinary chemical means. Furthermore, plasma can produce energetic species that can initiate chemical reaction difficult or impossible to obtain using ordinary chemical mechanisms. The energetic species generated cover a wide spectrum, e.g., charge particle including electron, ion, and radical; highly reactive neutral species such as reactive atoms (e.g. O, F, etc) [7].

1.2 PLASMA PHYSICS

1.2.1 BASIC GAS DISCHARGE

Plasma refers to an ionized gas, in which approximately the same number of electron and ions. The electron density (n_e) and ion density (n_i) are substantially equal to another, and they are referred to as the plasma density [8]. Because electrons are able to travel freely within the plasma, it has conductive property. When a radio frequency (RF) power is applied on a pair of electrodes in chamber, electrons are accelerated by an electric field generated by the RF power, acquire kinetic energy, and collide with atom and molecule. If the kinetic energy of an electron is greater than the ionization energy, the electron in the outermost shell of the atom or molecule is expelled. As a result, the neutral atom or the molecule turns into an ion. On the other hand, the electron that has been expelled from the molecule or the atom adds to the first colliding electron to now make a total two electron. These electron are then accelerated under the electric field, collide with other atoms and molecule, and generate new ion and electrons. The number of ion and electron increase as in an avalanche and eventually exceed a threshold level over which a resulting discharge begins and creates plasma [9].

1.2.2 PLASMA PARAMETER

The plasma is classified in to complete ionized plasma, in which 100 % of electrons and ions are ionized, and weakly ionized plasma, in which the degree of ionization is low and a mixture of ions, electron, and neutral atoms and molecules coexist. As a result, plasma parameter from each type has differences. Table 1.1 represents typical values for the plasma parameter

associated with arc discharge plasma, which is strongly ionized plasma, and a glow discharge plasma, which is weakly ionized plasma [10] .

Glow discharge plasma is characterized by a lack of thermal equilibrium between electron temperature Te and gas temperature Tg. An electron temperature corresponds to the energy of the electrons, and its relationship to the kinetic energy $\frac{1}{2} m_e v_e^2$ is expressed as

$$\frac{1}{2} m_e v_e^2 = \frac{3}{2} k T_e \qquad \qquad ......(1)$$

Where m_e is the electron mass, v_e is the electron velocity, and k is Boltzmann's constant.

Table. 1 Type of plasma and plasma parameters

Type of plasma		Plasma density (cm^{-3})	Electron temperature T_e(K)	Ion temperature T_i (K)	Gas temperature T_g (K)
Arc discharge	Strongly ionized plasma (high-temperature plasma)	$>10^{14}$	6000	6000	6000
Glow discharge	Weakly ionized plasma (low-temperature plasma)	10^9-10^{12}	$\sim 10^4$	300-1000	300

Because electron very light, they are accelerated by the electrical field and acquire a large kinetic energy. The average electron energy in a glow discharge plasma is several electron volt. Say the electron energy is 2 ev; then the electron temperature Te is 23200 K, according to Eq. (1). On the other hand, the temperature of the neutral atoms and molecules, which is the

gas temperature T_g, is around room temperature (293K). In other words, $\dfrac{T_e}{T_g}$ is

around 80, and electron temperature T_e and gas temperature T_g are not in a thermal equilibrium. Although the electrons hav an energy level comparable to high temperature of 10^4 K or higher, the chamber and the wafer remain low temperature because the electron mass is small. For this reason, glow discharge plasma is also referred to as a low-temperature plasma. Because electrons have enough energy for causing the excitation, ionization, and dissociation of atoms and molecules, with the gas temperature remaining at close to the room temperature, diverse types of reactions are possible at low temperature. This is the reason the glow discharge plasma is used form semiconductor monitoring.

An arc discharge is strongly ionized plasma, and its plasma density is 10^{14} cm^{-3} or greater. The electron temperature T_e, ion temperature T_i, and gas temperature T_g are in a thermal equilibrium, and $T_e = T_i = T_g$ is approximately 6000K. For this reason, the arc discharge is referred to as a high-temperature plasma [11].

1.2.3 COLLISION PROCESS IN PLASMA

Electrons that have gained energy in plasma collide with atoms and molecules. This collisions are categorized as elastic collisions and inelastic collisions. Figures 1.3 shows the collision process in plasma. With an elastic collision, only the kinetic energy changes; the internal energy does not changes. These types of collision tend to take place when the electron energy is low. In the figure 1.3 the electron is bounced back in a different direction. Because a portion of the electron's energy is transferred into the kinetic

energy of the atom, the atom slightly gains a velocity. The electron loses a small amount of energy through the collision. With an inelastic collision, the internal energies are converted, and excitation, ionization, dissociation, and electron attachment take place [12].
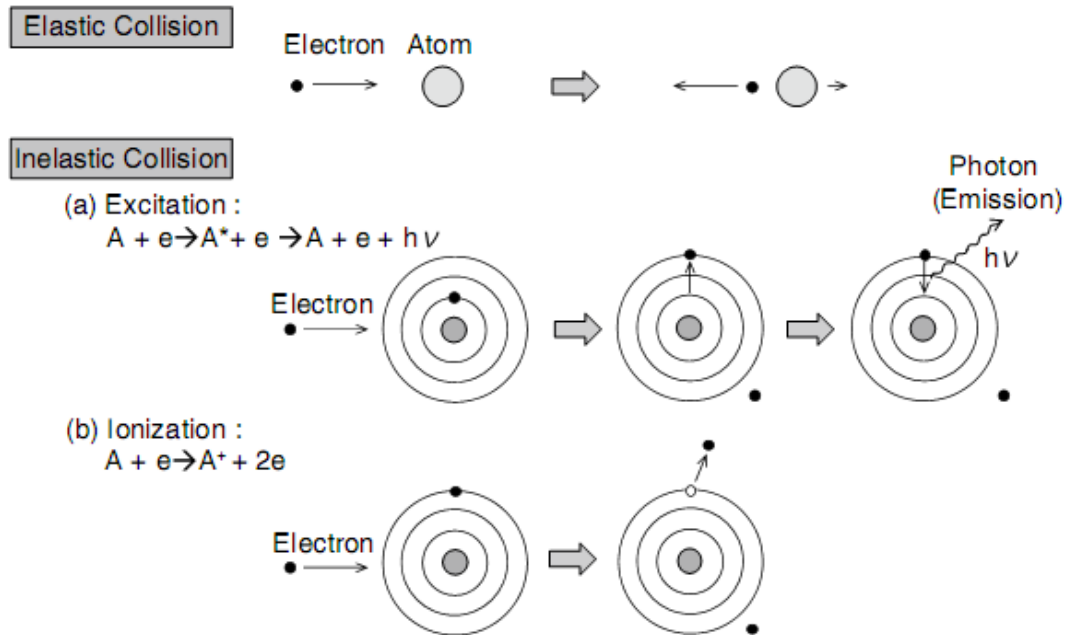
Figure 1.3 Collision processes in a plasma

The figure 1.3 represent collision process in plasma is divided into four type collisions.

a. Excitation

A colliding electron provides energy to the bound electron in an atom and enables it to jump to a higher energy level. In general, the excited state is unstable, and the excited electron would be able to remain in this state for only around 10^{-8} s, and then return to the ground state. Photon is emitted during this transition. The plasma glows because of this principle. An excitation reaction step is described as follows;

$$A + e \rightarrow A^* + e \rightarrow A + e + hv$$

where A represents a neutral atom, and A^* represent A in an excited state, h is Planck's constant, and v is the frequency of the emitted light

b. Ionization

As explained before, an electron in the outermost shell is expelled when the energy of the colliding electron is larger than the ionization voltage, and the neutral atom turn into a positive ion. This reaction step is described as follows;

$$A + e \rightarrow A^+ + 2e$$

c. Dissociation

Dissociation occurs when the energy given by the colliding electron is larger than the binding energy of the molecule. The reaction step is described as follows;

$$AB + e \rightarrow A + B + e$$

When a molecule is dissociated, its by products are chemically more active than the original molecule and turn into highly reactive particles. A particle in this activated stated is called a radical. It has been reported that CF_4 would easily be dissociated into a CF_3 radical ($CF_3^.$) and F radical ($F^.$) once excited [7]. This reaction step is described as follows:

$$CF_4 \rightarrow CF_4^* \rightarrow CF_3^. + F^'$$
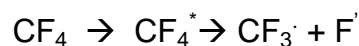
d. Electron attachment

The colliding electron attaches to the atom and turns it into a negative ion. This reaction step is described as follows;

$$A + e = A^-$$
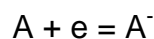
1.3 PLASMA GENERATION

1.3.1 DC DISCHARGES

Space and laboratory plasma are classified by their electron temperature (Te), and charge particle density (n) [13, 14]. A glow discharge is a kind of plasma consisting of equal concentration of positive and negative charges and a large number of neutral species. The DC-glow discharge plasma has been used for plasma application in the low and intermediate pressure region in modern technology [15]. Glow discharge plasma is a tool for heating, sputtering, etching, nitriding, and ionization as well as an activator for gaseous atoms and molecule. It is well known that a large number of ion, electron, and excited radical coexist in plasma. A wide variety of particles exits in the discharge in addition to ion and electrons, including for example radical, excited species, and various fractured gas molecules created by collisions between electronic and gas molecules or atom [16].
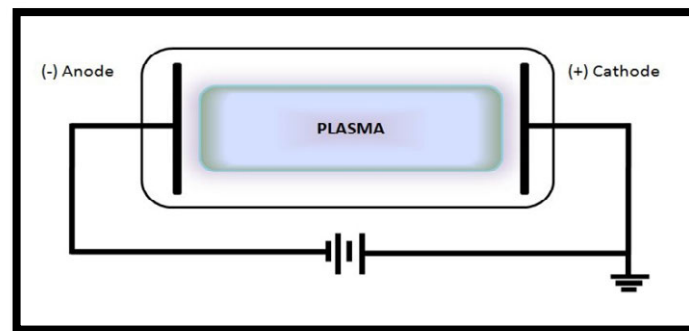
Figure 1.4 The schematic of DC glow discharge

The simple configuration of DC glow discharge plasma is depicted in the figure 1.4. Two plane metal plate are separated by a distance, d, in a chamber reactor filled with a particular gas at a pressure, p. Breakdown of the gas is achieved by applying an electric field or direct-current (dc) with cathode and anode biased negatively and positively, respectively. When the voltage

between the plates is low, the gas is a near-perfect insulator. As the voltage is increased, small fractions of electron present in a gas are accelerated towards the anode making collision with the background atoms. Some of these collisions create positive ion which are then accelerated towards the cathode. When the ion strikes the cathode, electrons are liberated from the metal surface as a result of neutralization (secondary electron emission). This process gives rise to an entire avalanche of electron leading to gas breakdown and discharge formation [17]. The voltage at which breakdown occurs is describe by Paschen's law. The breakdown voltage is found to depend only on the product p, d for a given gas and cathode material. At low p, d value, the breakdown voltage is small because of too few collisions (low pressure or small gap). At high p, d value, the breakdown voltage is high because of too many collisions (high pressure or large gap).

1.3.2 CAPACITIVE RADIO FREQUENCY DISCHARGE

Capacitive radio frequency discharge is also the most common types of discharges and the associated plasma processes. Commonly, this system utilizes parallel plate and the workhorse frequency is 13.56 MHz. Under these conditions, the electrons have a thermal energy of a few eV to bring atoms into excited states and dissociate molecule, which facilitates chemical reactions. On the other hand, the heat content of the electron gas is still small because of the low electron density. This allows bringing the plasma into contact with sensitive surface. This process is called cold heat [18].

Figure 1.5 represents typically capacitive radio frequency discharge plasma in common. It is mentioned by the parallel plate discharge belong to the capacitive RF discharge. By this condition the RF electric field results from

surface charges on electrode or dielectric. This distinguishes it from inductive discharges where the electric field is generated by a time varying magnetic field from an external antenna.
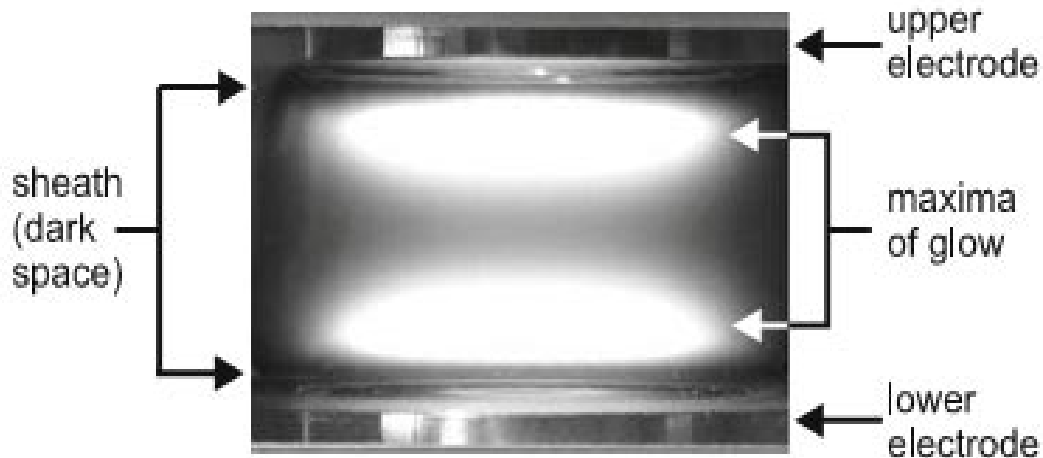
Figure 1.5 Typical capacitive radio frequency discharge plasma

The radio frequency (RF) type has advantage point compare with direct current (DC) type. When a dielectric substrate is put on one of the electrodes of parallel plate reactor, the DC current is interrupted and the plasma will seek a connection to the uncovered part of electrode. This hardly gives the desired homogeneous contact between plasma and substrate. However, when an RF voltage is applied, a displacement current will flow in the substrate that establishes the connection between plasma and electrode and provides homogeneity [19]. The parallel plate discharges fall into different classes of operation. First, the applied RF voltage determines whether the discharge operates in the α-regime, which is governed by ionization from electron avalanches, or in the γ – regime, where electrons are produced at the electrodes by secondary emission from ion bombardment. Second, the two RF electrodes of the discharge can have equal or different areas. Third, the

discharge can be operated through a blocking capacitor, which leads to a DC self bias from rectifying the RF voltage in the sheath region [20].

1.3.3 INDUCTIVELY COUPLED PLASMA

Inductively coupled plasma (ICP) became relevant for the semiconductor industry because of the necessity to achieve higher plasma density of $n_i = (1\text{-}3) \times 10^{17}$ m^{-3} in low pressure ($p = (0.11\text{-}2)$ Pa) discharges. Higher densities lead to faster reaction rate that boost the economy of the process [21]. Capacitive discharges were limited to achieve this regime because the plasma density was only increasing with the square root of the applied power. Moreover, the necessity to transport the applied power through the sheath region generated high voltage drop across the sheath, and ions gained energies of several hundred eV from the sheath potential, which could damage the integrated circuits. Inductive power transport to the plasma keeps the voltage drop across the sheath low and leads to moderate ion energies of (24-40) eV [22].
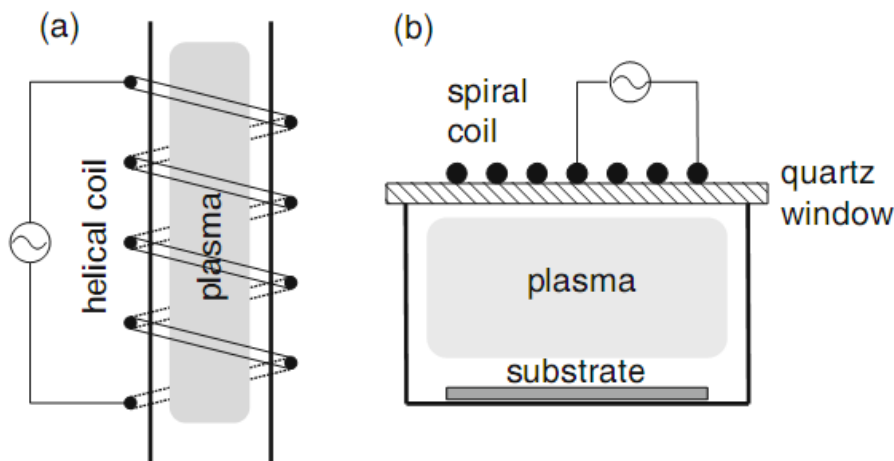
Figure 1.6 Typically ICP plasma system, a) ICP plasma with a helical coil wound around discharge tube, b) ICP with a flat spiral coil on a quartz window

12

An ideal ICP acts likes a transformer with the primary being a coil that is positioned close to the plasma, and the plasma forming a single-turn secondary. These typical arrangements for helical and flat coil design are sketched in the Figure 1.6. ICP plasma can be operated in a low-power electrostatic mode, or E mode, which is mostly found in the plasma density range 10^{14}-10^{16} m^{-3}. The real inductive mode or H mode is found for higher plasma density of 10^{16}-10^{18} m^{-3} [6]. The mechanism of E and H mode is illustrated in the Figure 1.7.
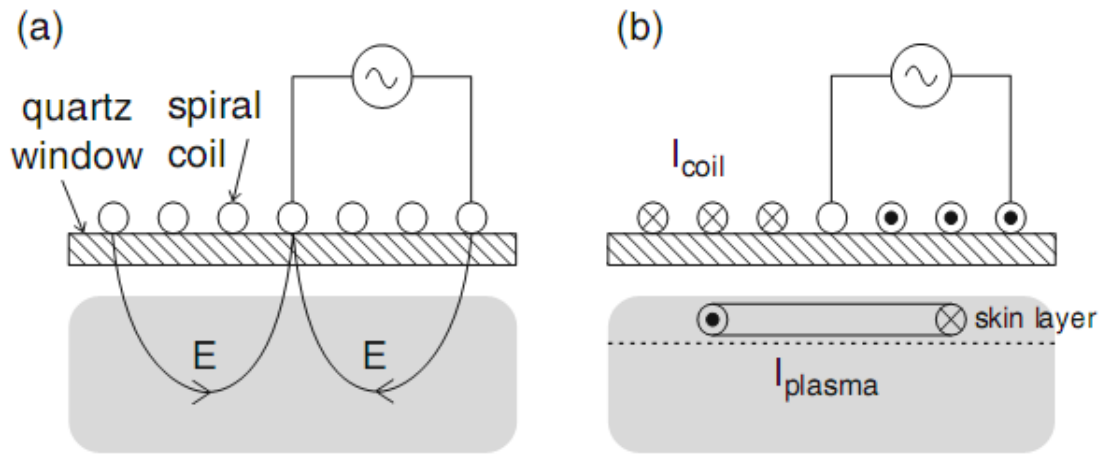
Figure 1.7 The mechanism process of a) E mode and b) H mode in the ICP plasma system

The E-mode is characterized by an RF electric field that originates from the RF voltage drop across the exciter coil ICP discharge. Plasma density in the E-mode is low and lead to a skin depth that is larger than the plasma dimension. The E-mode resembles the parallel plate discharge and leads to energetic ions from the sheath region. It is possible to suppress the E-mode by using a so-called Faraday shield consisting of a thin grounded copper sheet with slits that are oriented a right angle to the current flow in the antenna.

The H-mode as depicted in the figure 1.7 b) deposits the RF energy in the plasma by accelerating electrons by the ring-shaped induction field inside the skin layer. The electron flow represents a ring-current that has the opposite direction as the RF current in the excited coil. This current system is the single winding of an air-core transformer, which consist of the multi-winding exciter coil and the skin layer of the plasma [23].

1.4 PLASMA APPLICATION

Plasma technology has applied in many sectors, such as industrial sector, in the biomedical sector, nano technology sector and etc. In the industrial sector, plasma technology has applied for many purpose and function. One of the famous applications in this sector is for ashing or etching process. Plasma etching and ashing can be generated in many ways and type from plasma system. Recently, dry plasma etching and ashing has chosen for MEMS/NEMS fabrication due to high accuracy and short time processing [24].
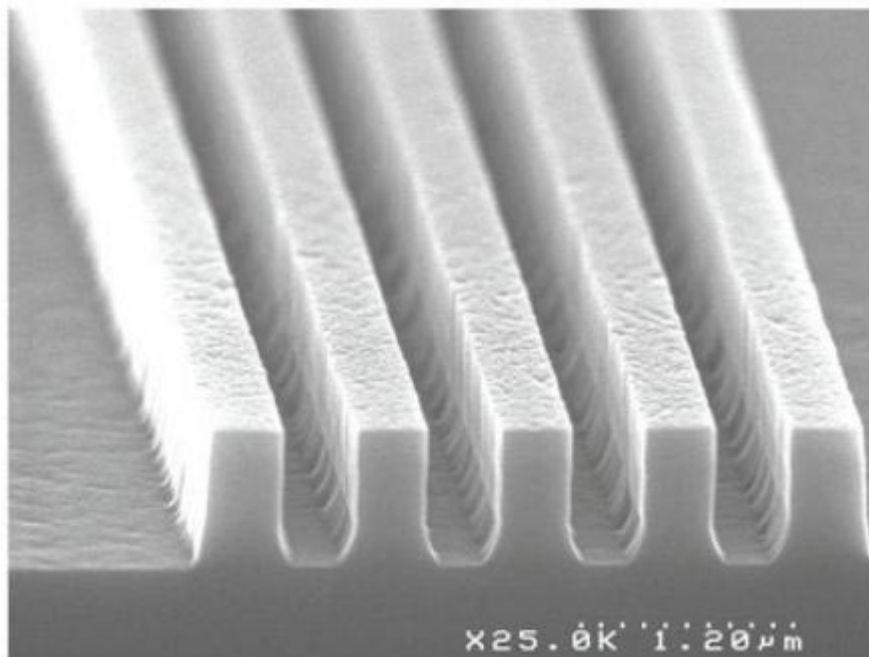
Figure 1.8 ICP plasma etching in the Si substrate

ICP plasma system has utilized to make etching process in the Si substrate as illustrated in the Figure 1.8. In this result anisotropic profile has obtained and imprinted in the Si substrate bu using low pressure gas [25].

In the biomedical sector, plasma has grown to replace the conventional method. Plasma applied for sterilization process. Plasma has utilized to kill the bacteria or virus in the medical instrument by treatment process [26]. With the high temperature in the plasma is expected to kill the bacteria or virus in the medical tools. Plasma has grown as scalpel in medical sector for helping doctor during operation process. One kind of the development plasma scalpel is depicted in the figure 1.8 [27].
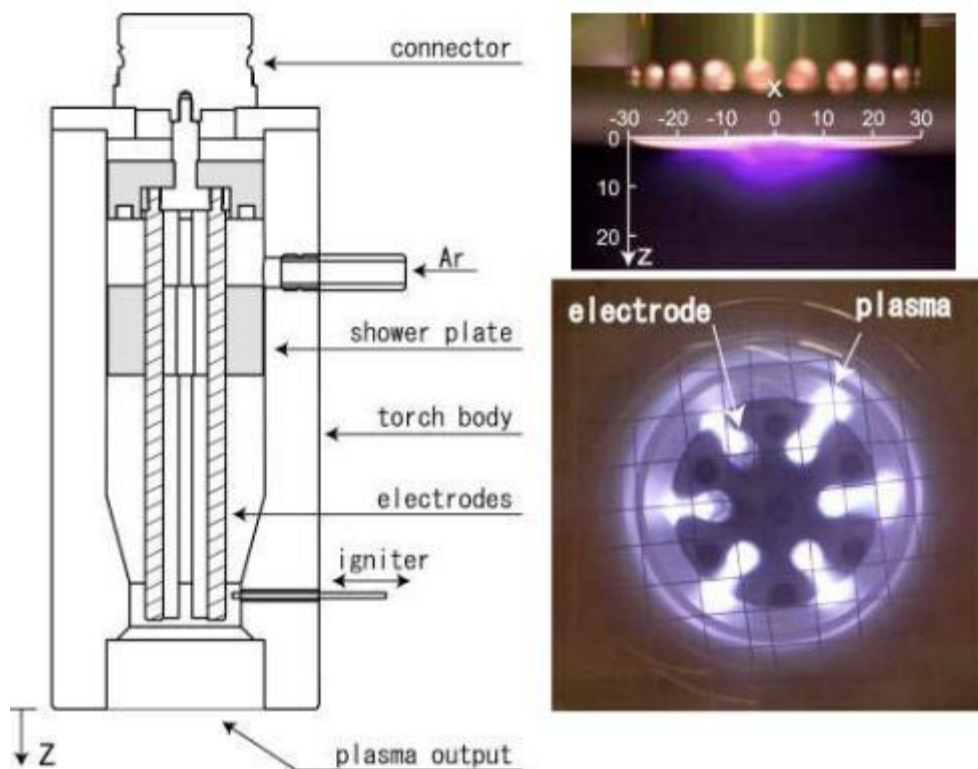
Figure 1.9 The application plasma technology for scalpel

1.5 THE PURPOSE OF THIS STUDY

The overall objective of the present study is in the understanding of the hollow cathode plasma system characteristic and applied for plasma application processing. Plasma generation can be done in many process and type. Each type has different behaviour and characteristic. Plasma characterization has become important process have to do before apply in some application process.

Hollow cathode plasma system has developed to obtain high ion and electron density. As we know, high ion and electron density are expected from each plasma system because it's useful for application process. In this study, hollow tube has placed inside the chamber to generate hollow cathode plasma. Hollow cathode plasma system is expected to have high ion density and electron density inside the hollow tube. Quantitative plasma diagnosis has utilized to measure and characterize hollow cathode plasma density by using Langmuir probe and Optical emission spectroscopy.

CVD diamond coatings have been widely utilized as protective coating of mechanical, functional and fashion-oriented parts besides tool and dies. CVD-diamond coating is the hardest coating material compare with other coating material. MEMS/NEMS is a key technology sensor for electronic devices with high speed performance. Most of these devices under development are mainly based on the silicon wafer. However, silicon has relatively poor mechanical properties; e.g. low Young's modulus of 130 GPa and low tribological properties. CVD-diamond diamond coating has grown up to replace silicon as material for MEMS/NEMS [28]. As we know, CVD diamond coating is a hard coating material and difficult in fabrication process.

Hollow cathode oxygen plasma etching with high plasma density is a solution to process CVD diamond coated for MES/NEMS.

CFRP (carbon fiber reinforced plastic) has grown to be a key structural composite material especially in aerospace and automobile industries. CFRP is difficult to be machined because of its high strength in tension and brittleness in compression [29]. Tooling with diamond coating become a solution to be free from the about difficulties. However its tool life is so short and the WC (CO) tool price is quite expensive, one of the solution is the used diamond coating must be recycle before reuse for practice. Many studies were reported in the literature on this removal of the used diamond coating. Mechanical and chemical polishing, EDM, laser, chemical ashing are kind the way to remove diamond coating from the substrate [30]. Certainly, there is advantage and disadvantage point from each process. Nowadays, high rate and fast ashing process is required to remove diamond coating. Importantly, low damage to the substrate material after ashing process is expected from each process. An alternative process is needed to solve this problem. Hollow cathode plasma ashing system is design to solve this problem. High ion and electron density inside hollow cathode is effective to remove the used CVD diamond coating material. And also, the rotating system has developed to make homogeneous plasma ashing in the CVD-diamond coating tools.

REFERENCES

[1] F. F. Chen, Introduction to plasma physics and controlled fusion, New York: plenum press. (1984), Vol. 1.

[2] M. Lieberman and A. Lichtenberg, Principles of plasma discharge and material processing, New York : John Wiley and Sons, (1994).

[3] R. J. Goldston and P. H. Rutherford, Introduction to plasma physics, London: Institute of Physics Publishing, (1995).

[4] E. A. Mason and E. W. McDaniel, Transport properties of ion in gases: John Wiley and Sons, (1998).

[5] I. Katz, J. Anderson, et al, One dimensional hollow cathode model, Journal of propulsion and power, (2003), vol 19, 595-600.

[6] L. Spitzer, Jr., Physics of fully ionized gases, New York : Interscience, (1962), 127-135.

[7] D. Bohm, The characteristic of electric discharges in magnetic fields, New York : McGraw-Hill, (1949). 1-76.

[8] S, I, Braginskii, Transport processes in a plasma, Plasma physic, (1965), 205.

[9] T. Panagopoulos and D. J. Economou, Plasma sheath model and ion energy distribution for all radio frequency, Journal of applied physics, (1999), 3435-3443.

[10] Q. Sun, Y. Li, The characteristic of surface arc plasma and its control effect on supersonic flow, Physics letters A, (2014), 2672-2682.

[11] C. A. Bishop, Vacuum deposition onto webs, films, and foild (third edition),(2015), 277-287

[12] V. M. Zhdanov, A. A. Stepanenko, Electron transport coefficients in molecular and atomic plasma with account for inelastic collision, Physic Procedia, (2015), 110-115.

[13] Z. Wronski and J. Filiks, Fe and Ti cathode sputtering by oxygen plasma in DC glow discharge, Vacuum, (2009), 77-80

[14] M. Hirano, M. Yamane, N. Ohtsu, Surface characteristic and cell-adhesion performance of titanium tread with direct-current gas plasma comprising nitrogen and oxygen, Applied surface science, (2015), 7-13.

[15] J. A. Baier-Saip, et al, Deep oxidation of aluminium by a DC oxygen plasma, Surface and coating technology, (2005), 168-175.

[16] R. H. Zhu, et al, High temperature thermal conductivity of free-standing diamond films prepared by DC arc plasma jet CVD, Diamond and related material, (2014), 55-59

[17] S. Khorram, M. S. Zakerhamidi, Polarity functions characterization and the mechanism of starch modification by DC glow discharge plasma, carbohydrate polymers, (2015), 72-78

[18] T. Kitajima, J, Nakashima, et al, Oxygen atom density in rare gas diluted O2 radio frequency plasma, Thin solid films, (2006), 489-493.

[19] Y. Ohtsu, Y. Hino, et al, Influence of ion bombardment energy on thin zirconium oxide films prepared by dual frequency oxygen plasma sputtering, Surface and coating technology, (2007), 6627-6630

[20] L. Wang, X. D. Zhu, et al, Effect of bia in patterning diamond by a dual electron cyclotron resonance-radio frequency oxygen plasma, Thin solid film, (2010), 1985-1989

[21] U. Cvlbar, N. Krstulovic, et al, Inductively coupled RF oxygen plasma characterization by optical emission spectroscopy, Vacuum, (2008), 224-227.

[22] A. Vesel, R, Zaplotnik, Inductively coupled oxygen plasma in H mode for removal of carbon from mixed a-C:H, W films, Nuclear engineering and design, (2013), 275-278.

[23] K. H. Rasmussen, S. S. Keller, SU-8 etching in inductively coupled oxygen plasma, Microelectronic engineering, (2013), 35-40.

[24] T.Aizawa, M. Masaki, Oxygen plasma ashing of used DLC coating for reuse of milling and cutting tools, International conference on Material processing technology, (2013), 15-20

[25] Z. Ren and M. E. McNie, Inductively coupled plasma etching of tapered via in silicon for MEMS integration, Microelectronic engineering, (2015), 261-266

[26] T. Kuwahara, T. Kuroki, et al, Development of strerilization device using air nonthermal plasma jet induced by atmospheric pressure corona discharge, Thin solid film, (2012), 2-5.

[27] O. Rabinovych, R. Pedrak, Nanojet as a chemical scalpel for accessing the internal 3D-strcture of biological cell, Micri and nano engineering, (2004), 843-846.

[28] K. Hanada, Fabrication of diamond dies for micro forming. Diamond related material. (2003).

[29] R. Hasegawa, Cutting tool for aircraft and application, Journal Japan society for precision engineering, (2009), 953-957.

[30] A. Rashid and K. Piglmayer, Laser induced simultaneous etching of silicon and deposition of carbon material, Applied surface science, (2012), 9167-9170

2. EXPERIMENTAL PROCEDURES

2.1 INTRODUCTION

Plasma ashing and etching are the famous method used to remove coating film from substrate. This method generally consists of the chamber, the electrode, the plate, the substrate, the carrier gas supply, and the RF or DC generator [1].

The electrons are able to travel freely to collide with atoms and molecules inside the chamber. The ions and new electrons are produced by this collision. The reactive species are transported and adsorb on the target film. The reaction take place at the surface of the target film and etching or ashing process is starting [2]. The etching or ashing process can be controlled by modifying the plasma parameters.

Plasma systems are generally falls into several categories: DC, RF, ICP and hollow cathode plasma. The hollow cathode plasma has some advantage in term of stabilization of the plasma, high ion and electron density, and as result powerful for etching or ashing process [3].

2.2 HOLLOW CATHODE OXYGEN PLASMA SYSTEM CONFIGURATION

Hollow cathode oxygen plasma has utilized to remove coating material from the substrate. Hollow cathode plasma consists of the hollow tube, the vacuum chamber, the plasma generator, the control unit, and the carrier gas supply. The chamber with diameter 11 cm is neutral in electricity; RF dipole electrode and DC-bias work independently to generate RF and DC plasma, respectively as shown in Fig.2.1 below [4]. The ionized species and activated radical in the RF plasma are attracted to the DC bias plate with kinetic energy. Either RF-plasma or DC plasma or, both are ignited by switching on either or

both on the control panel. In addition, there is no mechanical matching box for RF plasma generation in this system. Input and output powers are automatically matched by frequency adjustment around 2 MHz. After placing the diamond coated specimen, the chamber is evacuated to the base pressure, less than 5×10^{-3} Pa. The pure oxygen gas with the purity of 99.99% is supplied as carrier gas to the specified pressure [5].

Figure 2.1 High density plasma systems

The hollow tube is placed inside the neutral chamber and made from stainless steel. There are two kind of hollow tube with different size and shape in this experiment. For Ashing process, the cylindrical shape with diameter 2.5 cm and length 10 cm has utilized in this study. And also, rotation system has used in the whole of the experiment time to make homogeneous ashing result. For etching process, the cuboids shape with dimension 2 x 1 x 5 cm has

utilized to make etching process. Both of the hollow tubes are depicted in the Fig. 2.2.
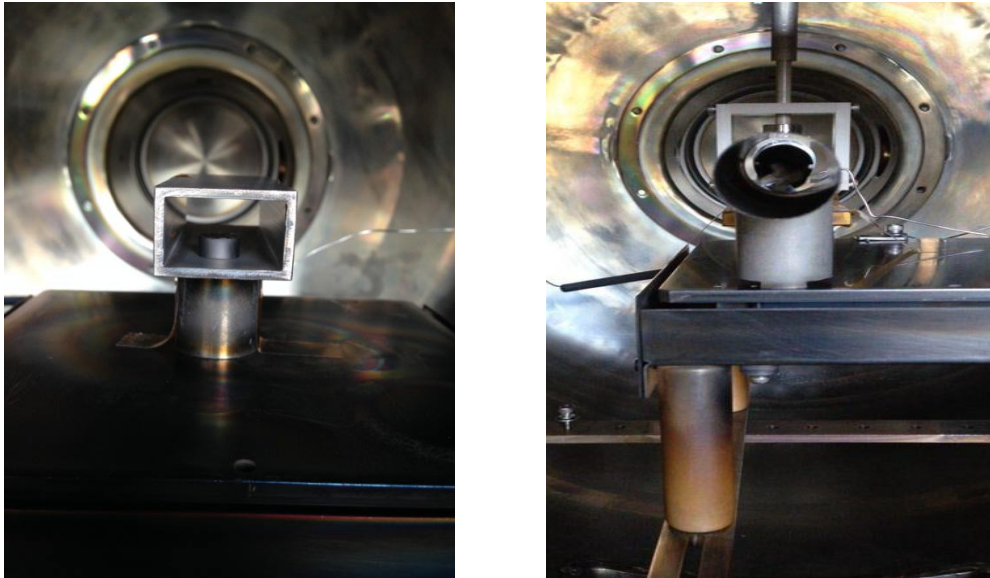
Figure 2.2 Hollow tube shape and dimension. a) for etching, and b) for ashing process

Different from the conventional hollow cathode plasma generator, this hollow is directly connected to DC-bias. Oxygen gases are introduced to the chamber. Due to the pressure gradient between chamber and hollow tube, oxygen gas flow inside the hollow tube. The plasma ignition is done by switching on RF plasma generation and DC-bias. As a result oxygen plasmas are formed inside the hollow tube.

2.3 HOLLOW CATHODE OXYGEN PLASMA CHARACTERIZATION

2.3. 1. CHARACTERIZATION BY USING LANGMUIR PROBE

The centralized generations of hollow cathode oxygen plasma provide high electron and ion densities. Variation in pressure, DC-bias, and RF-voltage give different result in plasma density. The plasma characterization is needed to understand and to describe the hollow cathode plasma. In this case,

plasma characterization has done by using Langmuir probe and optical emission spectroscopy [6]. The schematic diagnostic is depicted in Fig. 2.3.
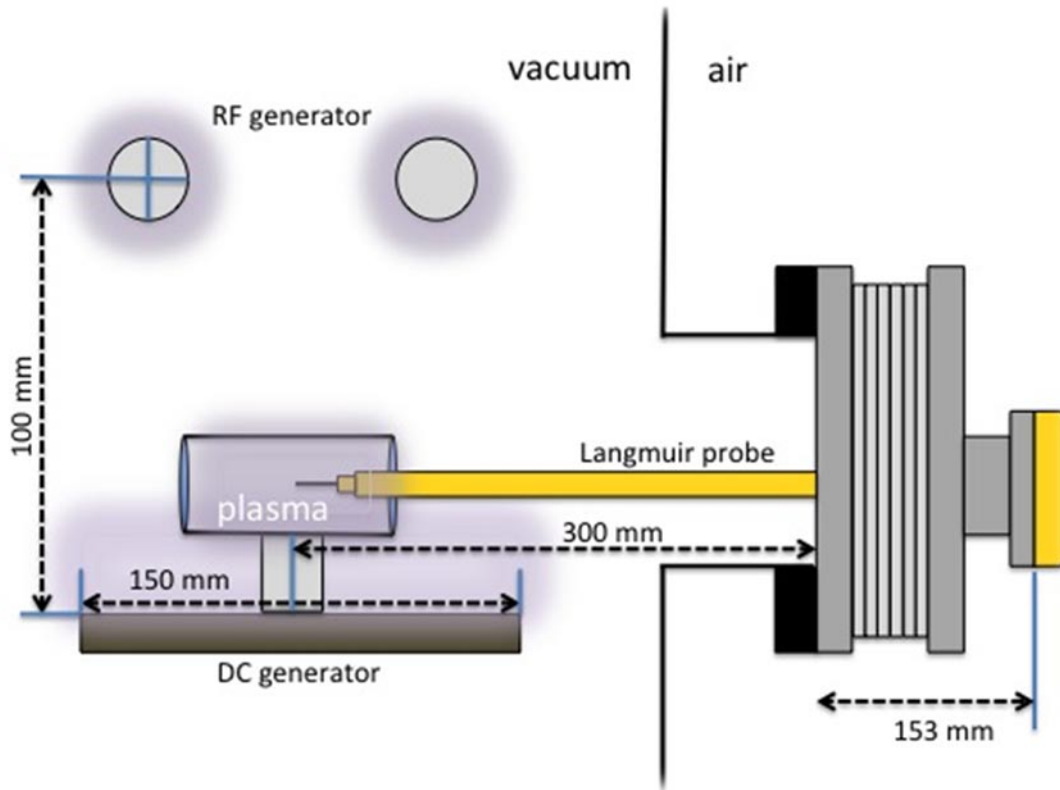
Figure 2.3 The schematic plasma characterization by using Langmuir probe and optical emission spectroscopy

Plasma parameter has measured with a single Langmuir probe analysis (Impedans ALP System). The probe has radius 3.5×10^{-4} m, length of 0.01 m, and resistance of 36 ohm. Plasma density has measured in all area of hollow tube by moving the probe position from outside to inside of the hollow tube. In this condition, only oxygen gas is utilized without using sample. The pressure, DC-bias, and RF voltage are varied to describe the plasma density and to get the optimum condition for ashing or etching process [7]. The plasma parameter such as ion density (ni), electron density (ne), electron temperature (Te), and plasma potential are measured and transferred to display.
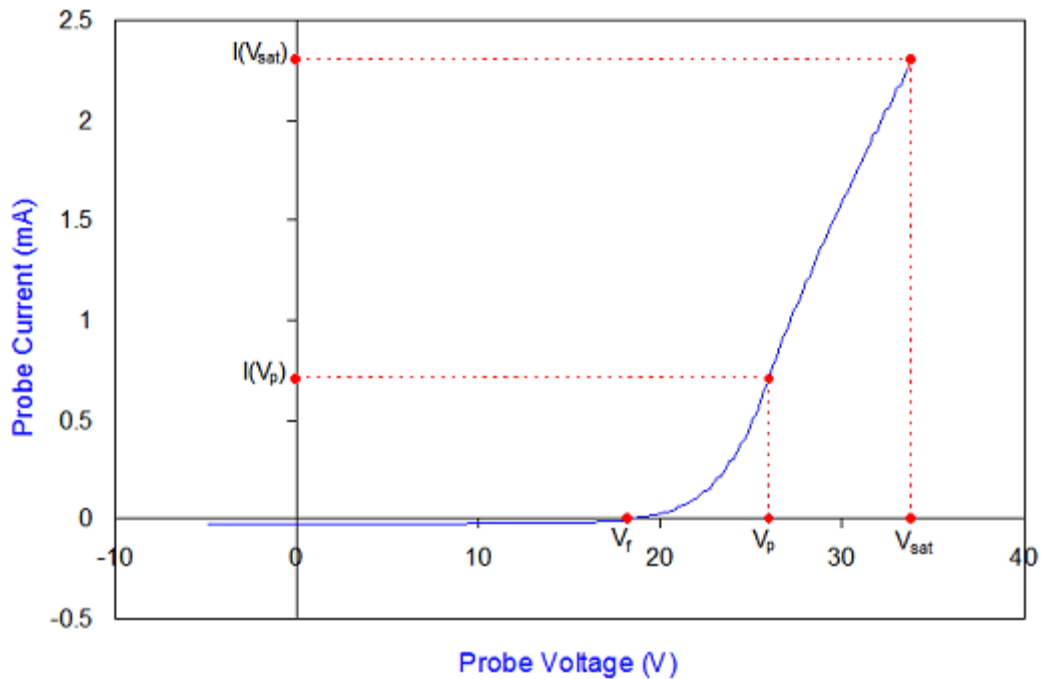
Figure 2.4 Typical I-V curves characteristic

The Langmuir probe works with the principle of I-V curves and divided in three regions as depicted in Fig. 2.4. The first region is the region to the left of Vf where the probe bias is increasingly more negative, with the respect to the plasma potential. The electrons are repelled and the probe current is dominated by the positive ions. This region is called Ion saturation condition. Moving from Vf to Vp the probe collects increasingly more electron current as the potential barrier formed between the probe and plasma decreases (becoming 0 at Vp). The electron current increases exponentially when the electrons are in thermal equilibrium. This region is called electron retardation condition. The last condition is to the right of Vp the probe potential attracts plasma electrons and electron saturation occurs. This region is called electron saturation condition [8].

2.3.2. CHARACTERIZATION BY USING PHOTONIC MULTICHANNEL ANALYZER (PMA 11)

The photonic multichannel analyzer (PMA-11) has utilized to measure and characterize the spectrum from hollow cathode oxygen plasma. The PMA-11 is compact spectral measurement apparatus that combines a spectrometer and optical detector into one unit. An optical fiber with a 1 mm effective diameter is used and mounted in the chamber during plasma etching and ashing process [9]. The set-up experiment setting as depicted in fig. 2.5.
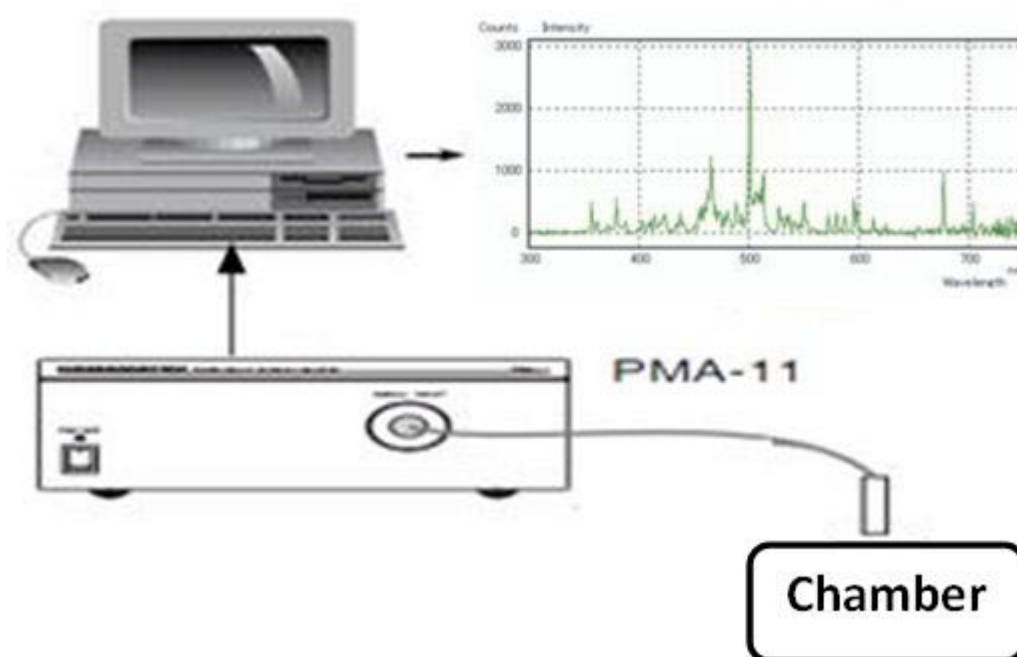
Figure 2.5 Hollow cathode spectrum measurement by using PMA-11

The optical fiber has mounted in the quartz window on the top of the chamber perpendicularly to the sample. The lights from plasma in the hollow cathode are detected by optical detector. This measurement is transferred to the computer. The spectrum software inside the computer processes this data and then displayed the spectrum in the computer screen as online. The peaks from the spectrum represent atomic, molecule, activated molecule and radical

peaks from the plasma. In this study, oxygen gas was utilized to generate hollow cathode plasma. Diamond coated was placed inside the hollow cathode. During the plasma processing, hollow cathode oxygen plasma attack to the diamond coating. The peaks from oxygen atomic, oxygen molecule, and activated molecule were displayed in the computer as online.

2.4 PREPARATION OF DIAMOND COATING FOR ETCHING

The hollow cathode oxygen plasma was proposed to make plasma etching in the diamond coating. In this case diamond has coated in the WC (Co) substrate in cylindrical shape. The thickness of diamond coating reaches to 20 μm as depicted in the fig. 2.6.a Micro line was the goal in this step. A stainless sheet mask as depicted in fig. 2.6.b with the thickness of 50 μm was used for masking to make micro line pattern in the diamond coating [10].
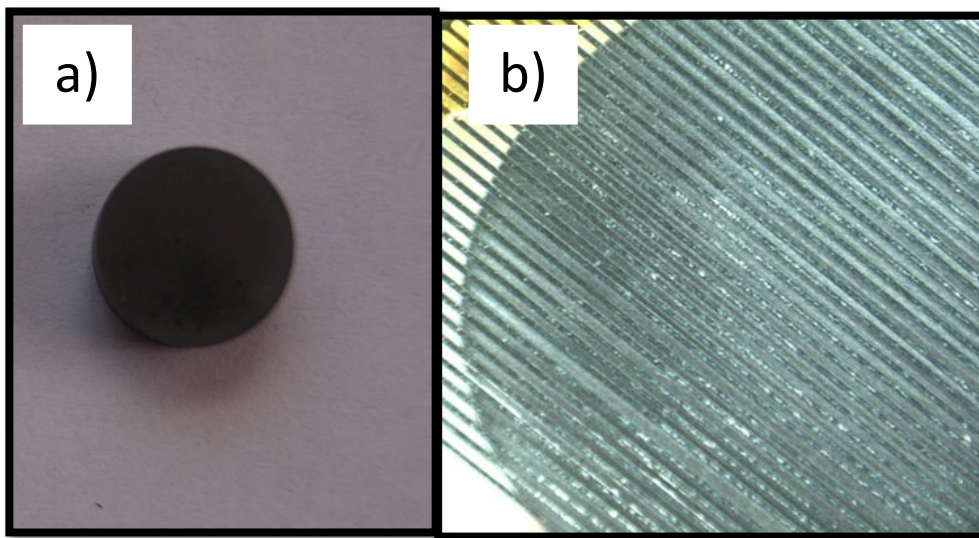
Figure 2.6 The specimen for etching process, a) diamond coating on WC (Co) , b) micro lines mask on the diamond coating

The WC (Co) specimen has diameter 10 mm and thickness 5 mm. The stainless steel mask has dimension 30 x 30 mm. The stainless steel mask was placed on top of WC (Co) diamond coating. A tape has utilized to make

the stainless steel mask stay on the position during the etching process. The diamond coating and stainless steel mask were placed inside the hollow cathode. The plasma etching condition was showed in the table below.

Table. 1 The plasma etching experiment set-up

RF- voltage (V)	250
DC-bias (V)	-550
Pressure (Pa)	30
Time (s)	7200

2.5 PREPARATION OF CUTTING TOOLS DIAMOND COATING FOR ASHING

The other purpose from hollow cathode oxygen plasma was used to make homogenous and perfect plasma ashing on the end-milling tools. The end-milling tools have a length 7 cm and thickness 15 μm of diamond coating. The cutting tools were made from WC (Co) material. This material is a hard material which is characterised by an extraordinary hardness and wear resistance. The end-milling tool is depicted in the figure 2.7. In this study, the end milling tool was rotated with the constant speed 4 rpm. The experiment condition was set in RF=100 V, DC-bias -500 V, and pressure 45 Pa [11]. The end-milling tool was placed inside the hollow tube and tightening with the screw to keep in the position. The rotation machine was started and kept constant during the experiment. The only oxygen gas was used and introduced inside the chamber. The ashing process was set in 3600 second and no additional time.

Figure 2.7 CVD-diamond coated end-milling tools with the film thickness of 15 μm

2.6 MEASUREMENT ANALYSIS BY USING OPTICAL MICROSCOP

The optical microscope has utilized to check the specimen after ashing and etching result. The optical microscope made by Shimadzu with the series number STZ-168-TL has utilized in this study. This microscope has advantage smooth zooming mechanism, sharp images, large focusing working area, and easy to use. The specimen after ashing and etching has cleaned by using alcohol, after that the specimen was checked by using optical microscope to get the surface condition. In this case, the magnification of microscope can be change from 1.0 to 7.5 times [12]. The specification of optical microscope STZ-168-TL as depicted in the table 2 below.

Table. 2 The specification of microscope STZ-168-TL

Model	STZ-168-TL
Total Magnification	7.5 x ~ 5.0 x (1.125x ~ 320x by option)
Number of view	23 mm
An objective lens	Zoom type 0.75x ~ 5x zoom ratio of 1:67
Eyepiece	WF10x
Dioptre adjustment range	$\pm 5^0$
Eye width adjustment range	52 ~ 79 mm
Lens barrel	Three eye 35^0 tilt barrel 360^0 rotation strut slide rack and pinion two stage method eyepiece sleeve inner diameter 30 mm
Working distance	113 mm
The maximum field of view	30.7 mm
Size and weight	330 x 340 x 398 mm and 7 kg
Lightning systems	The incident light source 12 V 10 W halogen

The result from optical microscope has transferred and displayed in the computer. This microscope has integrated with the computer software to check and modify the image result. The image result was saved in jpeg, tif, and bmp file. The optical microscope STZ-168-TL model was depicted in fig. 2.8.

Figure 2.8 The optical Microscope Shimadzu STZ-168-TL

2.7 MEASUREMENT ANALYSIS BY USING SCANNING ELECTRON MICROSCOPE (SEM)

The SEM (Scanning Electron Microscope) has utilized to measure the specimen before and after etching and ashing process. The SEM JCM-6000 was made by Nikon has utilized in this study. This system consist of power supply, rotary pump, JCM-6000 base unit, PC, and LCD display as depicted in fig. 2.9. This compact electron microscope was a simple to operate as digital camera, but has the powerful electron optics of an SEM, with up to 60000 x magnification [13]. The SEM operation was via a touch screen and was simplified with auto focus, auto alignment, auto contrast and auto brightness controls. The neoscope operates in both low and high vacuum modes with three setting for accelerating voltage. The specification of SEM JCM-6000 was depicted in table.3.

Table. 3 The specification of SEM JCM-6000

Magnification	Secondary electron image: x10 to x60,000 Backscattered electron image: x10 to 30,000 (when image size is 128 mm x 96 mm)
Imaging mode	Secondary electron image, backscattered electron image
Accelerating voltage	Secondary electron image: 5 kV, 10 kV, 15 kV (3 stages) Backscattered electron image: 10 kV, 15 kV (2 stages)
Electron gun	Small gun with cartridge filament integrating wehnelt
Bias current	Auto bias
Specimen stage	Manual control for X and Y: X:35 mm, Y: 35mm
Maximum sample size	70 mm diameter x 50 mm height
Image memory	One, 1280 x 960 x 16 bits
Pixels	640 x 480, 1280 x 960
File format	BMP, TIFF, JPEG
Evacuation system	Fully automatic, TMP : 1, RP : 1

The sample was placed inside the JCM-6000 base unit. The high vacuum system has worked during the process. Focus and contrast were set automatically to get the clear image from the specimen on the display. The magnification was chosen from 50 x, 100x, 500x, and 600x as needed. The specimens were also rotated and change the tilt to get different image for

other side of the specimen. The tilt could be change from -15^0 to $+ 45^0$ and the rotations reached to 360^0. The image result has saved in computer and easy to transfer to other storage by using usb.
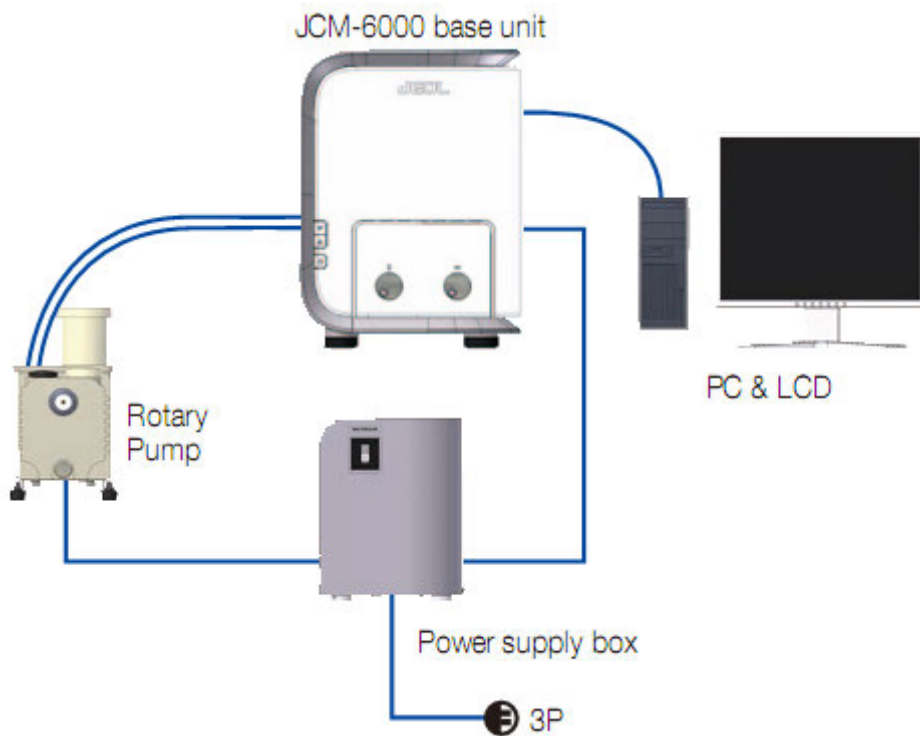
Figure 2.9 JCM-6000 SEM system composition

2.8 MEASUREMENT ANALYSIS BY USING SURFACE PROFILOMETER

The surface profilometer was also utilized to check the surface from the specimen after etching and ashing. The profilometer has used to get 3D surface profile after plasma etching. The surface profilometer was made by Keyence with the type VW-9000 high speed microscope. These systems consist of computer display and optical lens as depicted in the figure 2.10. Surface profilometer VW-9000 has some advantage compare with the other system. This system enables accurate filming of high-speed motion that conventional microscopes cannot capture, able to record up to 230000 fps, set up and record in minutes, automatically determine changes in motion, an

LCD monitor, light source, and HDD build into an all-in-one design [14]. The specification of Keyence VW-9000 has depicted in the table 4.

Table. 4 The specification of Keyence VW-9000 surface profilometer

Size	Color LCD (TFT) 10.4
Dimensions	• LCD : 210.4 mm (H) x 157.8 mm (V)
Number of pixels	1024 (H) x 768 (V) XGA
Display color	Approx 16,000,000 colors
Recording media	• Semiconductor memory 8GB • Hard drive 500 GB (includes reserved system space of 100 GB)
Image format	• Video : AVI, JPEG, WMV • Image : JPEG, TIFF
Light source	• Lamp : specialized metal halide lamp • Color camera : 60 W high color rendering • Monochrome camera : 80 W high-brightness • Lifetime : 2000 hours • Color temperature : 8000 K (color camera) , 6400 K (monochrome camera)
Sensor input	• Input channel number : 1CH • Measurement range : ±10 V, ±5 V, microphone • Input port : BNC, microphone jack • Resolution : 14bit

Power supply	• Power supply voltage : 100 to 240 VAC ± 10%, 50/60 Hz • Power consumption : 290 VA or less
Video input	1024 (H) x 768 (V) XGA
Weight	• Controller (main unit) approx 11kg • Optical fiber cable approx 800 g • VW console approx 180 gr

Keyence VW-9000 surface profilometer was easy to operate; the sample was placed on the table under the optical microscope. The software was selected in 3D mode photo image. The focus of optical lens was set and checked until the clear image show in the LCD display. After the clear image was gotten in the LCD display, the magnification of the lens was set and moved as needed to get the image from the specific area. Then, the figure will be captured and transferred to computer display. In the computer software, height, length, and distance of the figure can be measured by using software tools. The axis angle of the figure was possible to rotate until 360^{0} to get the image from each position. The image result was saved in jpeg, tiff file type and easy to transfer to other storage.
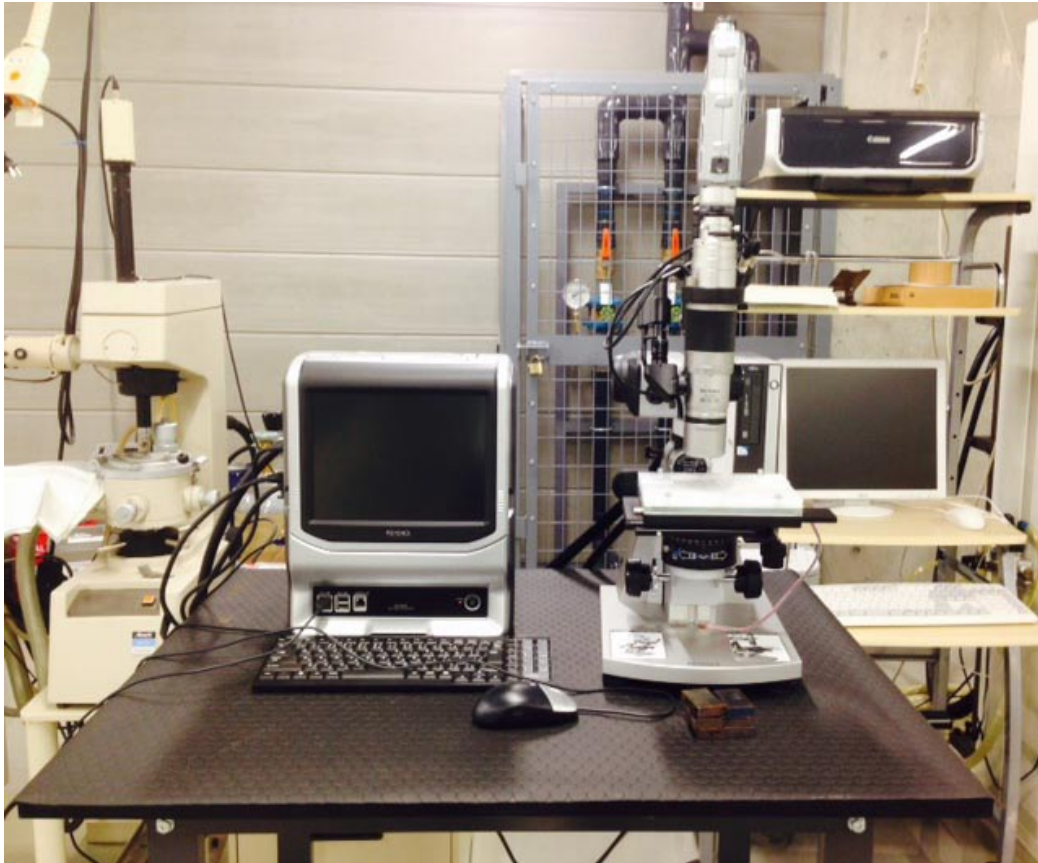
Figure 2.10 Surface profilometer VW-9000 high speed microscope

2.9 MEASUREMENT ANALYSIS BY USING RAMAN SPECTROSCOPY

Raman spectroscopy has utilized to check and prove the diamond coating has totally removed from the surface of specimen. InVia Raman spectroscopy made by Renishaw has utilized in this study. Invia Raman spectroscopy has high sensitivity for detecting weak signal, high speed in getting data, high resolution spectra, high stability, simple to use and safety. Invia Raman spectroscopy was integrated with high resolution of microscope as depicted in figure 2.11. Invia Raman microscopes support multiple lasers, with optimized beam path for each laser. The laser power was controlled manually for each measurement condition to get the optimum result from each sample [15].

Figure 2.11 Invia Raman spectroscopy

The sample was placed in the table inside the Raman spectroscopy machine. The sample was positioned as simple as possible to make laser checked the measurement area easily. In the plasma etching, the Raman spectroscopy has utilized to check the etched area and mask area. In this case the laser was directed to the both area to get the respond from diamond peak. The laser touched the sample surface in a few minute. The data from this measurement are transferred to the computer. The Raman spectroscopy software displayed the measurement result in the screen. The same condition was applied for plasma ashing. In this case the Raman spectroscopy has utilized to check the diamond peak on the end milling cutting tool before and after ashing process. The spectrum results before and after process have plotted and compared in one graph to get the information from ashing and etching process.

2.10 SUMMARY

Plasma ashing and etching were utilized to remove coating material from the sample. High plasma density was effective to remove coating material even for hard coating material such as diamond films. Hollow cathode plasma was developed to achieve high plasma density. Hollow cathode plasma system was developed by using metal hollow tube and bias directly during plasma generation. The bright discharge was produced inside the hollow tube. The characterization of hollow cathode plasma was done by using Langmuir probe and Optical emission spectroscopy (OES). The variations of pressure, DC-bias voltage, and RF-voltage were also done in the present study. The Langmuir probe was utilized to measure plasma parameters in the hollow cathode. Optical emission spectroscopy (OES) was utilized to measure the population inside the hollow cathode from the spectrum.

Two kind of sample were employed to make etching and ashing process. The first sample was a WC (Co) substrate in cylindrical shape. These substrates were coated with diamond film with the thickness 20µm. Metal mask with line width 100 µm has employed to make micro texturing onto WC (Co) substrate. The metal mask was installed above the diamond coating and fixed by using capton tape. The etching process was done by placing the substrate inside the hollow tube for 7200 second. The second sample was WC (Co) end milling tool with the length 7 cm and thickness 15µm of diamond coating. The end milling tool was placed inside the hollow cathode and rotating with constant speed 4 rpm. The homogeneous plasma ashing and little damage to the original substrate were the goal from the

second sample. The ashing process was done for 3600 second in the present study.

The analysis process after ashing and etching were done by using optical microscope, surface profilometer, SEM, and Raman spectroscopy. The optical microscope was employed with the purpose to check surface profile of substrate before and after ashing and etching process. Surface profilometer was utilized to check the surface profile of substrate after etching process in 3D after etching process. SEM was employed to check surface profile of the substrate more detail after etching and ashing process. Raman spectroscopy was utilized to check the diamond peak after and before processing. The measurements were done by placing the laser pointer to the mask and unmask area of diamond coating. The results were compared in one graph to see the diamond coating has left from the unmask area.

REFERENCES

[1] E. E. Yunata, T. Aizawa, D.J.H. Santyojo, Characterization of hollow cathode plasma, 8th SEATUC Sym. (2014), 86.

[2] R. Suenaga, E. E. Yunata, T. Aizawa, Quantitative plasma diagnosis on high density RF-DC plasma for surface processing , 7th SEATUC Sym. (2013), 113.

[3] L. Bardos, Radio frequency hollow cathodes for the plasma processing technology, Surface and coatings technology. (1996), 648-656.

[4] E. E. Yunata, T. Aizawa, R. Suenaga, D.J.H. Djoko Santyojo, Quantitative argon plasma characterization by Langmuir-probe method, 7th SEATUC Sym. (2013), 105.

[5] T.Aizawa, T. Fukuda, Oxygen plasma etching of diamond-like carbon coated mold-die for micro-texturing, Surface and coating technology, (2013), 364-368.

[6] E. E. Yunata, T. Aizawa, Micro-texturing into DLC/diamond coated mold and dies via high density oxygen plasma etching, 7th AWMFT, (2014), 28.

[7] T. Aizawa, E. Masaki, Y. Sugita, Oxygen plasma ashing of used DLC coating for reuse of milling and cutting tools, ICMPT, (2013), 15-20.

[8] J. P. Lebreton, S. Stverak, P. Travnicek, The ISL Langmuir probe experiment processing onboard Demeter scientific objectives, description, and first result, Planetary and space science, (2006), 472-486.

[9] P. G. Reyes, E. Measurements of electron temperature and ion density in a mixture of O_2 and Ar plasma, Journal of physics (2010), 1-4.

[10] E. E. Yunata, T. Aizawa, High density oxygen plasma processing for ashing of DLC and CVD-diamond coated tools. J. Coating. (2014) (to be submited)

[11] E. E. Yunata, T. Aizawa, K. Yamauchi, High density oxygen plasma ashing of CVD-diamond coating with minimum damage to WC (Co) tool substrates. Abstract. 42th ICMCTF,(2015) 123.

[12] N. T. Redationo, T. Aizawa, E. E. Yunata, Plasma micro-patterning onto diamond like carbon coating, 7th Seatuc, (2013) .

[13] E. E. Yunata, K. Yamauchi, T. Aizawa, Y. Sugita, Simultaneous oxygen plasma ashing of CVD diamond coated WC (Co) tools, 9th SEATUC (2015)

[14] K. Yamauchi, E. E. Yunata, T. Aizawa, High density oxygen plasma ashing of used CVD diamond coating for recycling of WC (Co) Tools. IFMMB (2015)

[15] E. E. Yunata, K. Yamauchi, T. Aizawa, High density oxygen plasma ashing of CVD diamond coated end-milling tools, 4th ASMP (2015)

3. THEORITICAL OF HOLLOW CATHODE PLASMA

3.1 INTRODUCTION

Hollow cathode discharges have been used for many years to produce plasma and ions for a large number of applications [1, 2]. Under typical operating conditions, hollow cathode plasma produces strongly ionized plasma with typical electron number densities of 10^{13} to 10^{15} cm^{-3} and electron temperatures of 1 to 2 eV [3]. As a plasma source, the hollow cathode has provided a valuable tool for research in atomic and molecular physic [4-6]. This device was used as a high current density ion source to heat plasmas in controlled thermonuclear reaction experiment. Moreover, the hollow cathode has been widely used as electron emitters in advanced ion thrusters, where they exhibit longer life time and greater reliability than oxide-coated or liquid metal cathodes [7]. Hollow cathode plasma provides high degrees of ionization, high electron density, and low contamination by cathode material.

Despite their broad utility, the physical processes inside hollow cathodes are still poorly understood. The inherently complex interaction between the plasma and the cavity walls does not lend itself to empirical modelling, and microscopic data on the plasma properties are sparse. By this point, the new model of hollow cathode plasma is developed in the present study. The hollow cathode plasma has developed by using metal hollow tube and placed inside the chamber. The glow discharge will be seen inside the hollow tube during plasma generation by this configuration. Theoretical and simulation was developed to describe and understand the new model of hollow cathode plasma.

3.2 ELECTRO-MAGNETIC ANALYSIS

3.2. 1 Theoretical of hollow cathode plasma

The present theoretical study is intended to identify and describe the major physical laws governing hollow cathode plasma. The figure 3.1 exhibits the schematic model of hollow cathode plasma in the present study. The gas pressure was introduced inside the chamber and flowing inside the metal hollow tube. The different dimension from metal hollow tube and chamber establish the pressure gradient, especially in the metal hollow tube. The high pressure flows inside the metal hollow tube. The RF-generator has applied and effect in electrons mobility inside the chamber. The electrons are accelerated by an electric field generated by the RF-generator, acquire kinetic energy, and collide with atom and molecule. At the same time, direct DC-bias has applied in the metal hollow tube. As a result, electric fields have also generated in the metal hollow tube inside the chamber.
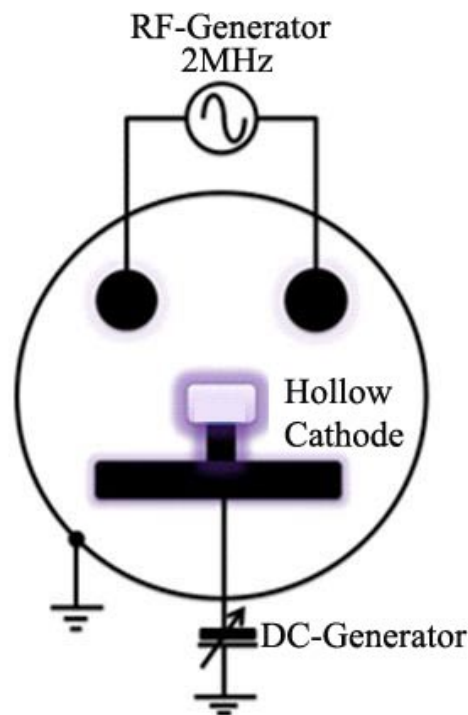
Figure 3.1 The schematic of hollow cathode plasma

Due to DC-bias voltage has higher than RF-voltage; the high electric fields are generated in the metal hollow tube area. The high percentage of ionization process localize in the hollow tube area. Theoretically, the electron in the metal tube is described by the Richardson-Dushman equation:

$$J = A\ T^2\ e^{-e\Phi/kT}, \tag{3.2-1}$$

Where A is a constant with a value of 120 A/cm^{2}K^2, T is the temperature in Kelvin, e is the charge, k is Boltzmann's constant, and Φ is the work function. The temperature correction for the work function is describe by the below equation;

$$\Phi = \Phi_0 + \alpha\ T, \tag{3.2-2}$$

Where Φ_0 is the classically reported work function and α is an experimentally measured constant. This dependence can be inserted into Eq. (3.2-1) to give

$$J = A\ e^{-e\Phi/kT}\ T^2\ e^{-e\Phi_0{}^{/kT}} = D\ T^2\ e^{-e\Phi_0{}^{/kT}}, \tag{3.2-3}$$

Where, D is a material-specific modification to the Richardson-Dushman equation.

In the presence of strong electric fields at the surface of the cathode, the potential barrier that must be overcome by the electron in the material's conduction band is reduced, which result effectively in a reduced work function. This effect was first analyzed by Schottky, and the effect of the surface electric field on the emission current density was written by

$$J = D\ T^2\ exp\left(\frac{-e\Phi_o}{kT}\right) exp\left[\left(\frac{e}{kT}\right)\sqrt{\frac{eE}{4\pi\varepsilon_o}}\right], \tag{3.2-4}$$

Where, E is the electric field at the cathode surface. This equation becomes significant inside hollow cathode where the plasma density is very high and the electric field in the sheath become significant.

High electric field in the metal tube area makes the electrons are difficult to leave the hollow tube. The free electrons are rappelled from each side of the hollow tube wall and stay in the centre of the hollow tube. The pressure provides gas molecule inside the hollow cathode. In this point, free electrons inside the hollow tube are ready to make ionization process. As a result, ion and secondary electron are generated inside the hollow cathode. The ionization is occurred many times and secondary electron support for ionization process. As a result, localize ionization process are produced by using hollow cathode and provide high plasma densities inside the hollow tube.

3.2. 2 Simulation of hollow cathode plasma

The simulation model was build to study electric field distribution in the hollow cathode plasma system. By using J-MAG software, the simple model of hollow cathode plasma was build to study the distribution of electric field in the hollow cathode plasma. First, the model was build without hollow cathode plasma. Second, the hollow cathode plasma was build inside the first model. The comparison from both model were studied to get the information about the distribution of electric field inside the hollow cathode plasma.

The plasma modelling has described in the Figure 3.2 without using hollow cathode device. The figure 3.2 represents the electric field distribution inside the chamber during plasma generation. Figure 3.2 a) exhibits the RF-electrode in 250 V and DC-bias (-) 100 V. The result indicates the strong electric fields are concentrated in the RF-electrode area. In other hand, the DC-bias plate has weak electric field in this step. The short distance between the RF-electrode and DC-bias produce strong electric field due to high voltage

differences. As a result, the electric field distribution can be seen as green colour in this region. In the figure 3.2 b), the DC-bias has higher than RF-electrode. In this case the DC bias was (-600) V and RF-voltage 250 V. The electric field distribution has changed and toward to DC-bias area. The strong concentrations of electric field stay in the DC-bias area. The electric field distribution between RF-electrode and DC-bias show the same trend with figure a) but has lower electric value.
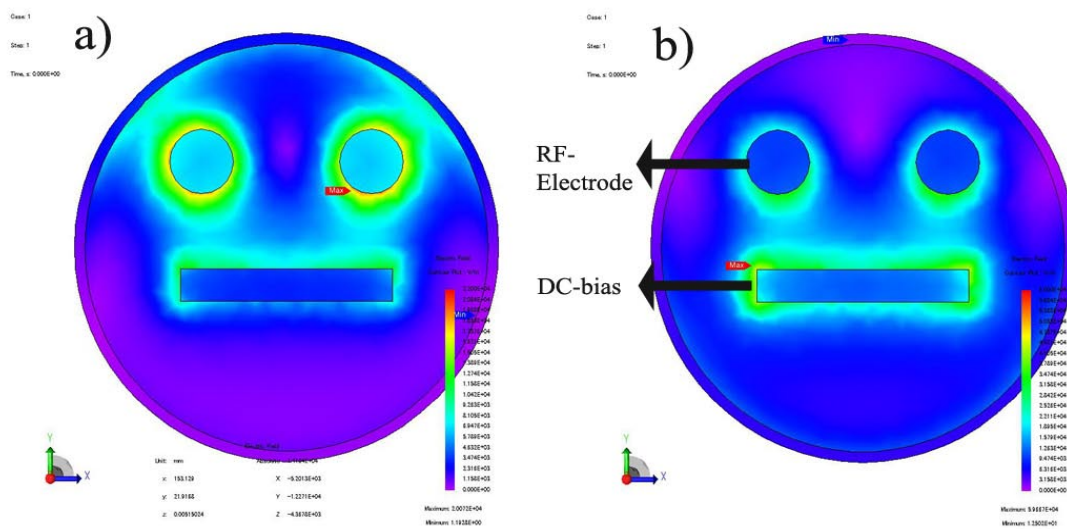
Figure 3.2 The electric field distribution in the plasma system without hollow cathode by using a) high RF voltage and low DC bias voltage, b) low RF voltage and high DC-bias voltage

The hollow cathode plasma model was built as depicted in the Figure 3.3. In this model, the hollow cathode was built in the cylindrical shape and was placed between RF-electrode and DC-bias plate. The RF-electrode was set in 250 V and DC bias was – (400) V. The electric field distribution toward to DC-bias due to high value of DC-bias compare with RF-electrode. The location between electrode and DC-bias show the same trend with the

previous model. The hollow cathode produces the strong electric field distribution as mention with yellow colour.
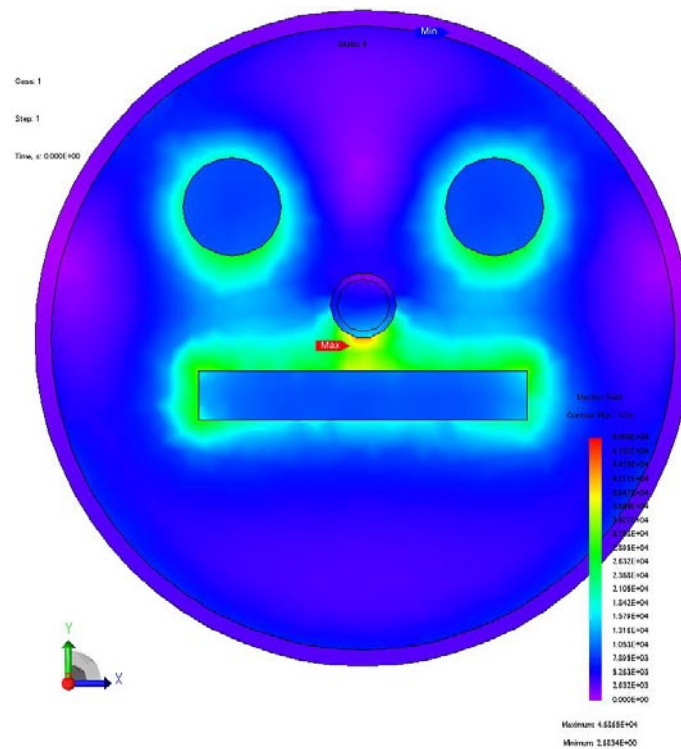

Figure 3.3 The electric field distribution in the hollow cathode plasma

The hollow cathode plasma model was placed in the DC-bias plate. In the same time the high voltage was applied in the DC-bias plate. By this condition, strong electric field distribute to DC-bias plate area. The hollow cathode has also affected by the strong electric field. The short distance between hollow tube and DC-bias plate produce high electric field. The electric field distribution covers the hollow cathode area by this effect. These modelling results support the experiment process and prove that hollow cathode has strong electric field and produce high plasma density.

3.3 PLASMA ANALYSIS

Plasma modelling has developed to understand plasma processing in theoretically. 1-dimension plasma model has build in the present study as depicted in the figure 3.4 by using COMSOL software. The plasma chamber

was modelled with the square shape with dimension 5 cm of the length. The thickness of cathode model was 0.2 cm and was placed inside the chamber. In the modelling process, argon gas was utilized and introducing inside the chamber. The chamber was grounded and the cathode was given negative voltage from – 350V to -450 V. The plasma parameter has measured in the z-axis from the cathode and the upper side of chamber.
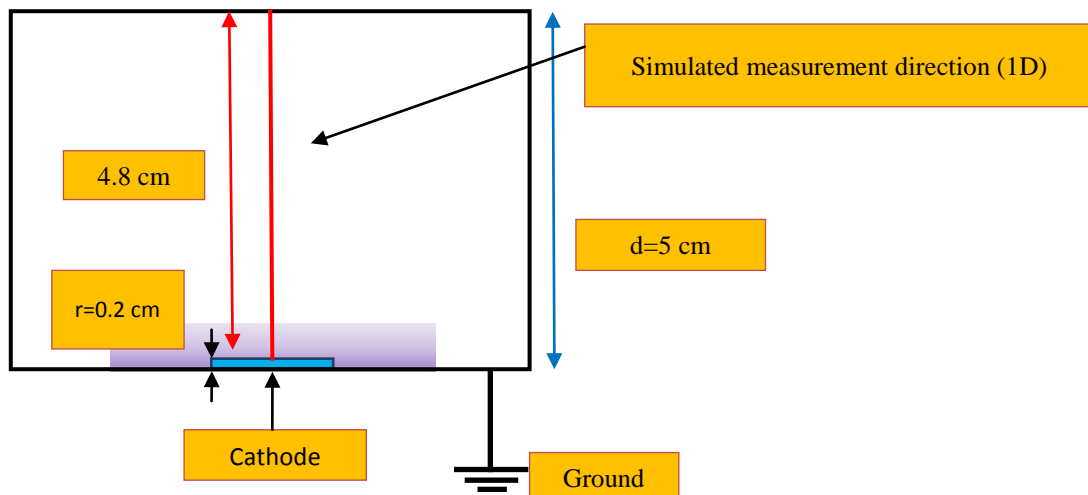
Figure 3.4 The schematic of 1 dimension plasma model

Plasma has generated in the chamber by applying DC-bias voltage in the cathode. The high electric field occur in the chamber and ionizing the neutral gas. The positive ion and electron are resulted from this process. Positive ions accelerate towards the cathode and electrons are repelled from cathode due to Coulomb Law. The ionization process produces more ions and electrons. The secondary electrons with sufficient energy have a role in new ionization process. The secondary ions move towards to the cathode and to sustaining the discharge. The electron density and mean electron energy are computed by using drift-diffusion equation. Convection of electron due to fluid motion is neglected. The equation for the number of electron density as depicted bellow [8]

$$\frac{\partial}{\partial t}(n_e) + \nabla.\left[-(\mu_e.\boldsymbol{E})n_e - \boldsymbol{D}_e.\nabla n_e\right] = R_e \qquad (1)$$

Where n_e is electron density (m^{-3}), μ_e denotes the electron mobility which is either a scalar or tensor (m^2/(V.s)), $\boldsymbol{E}$ is the electric field (V/m), $\boldsymbol{D}_e$ denotes the electron diffusivity which is either a scalar or tensor, and R_e is the electron rate expression (1/m^3.s). The migration of the electrons due to the electric field and diffusion of electrons from regions of high electron density to low electron density are represents in the second term on left side of equation 2 and the electron density rate are represent in the first term on left side of equation 1.The equation for electron energy density is:

$$\frac{\partial}{\partial t}(n_\varepsilon) + \nabla.\left[-(\mu_\varepsilon.\boldsymbol{E})n_\varepsilon - \boldsymbol{D}_\varepsilon.\nabla n_\varepsilon\right] + \boldsymbol{E}.\left[-(\mu_e.\boldsymbol{E})n_e - \boldsymbol{D}_e.\nabla n_e\right] = R_\varepsilon \qquad (2)$$

Where n_ε is electron energy density (V.m^{-3}), μ_ε denotes the electron energy mobility (m^2/(V.s)), $\boldsymbol{E}$ is the electric field (V/m), $\boldsymbol{D}_\varepsilon$ denotes the electron energy diffusivity (m^2/s, and R_e is the energy loss/gain due to inelastic collisions (V/m^3.s). The migration of the electrons due to the electric field and diffusion of electrons from regions of high electron density to low electron density are represents in the second term on left side of equation 2 and the electron density rate are represent in the first term on left side of equation 1. This equation for electron energy density is solved in conjunction with equation 2. Remember that subscribe ε is refers to electron energy. The heating of the electrons due to an external electric field are represents on the left side equation third term. For a Maxwellian electrons energy distribution function, the following relationships hold:

$$\boldsymbol{D}_e = \mu_e T_e, \mu_\varepsilon = \left(\frac{5}{3}\right)\mu_e, \boldsymbol{D}_\varepsilon = \mu_\varepsilon T_e \qquad (3)$$

Here T_e is electron temperature correlates with electron energy. The electron temperature correspondent with mean electron energy with equation:

$$\bar{\varepsilon} = \frac{n_\varepsilon}{n_e}, \text{ and} \tag{4}$$

$$T_e = \left(\frac{2}{3}\right)\bar{\varepsilon}$$

3.4 DISCUSSION

The result has achieved by setting the gas temperature at 400K, DC-bias -400V, and gas pressure 70 Pa. The plasma parameters have measured in the area between cathode and top of chamber. The plasma parameter distribution from this modelling is depicted in the figure 3.5.
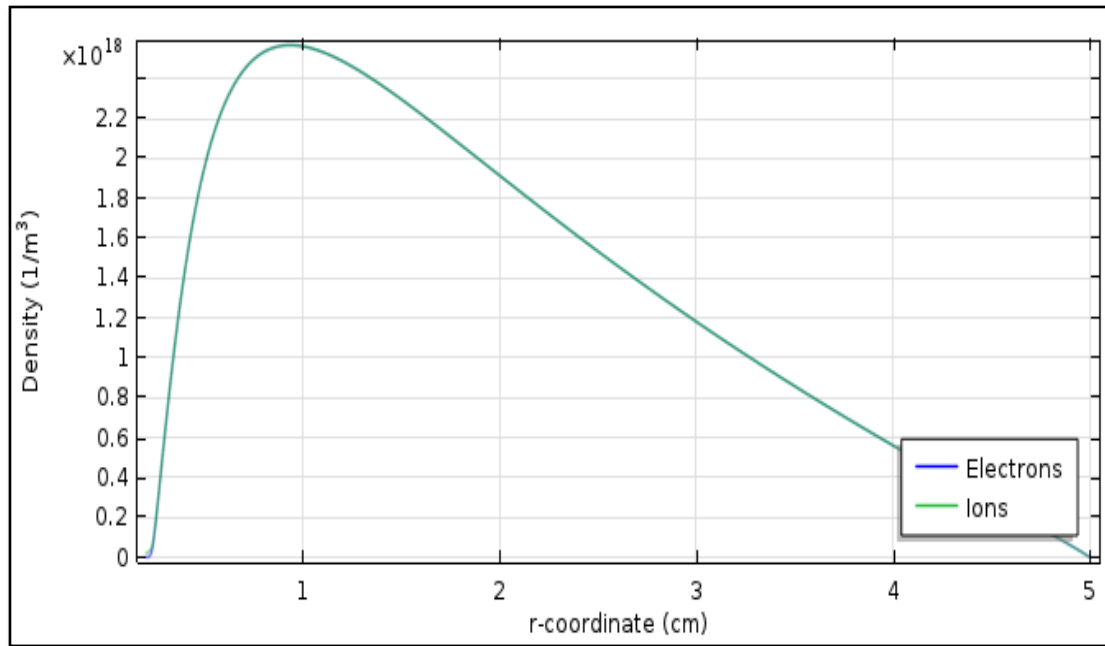
Figure 3.5 The electron and ion density distribution at t = 0.1s

The modelling result indicates the ion and electron density have the same quantity in the chamber. The electron and ion density distribute from the cathode toward to the wall. The highest values of ion and electron density are resulted in the range 1 cm and near the cathode area. It is caused by high ionization process occurs in the cathode area. High supply of DC-bias voltage produces high quantity of electron for ionization, as e result much more

secondary electrons are produced in this area. The secondary electrons with sufficient energy collide with neutral atoms and enhance the ionization result. Both of electron and ion density have high value in the cathode area. In the range 2 to 5 cm show the decreasing trend from ion and electron density. It is caused by the electron and ions are repelled towards to the wall. The highest value of plasma density reach to 2.6 x 10^{18} m^{-3} and the lowest value reach to 1.36 x 10^{15} m^{-3}. The quantity of electron and ion density in this modelling relative have the same value and prove that plasma is quasi-neutral ($n_e=n_i$).
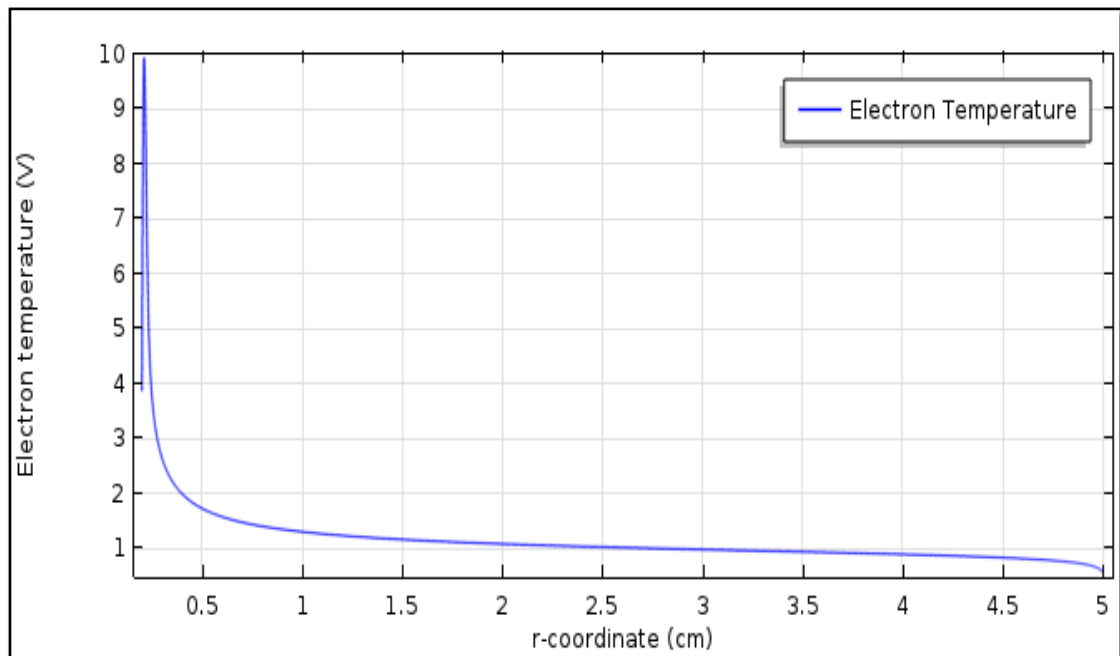
Figure 3.6 The electron temperature distribution at t=0.1s

The electron temperature distribution is depicted in the figure 3.6. The figure indicates the high electrons temperature occurs in the cathode area in the range 1 cm. It is caused by high different potential from cathode and the wall accelerates electrons. The electrons travel to the wall with high speed and as a result high electron temperature occur in this distance. The decreasing of electron temperature due to the electrons collides with the

argon gas in the chamber. The electron lost their energy due to the collision. It is expressed by low electron temperature in the distance more than 2 cm.

The pressure has varied in the range 30 to 150 Pa. The effect in the electron density has depicted in the figure 3.7.
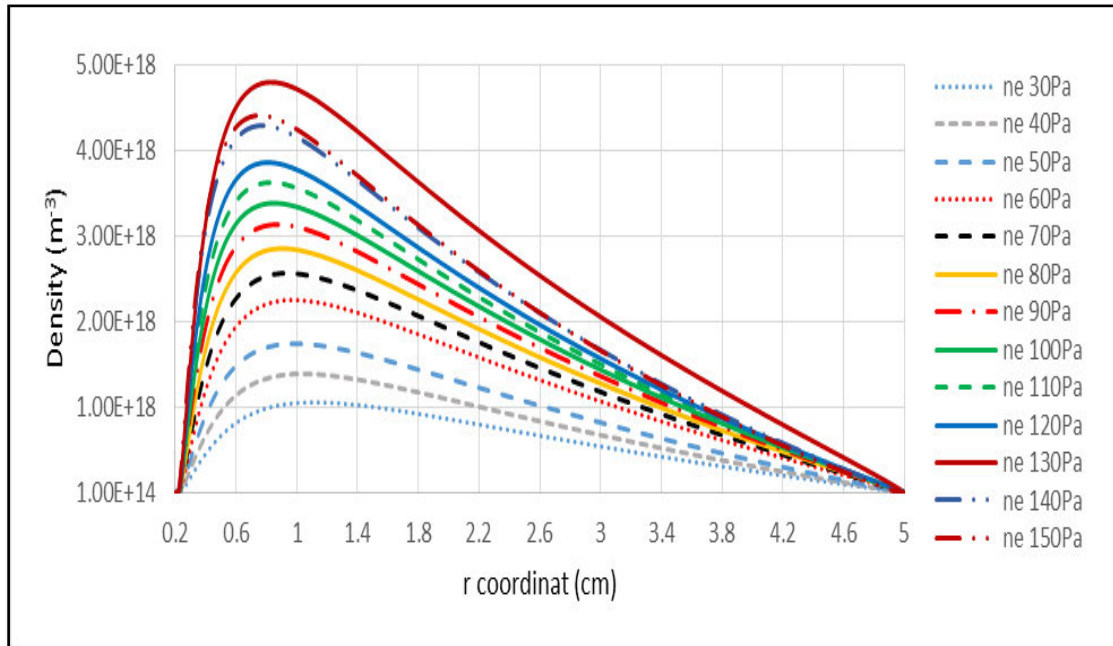
Figure 3.7 The effect of pressure in the electron density

The pressure has a significant effect in the electron density distribution. The figure 3.7 indicates the electron density increase by increasing the pressure. In the low pressure a few gas are introduced in the chamber. The electrons ionize the neutral gas and as a result ion and secondary electron are produced after ionization. By increasing the gas pressure, the quantities of neutral gas are increase inside the chamber. The collisions for ionization process are increased inside the chamber. As a result, high ion and electron density are produced in the high pressure.

The variation of DC-bias has also applied in the present study. The DC-bias voltage has varied in the range – 200 V to – 600 V. The variation result has depicted in the figure 3.8.
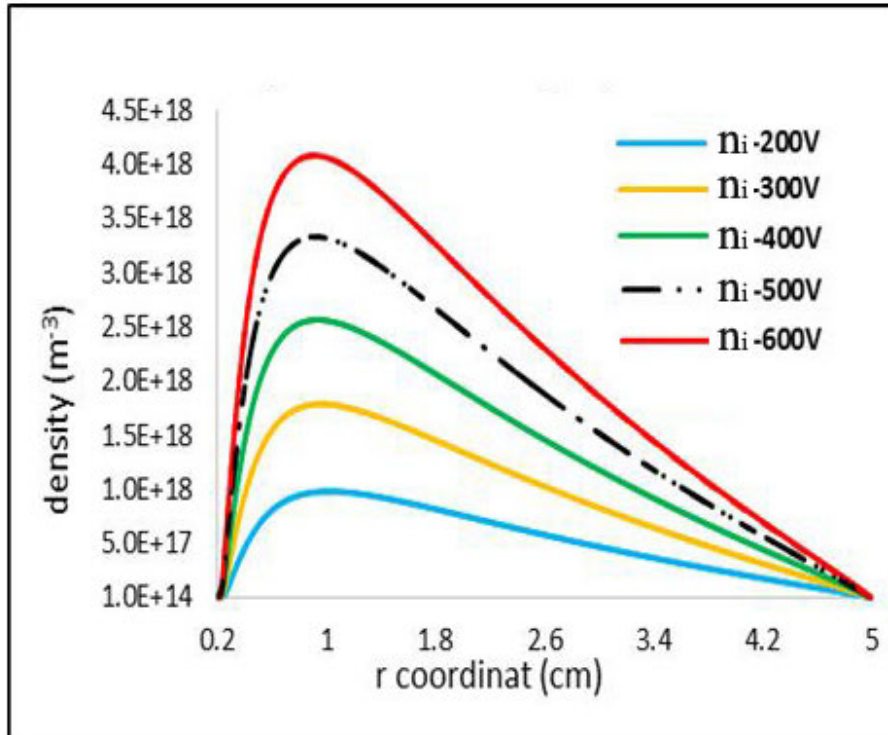
Figure 3.8 The effect of DC-bias voltage in the ion density

The DC-bias voltage has a role in supply the energy to the electrons for ionization processing. In the low DC-bias voltage, electrons get a low energy supply to make collision with neutral gas. By increasing the DC-bias, high supply energy is gotten to the electrons. As a result, electrons have capability collide with neutral gas more than one time. In other hand, the secondary electrons still have high energy to make the next collision with neutral atoms. The percentage of ionization process enhances many time and result in high ions density. The distribution result indicates the high concentration of ion density in the area bellow 1.8 cm. It is caused by this area are near with cathode and the cathode supply DC-bias voltage. The electrons are supplied with high energy and the ionization process occurs many times in this region. In the area far from cathode, the electrons energy are lower than near the cathode and reduce the ionization process. As a result, the ion densities in

this area become smaller than near cathode. The same trend of the ion distribution has done by Aflori et al [9], the ions density increase with increasing the power. It is means, power and DC-bias voltage supply energy to electron to enhance the ionization process inside the chamber.

3.5 SUMMARY

The theoretical and modelling of hollow cathode plasma system have done in the present study. The hollow cathode plasma produces high electron and ion density inside hollow cathode. It is caused by high probability of ionization process are taken place inside the hollow cathode plasma. High probabilities of ionizations are affected by high electric field in the hollow cathode plasma system. The high electric field cover the hollow tube and the free electrons inside the hollow tube are difficult to leave the hollow tube. The free electrons are repelled from each side due to the same charge and as a result free electrons oscillate and collide with neutral gas. The result from this collision is increase the ionization and produce high ion density inside the hollow tube. The electric field distribution modelling exhibit by using hollow cathode produce strong electric field in the hollow tube area and also from the theoretical explain the electrons in the metal tube are affected by temperature and electric field in the system.

The plasma modelling has build in the one dimension by using Comsol software. The voltage and pressure variation have done in the present study. The pressure has significant effect in the plasma density. By increasing pressure, the population of neutral gas are increase inside the chamber. As a result ionization process occurs many times. High ion and electron density are resulted from this process. The DC-bias voltage has the same effect to the ion

and electron density inside the chamber. Low DC-bias voltage supplies a little energy to electron ionizing the neutral gas. As a result, low electron and ion density are produced in this condition. Conversely, high DC-bias voltage makes electrons have more energy to ionize the neutral gas. The collision occurs in many times due to electron and secondary electrons have sufficient energy to make ionization process. As a result, high ion and electron density are produced in this condition.

REFERENCES

[1] N. Baguer, A. Bogaerts, R. Gijbels, Hybrid model for a cylindrical hollow cathode glow discharge and comparison with experiments, Spectrochimica acta part B, 57, (2002), 311-326.

[2] L. Bardos, Radio frequency hollow cathodes for the plasma processing technology, Surface and coatings technology, 86-87, (1996), 648-656.

[3] C.M.Ferreira andJ. L. Delcroix, Theory of the hollow cathode arc, J. Appl. Physics, 49, (1978), 2380-2395.

[4] A. Bogaerts, E. Neyts, et al, Gas discharge plasma and their applications,, Spectrochimica acta part b, 57, (2002), 609-658.

[5] D. M. Goebel, K. K. Jameson, et al., Hollow cathode theory and experiment. I. Plasma characterization using fast miniature scanning probes, Journal of applied physics, 98, (2005), 113302.

[6] R. V. Kennedy, Theory of the arc hollow cathode, Journal of physics D: applied physics, 34, (2001), 787-793.

[7] D. Mihailova, M. Grozeva, et al., Theoretical and experimental studies of the plasma processes in hollow cathode discharge lasers, 28th ICPIG, 98, (2007), 533-536.

[8] G. J. M Hagelaar and L. C. Pitchford, Solving the Boltzmann equation to obtain electron transport coefficients and rate coefficients for fluid models, Plasma sources sci. Technol, 14, (2005), 722-733.

[9] M. Aflori, et al., Estimating electrons and ions energies in an RF capacitively-coupled argon discharge, Rom. Journ. Phys, 51, (2006). 225-230.

4. HIGH DENSIFICATION FOR ETCHING AND ASHING

4.1 INTRODUCTION

Micro-texturing and micro-patterning has applied in many sector, such as electronic, industrial and manufacturing. The present electronic device has utilized micro-texture technology, especially in the sensor [1]. There are many ways to build micro-texture and micro pattern; e.g. by using chemical solution, lithography, laser, or dry process [2]. In the dry process, plasma etching is one kind of effective technique to build micro-texturing and micro-patterning on the specimen. Reactive ion etching is the key technology to remove coating material from the specimen [3]. DLC (Diamond like carbon) and CVD diamond coating are kind of coating material used in fabrication technology [4].

In the dry etching and ashing process, a plasma density is an important factor for influence the etching and ashing result. The low plasma density gives weak bombardment during the etching and ashing process. Otherwise, high plasma density gives strong bombardment in the coating material, even for high coating material. Hollow cathode plasma is purposed to generate high plasma density and strong bombardment for hard coating material [5]. High concentrations of plasma density are effective to remove hard coating material. The characterization of hollow cathode plasma is required in this study to achieve the optimization condition and controlling during plasma etching and ashing process. Langmuir probe and Optical emission spectroscopy have utilized to make quantitative plasma diagnosis in this study [6]. Furthermore, quantitative plasma diagnosis is accompanied by theoretical understanding of hollow cathode plasma in this characterization.

4.2 QUANTITAVIE PLASMA DIAGNOSIS

4.2. 1 Quantitative plasma diagnosis in the hollow cathode plasma by using Langmuir probe

Langmuir probe and Optical emission spectroscopy have utilized to make quantitative plasma diagnosis in the hollow cathode plasma systems. Ion density, electron density, electron temperature have measured by using Langmuir probe. Atomic peak, molecule peak, radical and activated molecule peaks have measured by using Optical emission spectroscopy. Commonly, plasma density has a range from $10^{15} - 10^{16}$ m^{-3} from each plasma system [7, -9]. Low concentration of plasma density has difficulty for an application, such as difficult to remove hard coating material. Hollow cathode plasma system has employed to solve this problem by increasing plasma density. Theoretically reason has proven hollow cathode plasma produce high concentration of ion and electron density as mention before [10].

The quantitative plasma diagnosis in the hollow cathode plasma has done by varying RF-voltage, DC-bias, and pressure respectively. First, Ion density and electron density have varied with changing of RF-voltage value, while pressure and DC-bias are fixed in 70 Pa and -600V, respectively. The results are depicted in the figure 4.1.
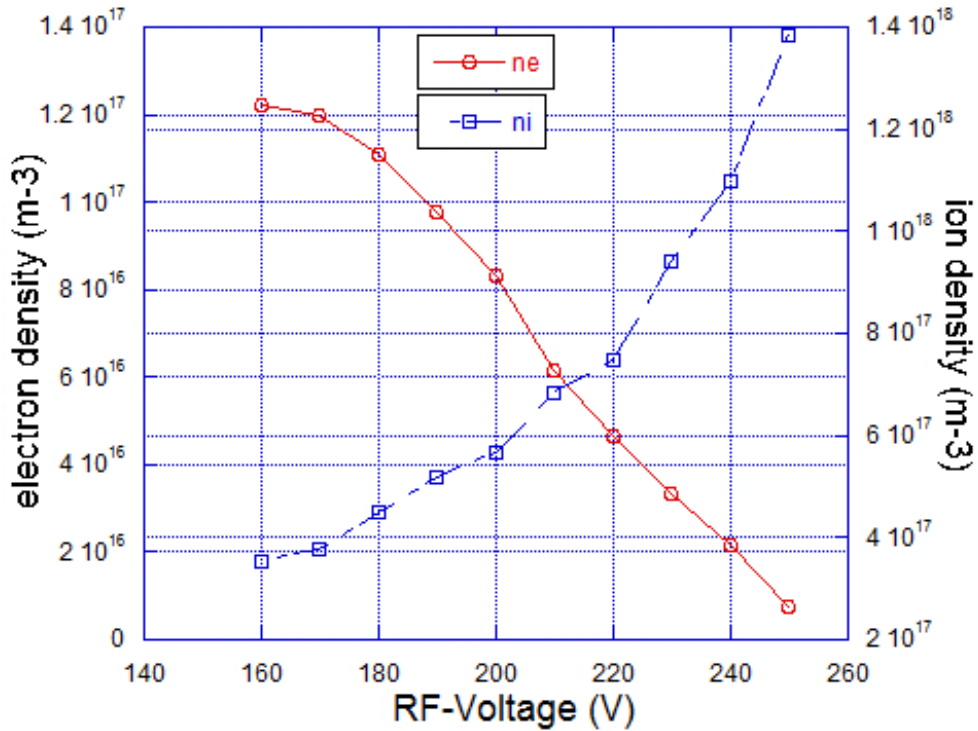
Figure 4.1 Electron (n_e) and ion density (n_i) from RF-voltage variation of hollow cathode plasma

The RF-voltage has varied from 160 V to 250 V in this plasma system. In the low value of RF-voltage (160 V), the electron density reach to 1.2×10^{17} m^{-3} and ion density reach to 2×10^{16} m^{-3}. In the maximum value of RF-voltage (250V), the electron density reaches to 7.37×10^{15} m^{-3} and ion density 1.38×10^{18} m^{-3}. By increasing the RF-voltage, the ion density increases while the electron density decreases. This trade-off indicates that high ionization process takes place inside the hollow cathode plasma.

In second, the quantitative plasma diagnosis has done by varying pressure while DC-bias and RF-voltage were fixed in -450 V and 150 V, respectively. The pressure was varied from 60 Pa to 110 Pa in this plasma system. The electron and ion density from this measurement were depicted in the figure 4.2.
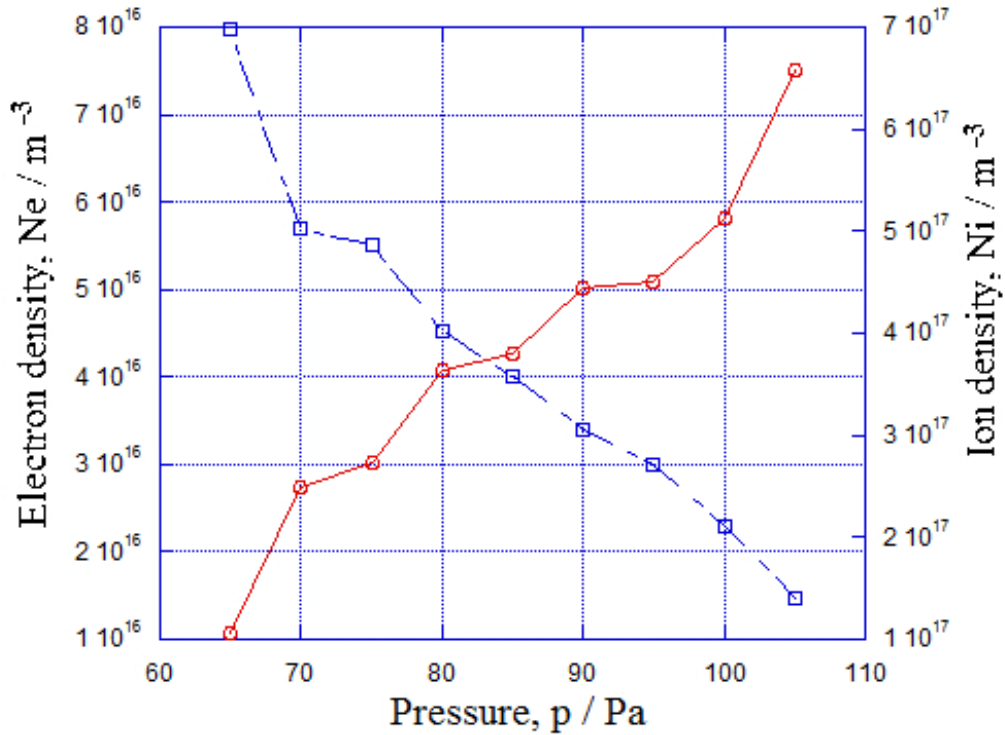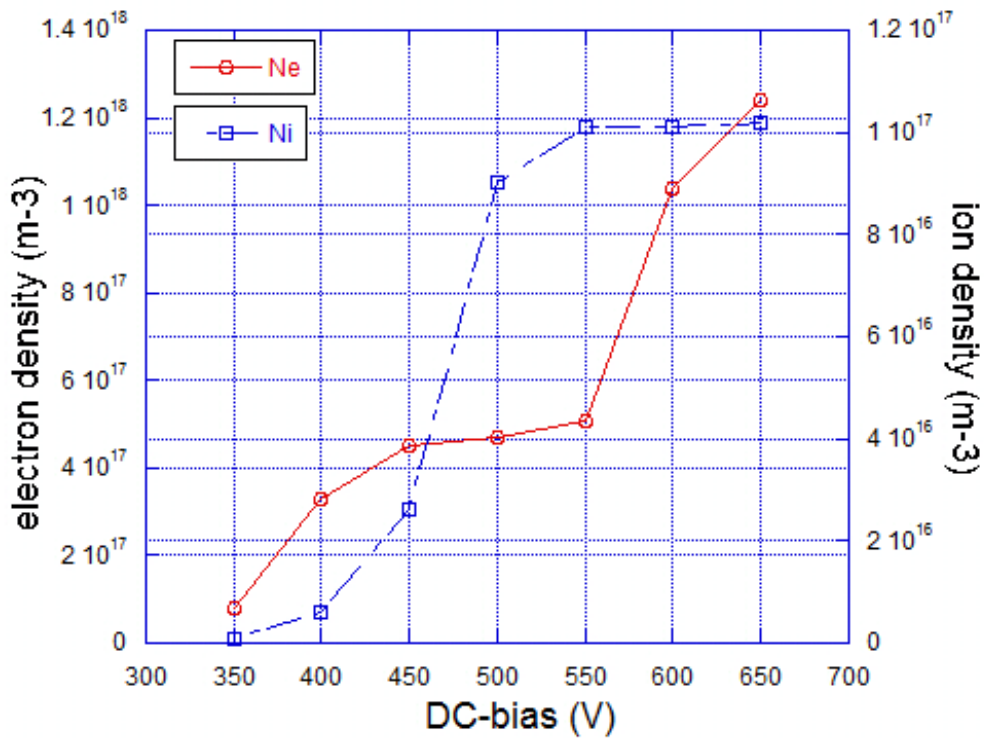
Figure 4.2 Electron (n$_e$) and ion density (n$_i$) from pressure variation of hollow cathode plasma

In low pressure (65 Pa) electron density reach to 1.0×10^{16} m^{-3} and ion density reach to 7×10^{17} m^{-3}. Otherwise, in the high pressure (105Pa) the electron density increase and reach to 7.5×10^{16} m^{-3} and ion density decrease to 1.5×10^{17} m^{-3}. This trend indicates ion density decrease by increasing the pressure and accompany by increasing of electron density. The pressure has role in control population inside the hollow cathode plasma.

In third, DC-bias was varied from – 350 V to -650 V. Pressure and RF were fixed at 75 Pa and 250 V, respectively. As shown in figure 4.3, both electron and ion density increase with increasing the DC-bias. At the lower DC-bias, $n_e = 8.67 \times 10^{14}$ m^{-3} and $n_i = 8.09 \times 10^{16}$ m^{-3}. By increasing the DC-bias, both n_e and n_i increase up to 1.02×10^{17} m^{-3} and 1.24×10^{18} m^{-3},

respectively. This implies that DC-bias enhances the ionization process in the
hollow cathode plasma.

**Figure 4.3 Electron (n_e) and ion density (n_i) from DC-bias variation of hollow
cathode plasma**

4. 2. 2 Spectrum analyses in the hollow cathode plasma by using optical emission spectroscopy (OES)

Optical emission spectroscopy has utilized to describe emission light
spectrum of hollow cathode oxygen plasma. The hollow cathode oxygen
plasma spectrum was shown in the figure 4.4. The wavelength of hollow
cathode oxygen plasma has measured from 300 to 900 nm. The spectrums
consist of oxygen atomic peaks, molecule peaks, and activated molecule
peaks. The plasma parameter was fixed in pressure 60 Pa, DC bias -450 V,
and RF-voltage 150V, respectively.
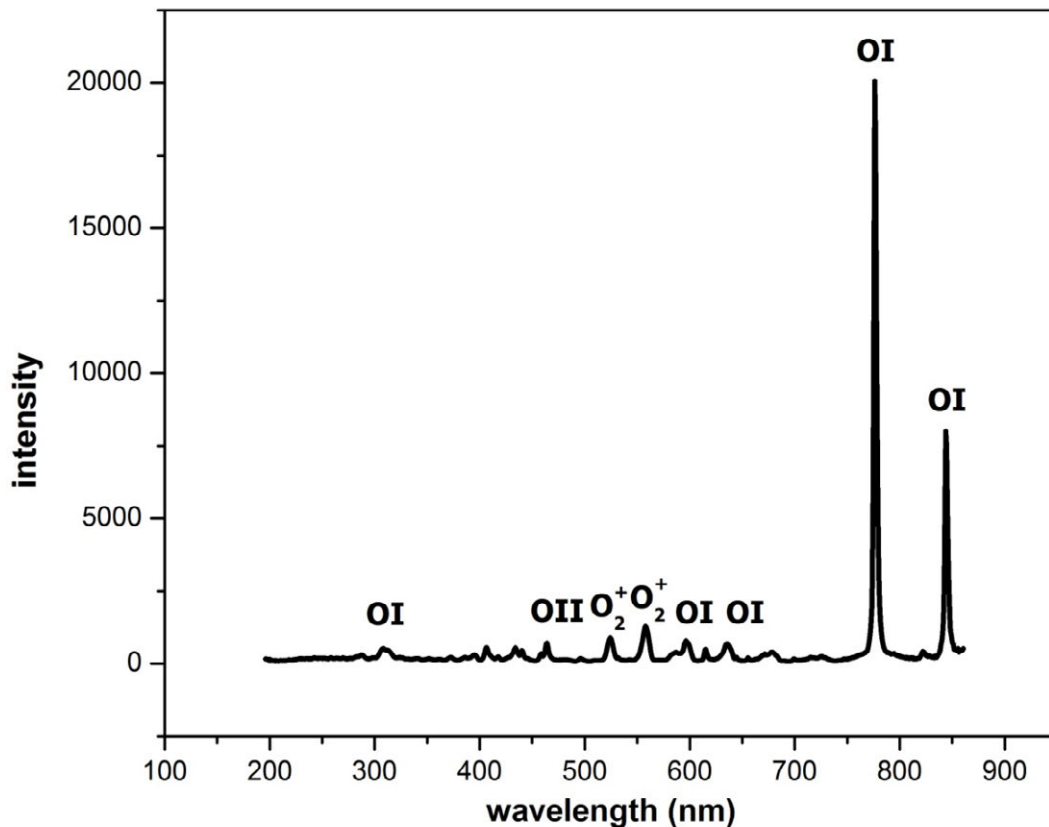
Figure 4.4 Emission light of hollow cathode oxygen plasma spectrum

Two strong peaks were observed at 776.34 nm and 843.778 nm. The former was identified as an atomic oxygen (OI) and the latter corresponds to the oxygen atom transition O ($3p^5P \rightarrow 3s^5S$) and O ($3p^3P \rightarrow 3s^3S$) respectively. Other peaks in a range from 400 nm to 749 nm have weak intensities. That is, singly ionized oxygen (OII) at 433.988 nm, atomic oxygen (OI) at 615.164 nm and 635.23 nm, molecular species (O_2^*) at 524.124 nm and (O_2^+) at 557.775 nm are never dominant in the hollow cathode plasma. However, it has higher intensities for almost all species than the conventional oxygen plasma. For an example, the atomic oxygen peak (OI) at 777nm was reported to have peak intensity of 16000 counts. In this hollow cathode plasma, atomic oxygen peak at 776.34 nm has peak intensity by 20000. That is, hollow cathode oxygen plasma has more activated species than conventional oxygen plasma.

4. 2. 3 Comparison electron and ion density in the hollow cathode plasma and without hollow cathode plasma by using Langmuir probe

Langmuir probe has utilized to measure plasma density inside hollow cathode plasma and without hollow cathode plasma. The variation of pressure was chosen in this measurement due to pressure has contribute to determine population inside the chamber. Pressure was varied from 65 to 105 Pa while DC-bias and RF-voltage were fixed in -450 V and 150 V, respectively. First, langmuir probe has utilized to measure electron and ion density in the plasma system without using hollow cathode. The measurement result exhibit in the figure 4.5.
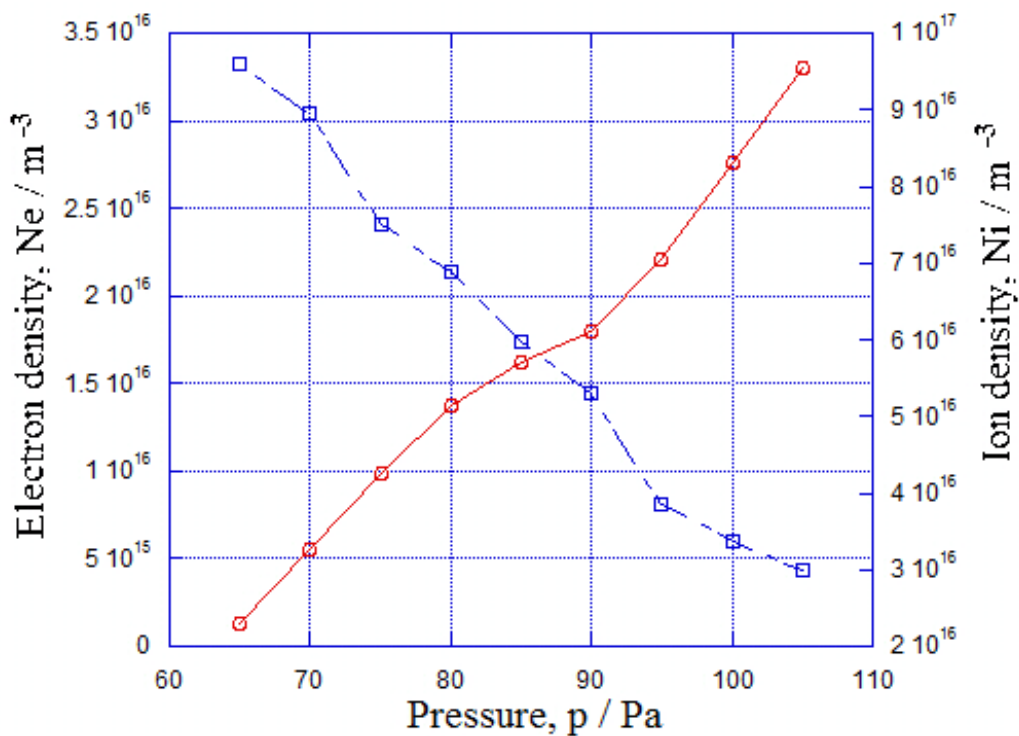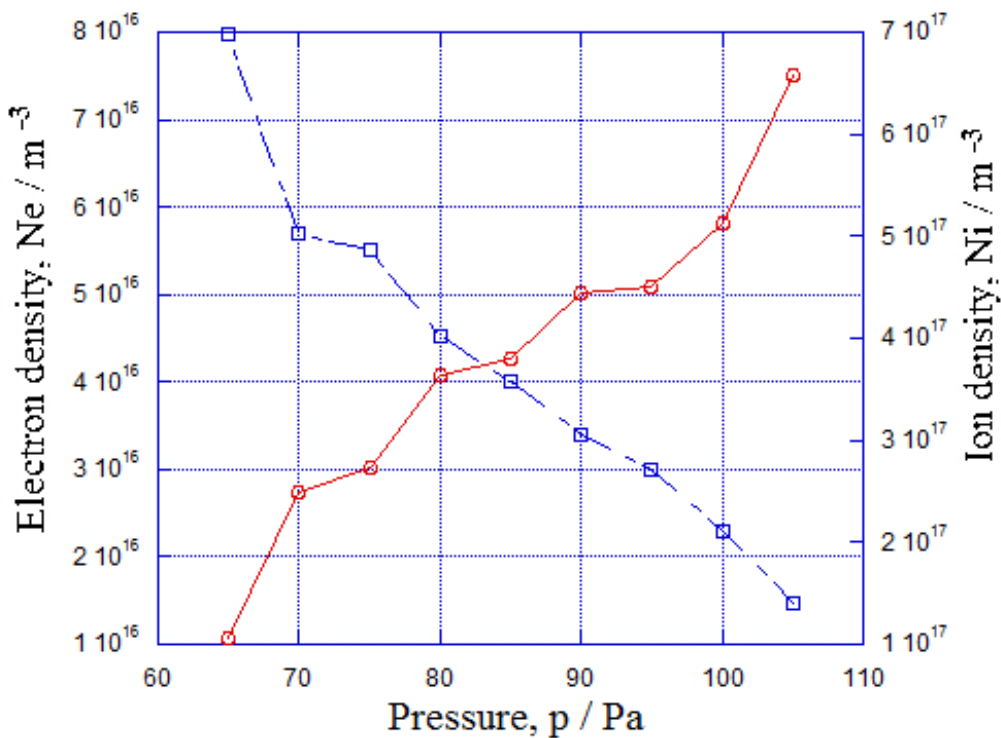

Figure 4.5 Electron (n$_e$) and ion density (n$_i$) with pressure variation in the plasma system

The measurement result exhibit in the low pressure ion density has high value and reaches to 1 x 10^{17} m^{-3}. In the same pressure, electron density show low

value and reach to 1×10^{15} m^{-3}. By increasing the pressure, ion densities are decrease and reach to 3×10^{16} m^{-3}. However, electron densities are increase and reach to 3.5×10^{16} m^{-3}. In the low pressure, the percentage of ionization is increase due to the collision between electron and oxygen molecule. However, in the high pressure the percentage of ionization are decrease due to electron collide each other inside the chamber.

In second, hollow cathode has utilized to measure electron and ion density with pressure variation. The plasma system was fixed in the same condition with the previous measurement. The measurement result was depicted in the figure 4.6.

Figure 4.6 Electron (n_e) and ion density (n_i) with pressure variation in the hollow cathode plasma system

The figure indicates ion density has high value in the low pressure, but at the same time was accompanied by low value of electron density. In the high pressure, much more electron stays inside hollow cathode and gives effect in

the low percentage of ionization process. The high value of electron density was accompanied by low value of ion density. Both of the measurement results have compared to get the differences from each system as depicted in the figure 4.7.
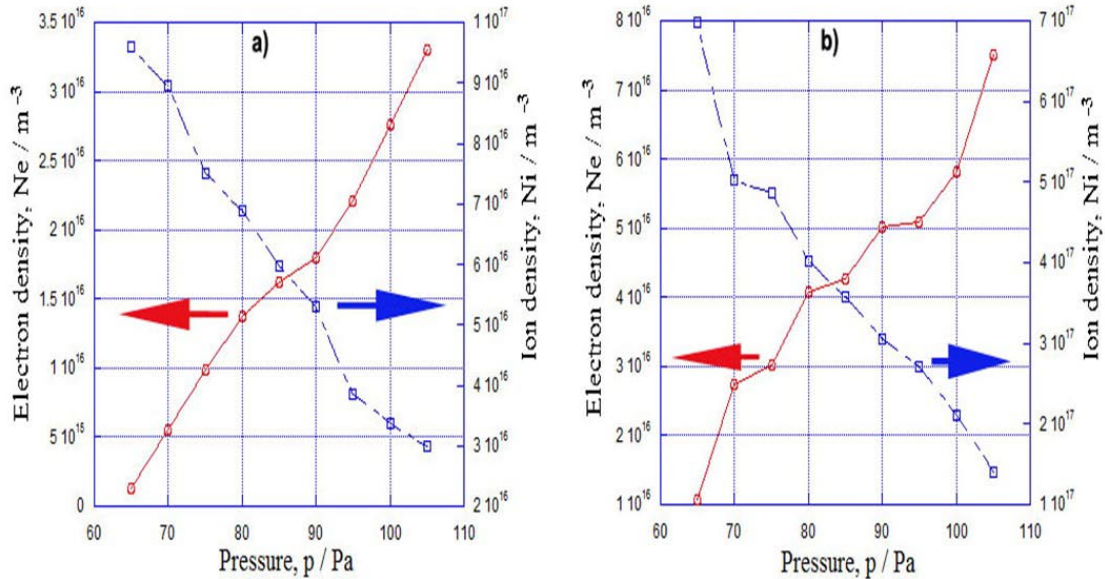
Figure 4.7 Comparison on the variation of electron (n_e) and ion density (n_i) with the pressure variation in the plasma a) without hollow cathode plasma and b) with hollow cathode plasma

The figure 4.8 represents the same trend from without and with using hollow cathode plasma. Both of the systems produce high ion density in the low pressure. It is means low pressure is effective to make plasma processing and application. The differences from two systems are in the value from ion and electron density. In the low pressure without using hollow cathode, the ion density reaches to 1 x 10^{17} m^{-3}. However, in the hollow cathode plasma system reach to 7 x 10^{17} m^{-3}. It is mean by using hollow cathode plasma; the ion density is seven times higher than without using hollow cathode. It is caused by in the hollow cathode plasma system provide electric field barrier which make electron difficult to leave the hollow tube. The ionization has

taken placed and concentrated inside the hollow tube. The low pressures provide a few electrons and a few gas molecules inside the hollow tube. Due to electric field in the hollow tube the percentage of ionization is increase and the electron difficult to leave the hollow tube.

4. 2. 4 Comparison spectrums in the hollow cathode plasma and without hollow cathode plasma by using optical emission spectroscopy (OES)

The optical emission spectroscopy has utilized to measure plasma spectrum from hollow cathode and without hollow cathode plasma. The plasma parameters were fixed with same condition with the previous measurement experiment. Figure 4.8 compares the emissive light spectra from plasma with and without the hollow cathode.
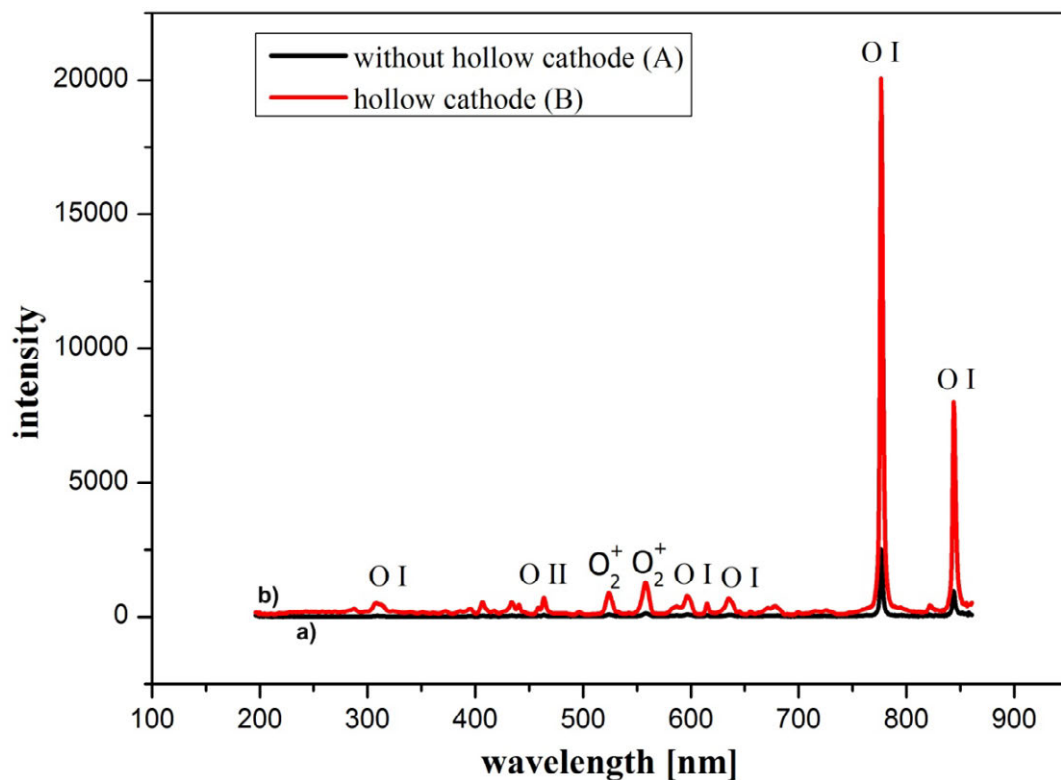

Figure 4.8 The optical emission spectroscopy comparison between a) without hollow cathode plasma, b) by using hollow cathode plasma

The oxygen ion { O^+, O^{2+}} or { OII, OIII, OIV} and activated oxygen molecules O_2^+ are seen in the both spectrum. Two strong peaks have identified with different intensity value from both systems. The peak intensity OI at 776.34 nm without the hollow cathode is only 2.5 x 10^3 counts; while it reaches to around 2 x 10^4 counts with use of hollow cathode. The high intensity indicates the oxygen atom is a main species in the generated oxygen plasma and its population is enhanced by using hollow cathode.

4.3 DISCUSSION

Hollow cathode plasma is a new method in the plasma system to generate high concentration of plasma density in the certain area. Hollow cathode plasma utilizes a hollow tube and placed inside the chamber. Plasma has generated inside the hollow tube. High concentration plasma density has concentrated inside the hollow tube. The quantitative plasma diagnosis has done by using Langmuir probe and Optical emission spectroscopy to measure plasma density inside the hollow tube. The result indicates by using hollow cathode system, plasma density reach to 10^{17} to 10^{18} m^{-3}. The plasma density value from this system is higher compare with the other system.

Theoretically, gas was introduced inside the chamber. The different pressure has occurred inside the chamber due to the hollow tube has different diameter in dimension. By this effect, high pressure flow inside the hollow tube. RF and DC generation provide electric field barrier in the hollow tube area. The electrons are emitted from the dipole electrode and enter to hollow cathode. The electrons collide with the gas molecule and ionization process has taken placed inside the hollow tube. The confinements of electric field in the hollow cathode area make ion and electron difficult to leave hollow

cathode. The DC bias voltage value has a role in determine electric field force. This condition make electron difficult to leave the hollow tube and freely travel inside the hollow cathode area. In the position inside the inlet of the hollow cathode, the percentage of ionization is increased due to free electron ionize the gas molecule flow inside the hollow tube. The ion density concentrates in the central and near outlet of the hollow cathode.
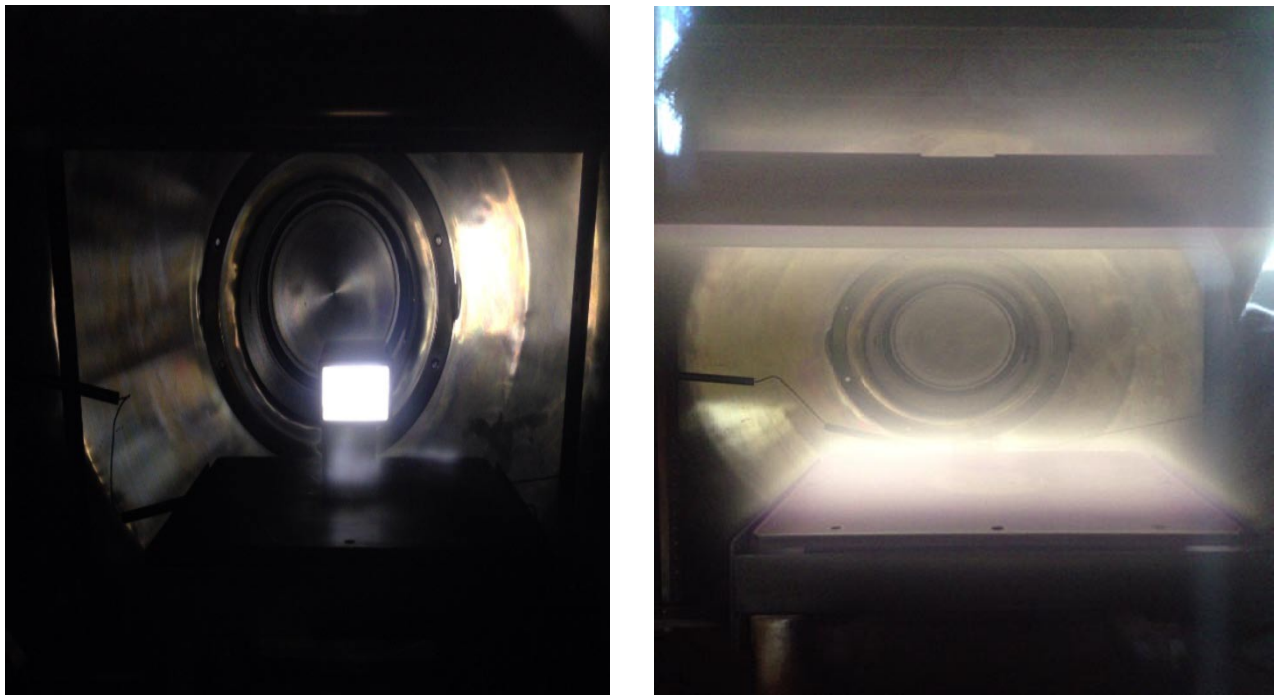
Figure 4.9 The glow discharge comparison by using a) hollow cathode plasma, b) without hollow cathode plasma

The figure 4.9 shows the different glow discharge from hollow cathode plasma and without hollow cathode plasma with the same condition. The strong bright light has shown in the plasma system by using hollow cathode and limited in the rectangular area. However, in the condition without hollow cathode the glow discharge show in all area of the chamber. Direct apply of DC bias to the hollow tube generate electric field barrier. The electrons movement are limited only inside the hollow tube. By this condition, the percentage of ionization process increase and as a result high ion density

produce inside the hollow tube. The strong bright light represents high movement of electron inside the hollow tube for ionization process. In other hand, large size area of the chamber make electron freely to travel everywhere. The ionisation process occurs almost in all area of the chamber. There is no confinement area to limit the movement of electron. As a result low ion and electron density compare with the hollow cathode system.

4.1 SUMMARY

Hollow cathode oxygen plasma has developed in the present study. The characterization of hollow cathode plasma has done by varying pressure, RF-voltage, and DC-bias voltage respectively. The optical emission spectroscopy (OES) and Langmuir probe have employed to measure plasma density and spectrum of hollow cathode plasma. The only oxygen gas without has utilized to generate plasma. The characterization result has compared with the measurement result in the plasma without using hollow cathode.

The RF voltage variation in the hollow cathode plasma has effect in the ion and electron density. By increasing RF-voltage, the ion density is increased and decreasing of electron density. RF-voltage has role in supply energy to the electron to make ionization process. High RF-voltage supplies high energy to electron for ionization process. As a result, increase the ion density inside the hollow tube. Pressure has also varied in the present study. The pressure has a role in determine the population inside the chamber. Low pressure supply a few gas inside the chamber, but increase the ionization process. In the low pressure, a few gases enhance the percentage of ionization process. The effective collisions occur in the low pressure and as a result increasing the ion density. However, in the high pressure supply much

more gas in the tube. The electron collide each other and decreasing the percentage of ionization. As a result, high electron density accompany with low ion density in this condition. DC-bias voltage variation has a result in increase ion and electron density. High DC-bias supplies high energy to make ionization process. The electrons have sufficient energy to make collision to the neutral gas many times and the secondary electrons still have high energy to make simultaneous collision for ionization process. The optical emission spectroscopy provides high intensity of oxygen plasma by using hollow cathode. High intensity of oxygen atomic peaks indicates high density of oxygen plasma inside the hollow tube. High plasma density is effective for bombardment to the sample surface.

The hollow cathode plasma characterization has compared with the plasma characterization without using hollow tube. The comparison result indicates hollow cathode plasma systems provide high ion and electron density in the order 10^{17} to 10^{18} m^{-3}. In the plasma system without hollow cathode provides ion and electron density in the order 10^{16} to 10^{17} m^{-3}. In the pressure variation, hollow cathode system has ion density 7 times higher compare with without using hollow cathode. The optical emission spectroscopy comparison result indicates hollow cathode plasma produce high intensity almost in all peaks compare with without using hollow cathode. High intensity provides strong bombardment during plasma processing. The glow discharges of hollow cathode and without hollow cathode provide different strong brightness of discharge. Hollow cathode plasma has strong and bright discharge in the hollow tube area and without hollow cathode the glow discharge are spread in the chamber area.

REFERENCES

[1] V. R. Mamillas and K. S. Chakradhar, Micro Machining for Micro electro mechanical system, procedia material science, (2014), 1170-1177.

[2] B. Schurink, J. W, Berenschot, Highly uniform sievinf structure by corner lithography and silicon wet etching, Microelectronic engineering, (2015), 12-18.

[3] T. Aizawa, E.Masaki, Y. Sugita, Oxygen plasma ashing of used DLC coating for reuse of milling and cutting tools, MAPT, (2013), 15-20

[4] M. Lessiak and Roland Haubner, Diamond coatings on hardmetal substrates with CVD coating as intermediate layers, Surface and coating technology, (2013), 119-123.

[5] J. Cho, J. Yang, High density large area hydrogen plasma by hollow cathode plasma array, Surface and coating technology, (2010), 1532-1535.

[6] E. E. Yunata,T. Aizawa, D.J. Djoko, Characterization of hollow cathode plasma for etching and ashing process, Proc. SEATUC UTM, (2013), 1-4.

[7] T. Panagopoulos and D. J. Economou, Plasma sheath modeland ion energy distribution for all radio frequencies, Jornal applied physics, (1999), 3435-3443.

[8] M. B. Hopkins. Langmuir probe measurement in the gaseous electronics conference RF reference cell, Journal of research of the national institute of standars and technology, (1995), 415-425.

[9] X. Zhu, W. Chen, Electron density and ion energy dependence on driving frequency in capacitive coupled atgon plasma, J. Physics, (2007), 7019-7023.

[10] E. E. Yunata and T. Aizawa, Micro-texturing into DLC/diamond coated molds and dies via high density oxygen plasma etching, Manufacturing review, (2015), 13.

5. PLASMA ETCHING OF DIAMOND COATING

5.1 INTRODUCTION

Micro-electromechanical system (MEMS) has a characteristic length of less than 1 mm but more than 100nm; it is composed of electrical and mechanical components. Nano-electromechanical system (NEMS) refers to nanoscopic devices that have characteristic length of less than 100 nm with electrical and mechanical components [1]. MEMS/NEMS have been utilized in variety of engineering areas; e.g. biomedical, environmental, transportation, manufacturing, robotic, and computing system [2]. Basically, MEMS has been used for micro electrode, pure sensor, or lab-on-chip. Most of MEMS fabrication techniques are mainly based on the silicon (Si) because of the available surface machining technology [3]. However, silicon has relatively poor mechanical properties; e.g. low Young's modulus of 130 GPa and low tribological properties. Diamond coating by CVD (Chemical Vapour Deposition) has grown as a next generation to replace silicon since the diamond has unique properties such as high hardness, low friction coefficient and available to work in high temperature [4-8].

A promising sensor and micro device require for fine micro-texturing on the diamond coating. Micro-EDM, laser, wet-etching, and lithography have been utilized to make micro-texturing onto the diamond films; in each method, its disadvantage more than its advantage [9-10]. The RF-DC oxygen plasma etching system has developed for micro-texturing onto diamond coating material [11]. The hollow cathode has placed inside the chamber of RF-DC oxygen plasma etching to generate high plasma density. The CVD diamond coated WC (Co) with metal masks was prepared to make micro-patterning by

using RF-DC oxygen plasma etching. The hollow cathode oxygen plasma etching has high etching rate 10 μm/ H for diamond films [12]. With this advantage, hollow cathode oxygen plasma etching is expected to make fine and fast rate etching into CVD diamond coating. Optical microscopy, SEM, surface profilometer and Raman spectroscopy have utilized to evaluate the surface profile and micro-texturing of CVD diamond coating before and after etching process.

5.2 OPTICAL MICROSCOPY ANALYSIS

The optical microscopy was utilized to measure surface profile from CVD diamond coated specimen after plasma etching. The magnification of the microscope was set to get the clear image in the computer display. Figure 5.1 shows the surface profile of CVD diamond coated WC (Co) specimen after plasma etching process.
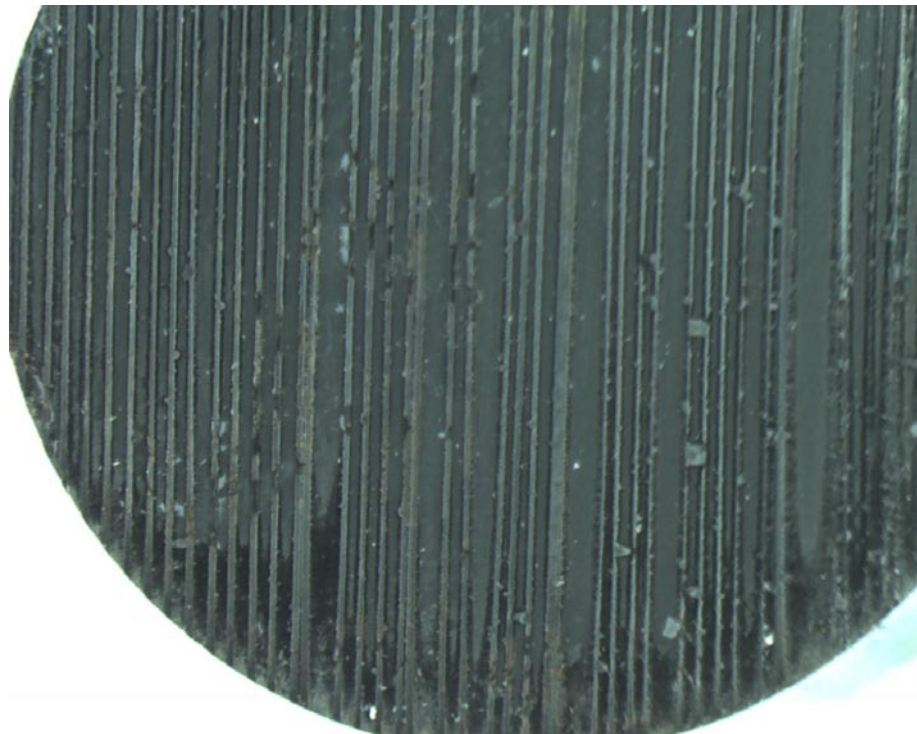
Figure 5.1 Surface profile of CVD diamond coated WC (Co) specimen after etching process

The magnification 1x from the optical microscopy was chosen to get the full image of the surface after etching process. The figure 5.1 exhibits the view from the top side of the specimen. The result indicates micro-texturing has imprinted in the all surface of diamond coated specimen. From this side, the line pattern has imprinted successfully in the centre and left side of the sample and indicates by clear image result. In the down side of the sample, the black view represent, there was a diamond in the un-mask area. It caused by the metal mask was not perfectly adhering in the specimen surface. This condition makes the ion bombardment direction not perpendicular to the diamond coating. The ion bombardment attack to the metal mask an repeal to another direction. As a result a little diamond coating stays in the un-mask area.
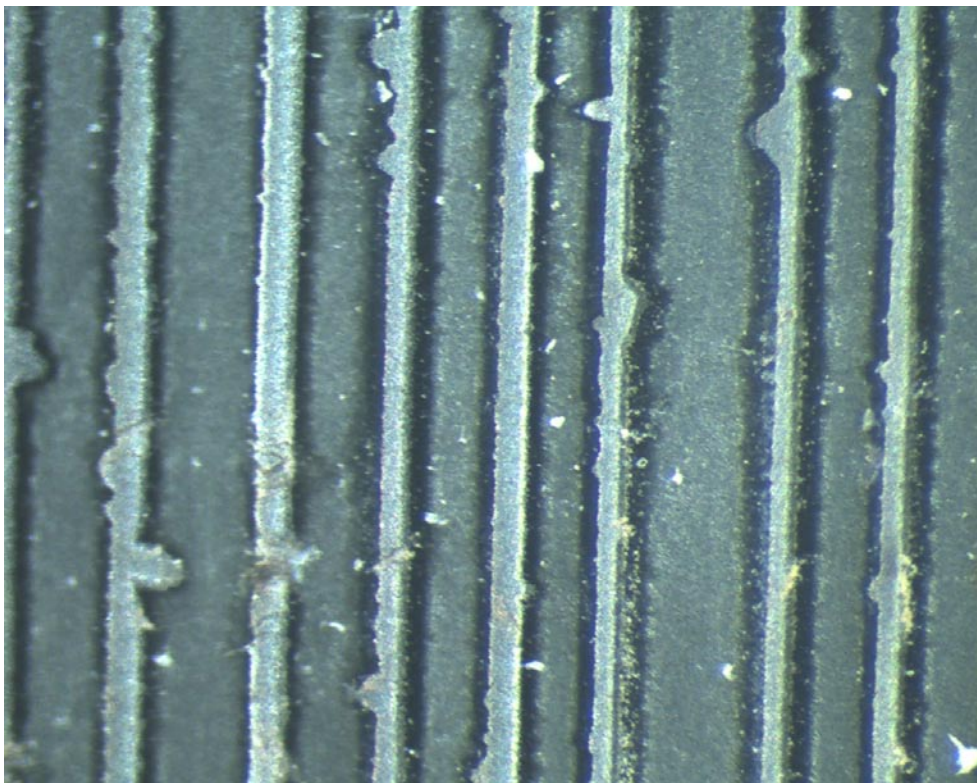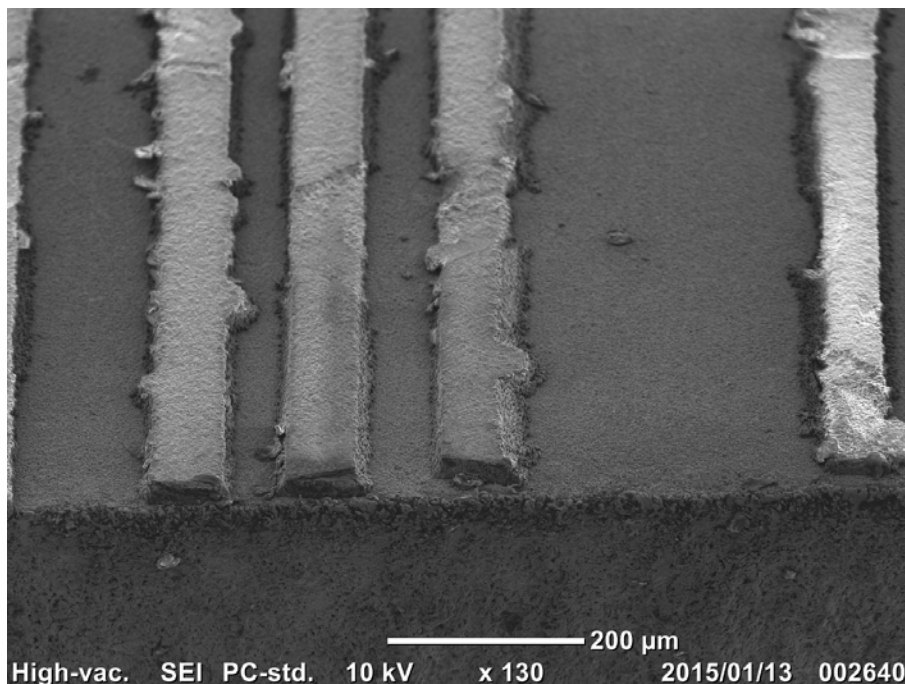

Figure 5.2 Surface profile of CVD diamond coated WC (Co) specimen

after etching process in the centre area

The magnification of the optical microscope was changed to 5 x and concentrated to the centre area of the specimen. Figure 5.2 represent the centre area of specimen after etching process. The clear image has showed from the figure 5.2. The line pattern has formed in the centre area of the specimen. The homogeneous plasma etching has done in the un-mask area. The flat surface has showed in all area of CVD diamond coated specimen. The un-straight pattern has formed in several line of the specimen surface. It caused by imperfect shape of metal mask surface. The ion bombardment attack in unmask area and follow the metal mask shape. The straight line shapes of metal mask provide straight line of micro-texturing.

5.3 SEM ANALYSIS

The scanning electron microscope (SEM) was utilized to check surface profile of CVD diamond coated specimen in detail. Figure 5.3 represent SEM image from the specimen after plasma etching process.

Figure 5.3 Surface profile of CVD diamond coated WC (Co) specimen

after etching process by using SEM

The SEM image result indicates in clearly micro-texturing has formed in all CVD diamond coated specimen area. The flat surface area has formed in the un-mask area. It is mean diamond coating has removed from the surface specimen during etching process. The line pattern has formed in several lines as depicted in the figure. It indicates the metal mask is effective to protect diamond coating from ion bombardment in the mask area. The magnification of SEM was improved to check micro-texture more detail in limited area as depicted in the figure 5.4.
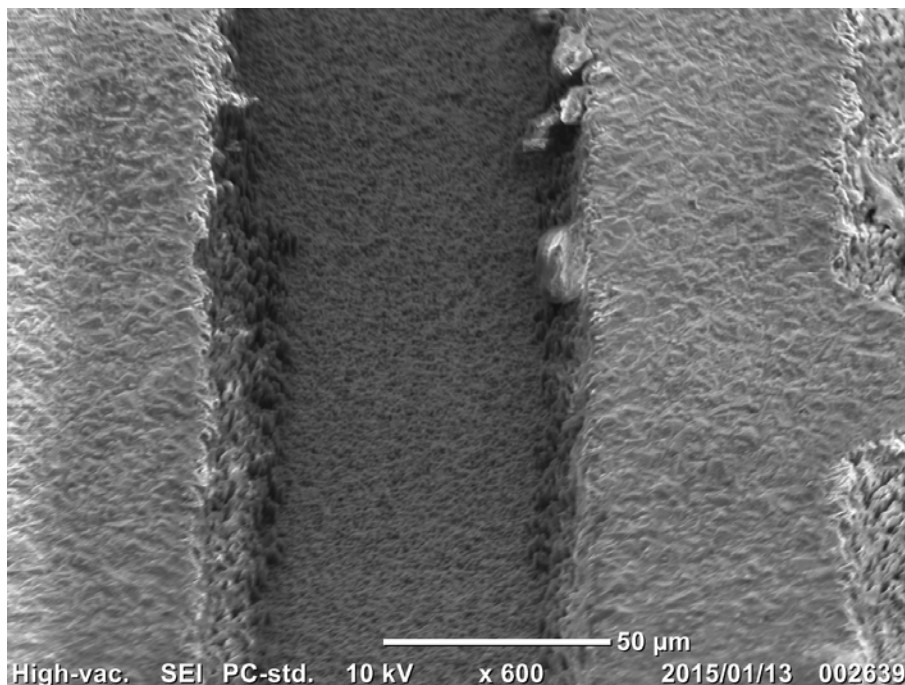

Figure 5.4 Micro-texturing in the CVD diamond coating after etching process

The homogeneous plasma etching has formed by using hollow cathode plasma systems. In this figure, the differences from mask and un-mask area are clearly seen. The homogeneous micro-line has formed in the un-mask area, while the diamond coating still in the mask area. Two hour or 7200 second was effective to make micro-texturing in the CVD diamond coating specimen by using hollow cathode plasma etching system.

5.4 SURFACE PROFILOMETER ANALYSIS

Surface profilometer was also utilized to get 2D and 3D image on the CVD diamond coated specimen after etching process. Figure 5.5 exhibit 2D-surface profile image after etching by using surface profilometer.
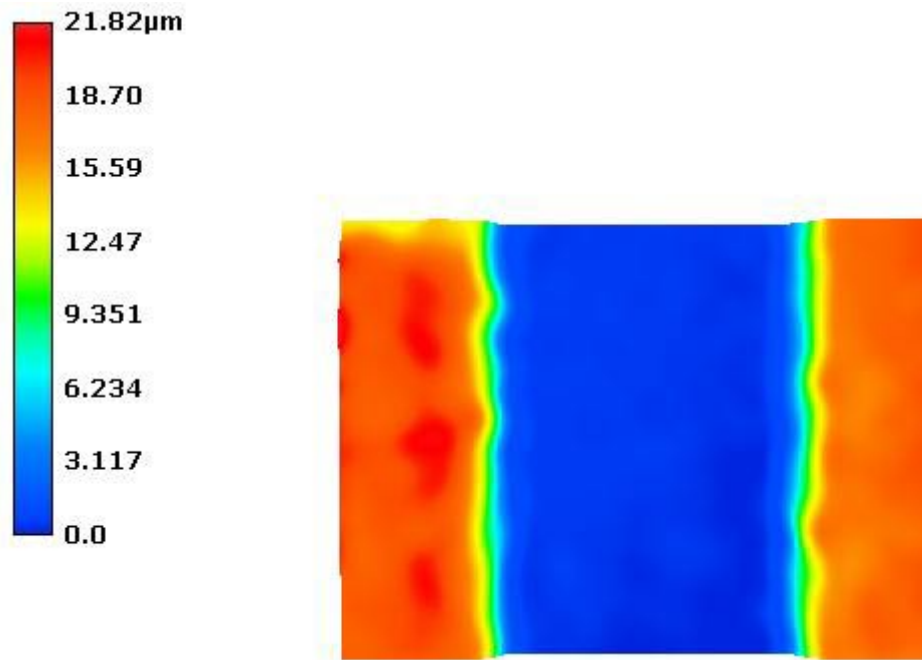
Figure 5.5 2D surface profile images after plasma etching process

Figure 5.5 represent surface profile of the specimen after etching process. The different colour represent different in depth of the surface area. The blue colour shows the un-mask area and all area have the same colour. Its means the homogenous plasma etching has successfully eliminate diamond coating in the surface area. The orange colour represents the mask area and from the both side have the same colour. It is indicated metal mask success preventing diamond coating area from electron bombardment during plasma etching process. The etching process has reached nearly 18.70 μm for two hours process and it is proved by the different colour from blue to orange.

Figure 5.6 represents 3D-surface profile of CVD diamond coated specimen after plasma etching process. The figure shows clearly the anisotropic surface shape of the specimen after etching.
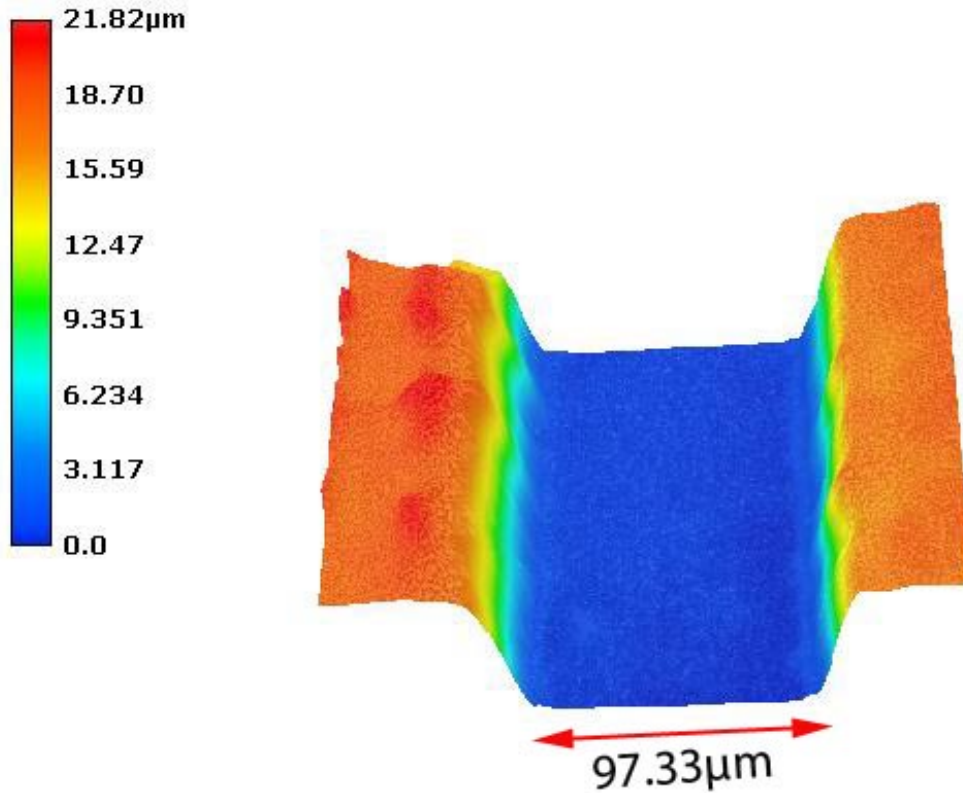

Figure 5.6 3D surface profile images after plasma etching process

The micro-line has depicted in the figure 5.6. The depth after etching reaches to 18.70 µm and the line width of the sample reaches 97.33 µm. The etching rate from this process reaches to 9.35 µm/H. Fast rate in plasma etching comes from plasma density bombardment inside the hollow tube. High electron and ion density are preserved by the electromagnetic confinement in the hollow tube. Then, bare diamond coating is removed from the substrate; while the metal mask endures against the oxygen plasma. The oxygen plasma only reacts with diamond coating on the un-mask region. The edge-sharpness reveals that the anisotropic etching takes place to form a stepwise microgroove in corresponding to the initial line pattern in masking.

5. 5 RAMAN SPECTROSCOPY ANALYSES

Raman spectroscopy has utilized to measure and check the diamond coating in the mask and un-mask area. The measurement result has depicted in the figure 5.7.
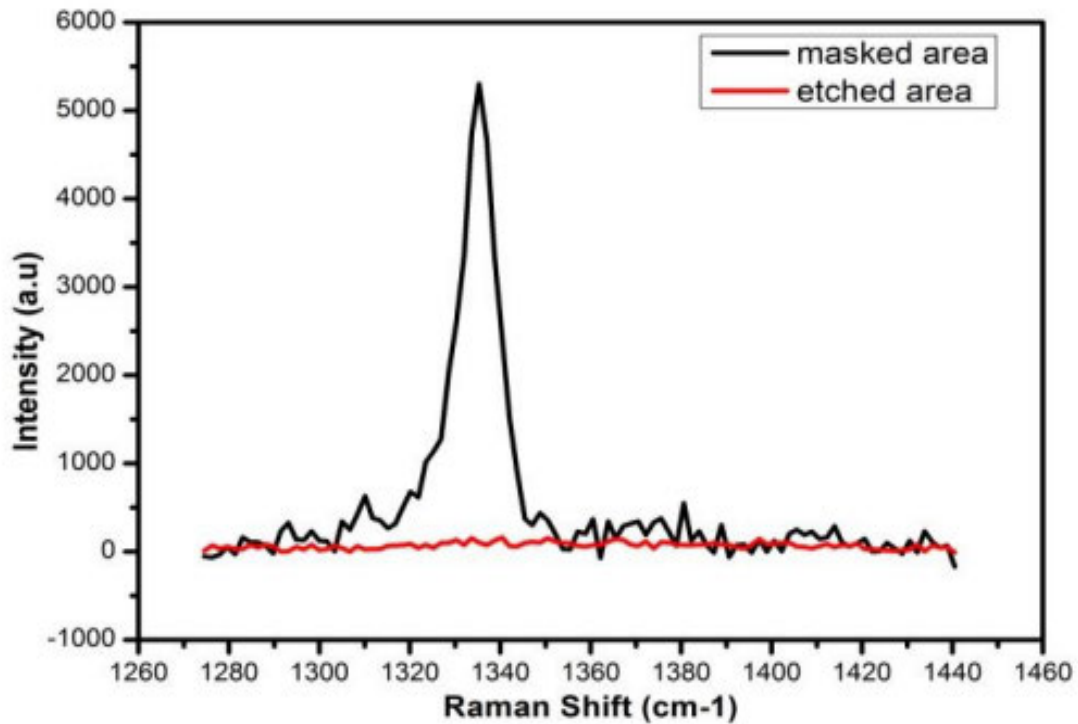

Figure 5.7 Comparison of Raman spectroscopy on the mask and un-mask area

The Raman laser was directed to the mask and un-mask area. The mask areas are characterized by typical Raman spectrum with the sp3 strong peak at 1330 cm^{-1}. Since its intensity reaches to almost 5500 counts, these regions remain to be the same as the diamond coating before etching process. The mask area results are mentioned with the black line. On the etched area, no significant peaks are detected in the range 1280-1440 cm^{-1}. It is proves that the diamond coating is completely remove from the un-mask area as mentioned with the red line. The comparison results have proved that hollow cathode plasma has effective to make micro texturing in the diamond coating.

5.6 DISCUSSION

Hollow cathode plasma etching has produced high ion and electron density. With use of the line-patterned stainless steel mask plate, the micro-grooves are machined into the diamond coating WC (Co) substrate.
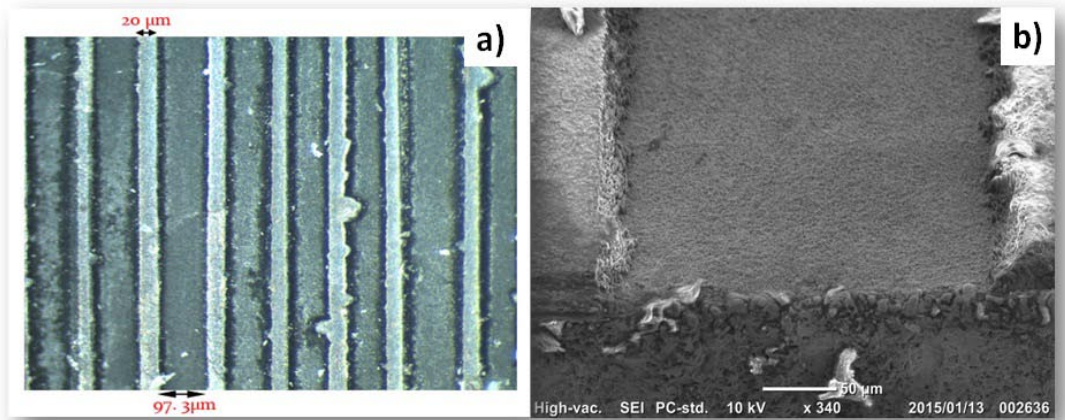
Figure 5.8 Micro-texturing in the CVD diamond coating by using a) optical microscope and b) SEM

Figure 5.8 a) depicts the alignment of CVD-diamond micro-lines formed on the WC (CO) surface. Although the width between lines fluctuates and burrs are formed in part, the regular lines with thickness of 18.70 µm, corresponding to the original CVD diamond film thickness are formed on the WC (Co) surface by the present homogeneous etching. Figure 5.8 b) shows a typical micro groove between two diamond lines. This micro-groove width or the distance between two lines on the WC (Co) bottom surface is 97.33µm; the side surfaces of diamond line have sharp edge again the substrate after etching process. Assuming that the un-mask line has the width of 100µm is completely removed away, the etched side surface of diamond line stand on the WC (Co) bottom surface with the tangential gradient by $\tan(\Theta) = 18.70$ µm / 1.33 µm = ((100 µm − 97.33 µm) /2) = 14.0. Since $\Theta = 87^0$., the CVD

diamond micro-lines are formed as a regularly rectangular line on the WC (Co) substrate.
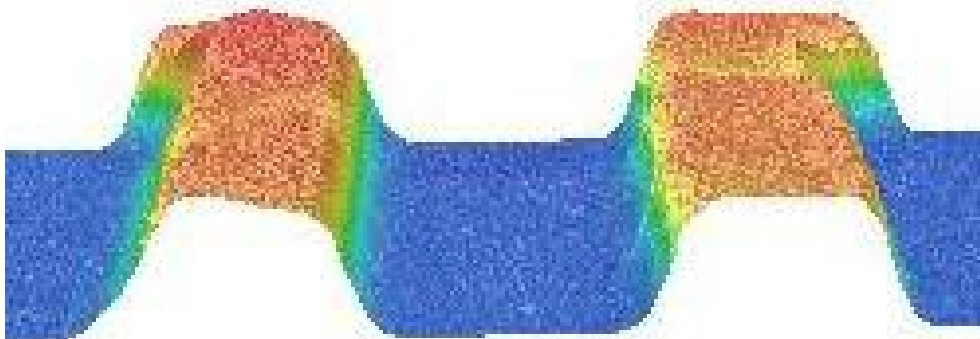
Figure 5.9 Homogeneous plasma etching in CVD diamond coating

The anisotropic etching has obtained by using hollow cathode oxygen plasma as depicted in the figure 5.9. Different from the conventional plasma [13-15], the etching process only by O_2 is driven by chemical reaction and physical bombardment. In the former, direct oxidation of carbon based films by C (in the diamond film) + O (in plasma) → CO (carbon mono-oxide) is responsible for etching. Hence, if this direct oxidation process were retarded by another chemical reaction, the etching rate could be lowered. In the letter, the physical bombardment effect in etching is enhanced by increasing the DC-bias to accelerate the flux of oxygen ions onto the specimen surface. In particular, the confined plasma in the hollow cathode device has a capacity to drive the etching process. In fact, the etched micro-groove pattern has the same size and dimension as the original mask pattern.

5.7 SUMMARY

The hollow cathode plasma has employed to make anisotropic plasma etching in the CVD diamond coated material. WC(Co) disk in cylindrical shape has coated with diamond film as a substrate. The thickness of diamond

coating films reach to 20μm. The metal mask has employed as a mask to make micro-texture in the substrate material. The etching result has indicated micro-texture has imprinted in the substrate after process. The optical microscope and SEM indicate clear figure for the micro texture. The anistropic etching has resulted in all area of the subtarte. The etching process has done in 7200ks. The metal mask is effective to block and repeal the oxygen ion bombardment during etching process. The surface profilometer has utilized to check the surface profile in 3D after etching process. As a result, homogeneus and anisotropic have depicted as a blue color in the bottom of surface and 87^0 of the sharp edge again the surface. The line width after etching process reach to 97.33μm as the same with the metal mask line width. Raman spectroscopy has employed to check the diamond has removed from the substrate. First, laser pointer has directed to the mask area in which there is a diamond film. Second, laser pointer has directed to the un-mask area. The comparison result indicates there is no diamond peak in the un-mask area. It is indicated the diamond films have removes homogeneously from the subtrates.

REFERENCES

[1] B. Bhushan, Nanotribology and nanomechanics of MEMS/NEMS and bioMEMS/bioNEMS material and device, Microelectronic engineering, 84, 2007, 387-412.

[2] T. S. Santra, T. K. Bhattacharyya, et al, Diamond-like Nanocomposite (DLN) film microelectro-mechanical system (MEMS), International Journal of computer application, 2011, 6-9.

[3] M. Bassu, L.M. Strambini, et al, Advances in electrochemical micromachining of silicon: towards MEMS fabrication , Procedia engineering. 25, 2011, 1653-1656.

[4] Erdemir and C. Donnet, Tribology of diamond-like carbon films: recent progers and future prospects, J. Physic. 39, 2006, 311-327.

[5] E. Kohn, P. Gluche, et al, Diamond MEMS a new emerging technology. Diamond and related material, 8, 1999, 934-940.

[6] M. W. Varney, D. M. Aslam, et al, Polycrystalline diamond MEMS biosensors including neiral microelectrode-arrays, 2011, 118-133.

[7] N. Kawasegi, H. Sugimori,et al, Development of cutting toolswith microscale and nano scale textures to improve frictional behaviour, Precis. Engs, 33, 2009, 248-254.

[8] T.Aizawa, Micro-texturing onto amorphous carbon materials as a mold-die for micro-forming, Applied Mechanics Material. 289, 2013, 23-37.

[9] T. Enomoto and T.Sugihara, Improving anti-dhesive properties of cutting tool surfaces by nano-/micro textures, Manufacturing Technology,59, 2010, 597-600.

[10] T. Aizawa, T. Fukuda, Oxygen plasma etching of diamond like carbon coated mold-die for micro-texturing. Surface Coating and Technology, 215, 2013, 364-368.

[11] T.Aizawa, T.Fukuda, Fabrication of micro-textured vi high density oxygen plasma etching for micro-embossing process. Res. Rep. Shibaura Institute of Technology. 57-1, 2013, 364-368.

[12] T. Aizawa, K. Mizushima,T.N. Redationo,M. Yang,Micro-imprinting onto DLC and CNT coatings via high density oxygen plasmaetching. Proc. 8th ICOMM, 2013, 459-466.

[13] Z. Yao, C. Wang, et al, Defined micropattern of platinum thin films by inductively coupled plasma etching using $SF_6/Ar/O_2$ mixture gas, Material science in semiconductor processing, 27, 2014, 228-232.

[14] K. R. Choi, J. C. Woo, et al, Dry etching properties of TiO_2 thin films in $O_2/CF_4/Ar$ plasma, Vacuum, 92, 2013, 85-89.

[15] V. Mondiali, M. Lodari, et al, Micro and nano fabrication of SiGe/Ge bridges and membranes by wet-anisotropic etching, Microelectronic engineering, 141, 2015, 256-260.

6. PLASMA ASHING OF DIAMOND COATING

6.1 INTRODUCTION

Plasma etching and ashing have become effective means to remove coating material from the substrate. The differences from etching and ashing are the removed area. In the plasma etching, the selective areas are removed from the surface. The other areas are protected by using mask or resistant material. But in the plasma ashing, all coating areas are removed from the surface [1,2]. With this advantage, plasma etching and ashing has applied in many sector such as industrial, technology, transportation and etc [3-6].

CVD-diamond coated WC (Co) cutting, drilling, and end-milling tools have been widely utilized for dry machining of the carbon fiber reinforced plastic (CFRP) or thermos-plastic (CFRTP) component an parts in the airplanes and automobiles [7,8]. This material is used for construction of main cabin and wings, a hundred of thousands holes must be machined or drilled into CFRP/CFRTP for each airplane in dry by using the diamond coated tools. Since the number of airplanes is expected to be doubled in the next eight years, the above tooling cost significantly increases in the total production cost. Event at present, the carbon fibers in CFRP/CFRTP have high strength and stiffness enough to make fatal damage and defect to the diamond coating of machining tools; the used or damaged diamond coated tools are often exchanged with new ones during machining and drilling process. Since the tools substrate is made from WC (Co), the substrate materials have to be recycled in many times and reused as long as possible [9-11].

Many studies were reported in the literature on this ashing or removal of diamond coatings. Chemical ashing, EDM, mechanical and chemical polishing

were difficult to removed diamond coating from the substrates [11-15]. The new system has proposed to make perfect removal of diamond coating in fast rate without any damage to the WC (Co) tool substrates.

The hollow cathode plasma ashing has proposed to solve this problem. The hollow cathode device is developed to dense the oxygen atoms and ions as well as electrons. In order to make full use of these activated species in the plasmas, the CVD-diamond coated tools are rotated in the hollow tube during plasma ashing process.

6.2 SCANNING ELECTRON MICROSCOPE (SEM) ANALYSIS

The hollow cathode oxygen plasma ashing has utilized to remove CVD-diamond coated material in the end milling tools under the condition listed in Table 1. The scanning electron microscope (SEM) has employed to measure end milling tool surface after ashing process. The plasma ashing result under the condition number one is depicted in the figure 6.1.

Table 6.1 The plasma ashing experiment set-up

|	RF-voltage (V)	DC-bias (V)	Pressure (Pa)	Processing time (ks)
1.	250	650	30	3.6
2.	250	500	45	3.6
3.	100	500	45	3.6

The plasma parameter has varied to get the optimum condition on ashing process. The only oxygen gas with purity 99.99% has used to generate hollow cathode oxygen plasma ashing. Each plasma parameter has a role and influence in the plasma ashing result.
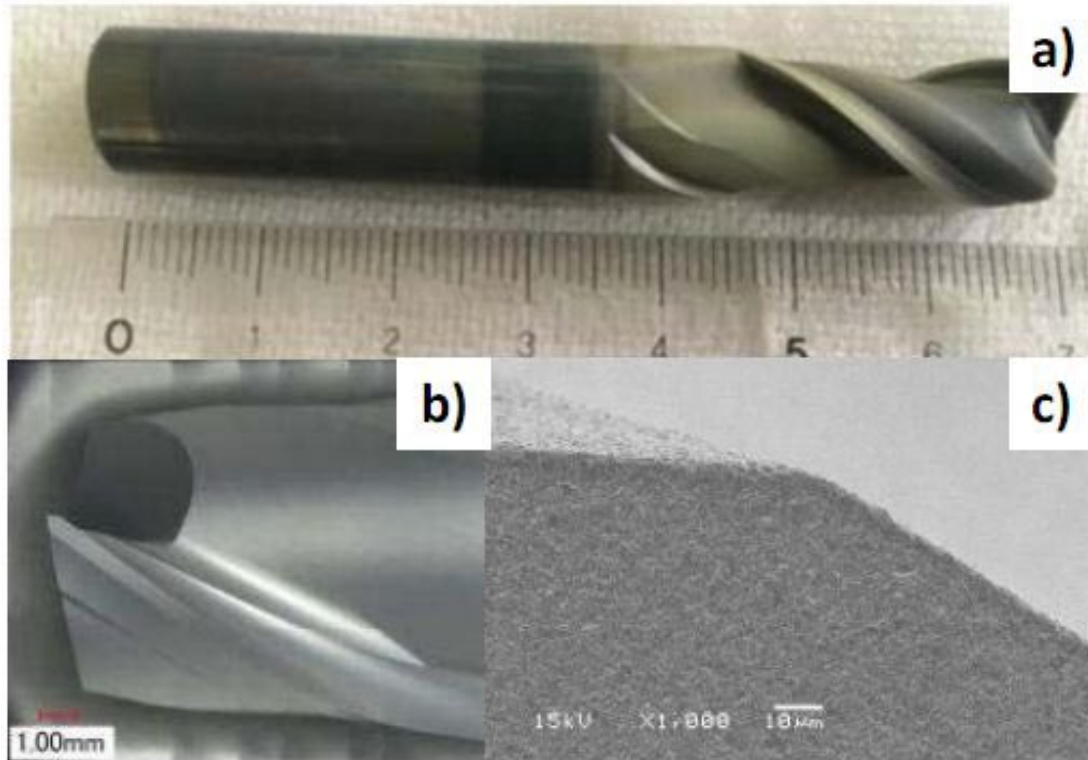
Figure 6.1 Ashed specimen by the present processing by the condition no 1 in the table 1. a) Outlook of ashed CVD-diamond coated tool, b) A top tooth of ashed tool after cleansing, and c)SEM image of tooth edge

The hollow cathode plasma ashing has utilized in the cutting tool by using the condition no 1 and the result as depicted in the figure 6.1. The figure a) represent the CVD diamond coating has removed from the cutting tool surface. It is indicated by the green colour after ashing process. Before ashing process, the cutting tool has a black colour represent the diamond coating. The green colour comes from the oxidation of tungsten and cobalt on the tool surface during ashing process. The figure b) represents the ashed cutting tool after cleansing. The ultrasonic vibration machine has used to clean cutting tool after ashing process. The result from this point shows no residual of CVD dimond coating were left event on the top toot surface. The figure c) shows the SEM image on the edge of cutting tools. The results show sharp tooth

edge and there was no damage even after ashing process. The high RF voltage, high DC bias and low pressure are effective to promote the physical bombardment in ashing process but give the risk of oxidation of tool substrate.
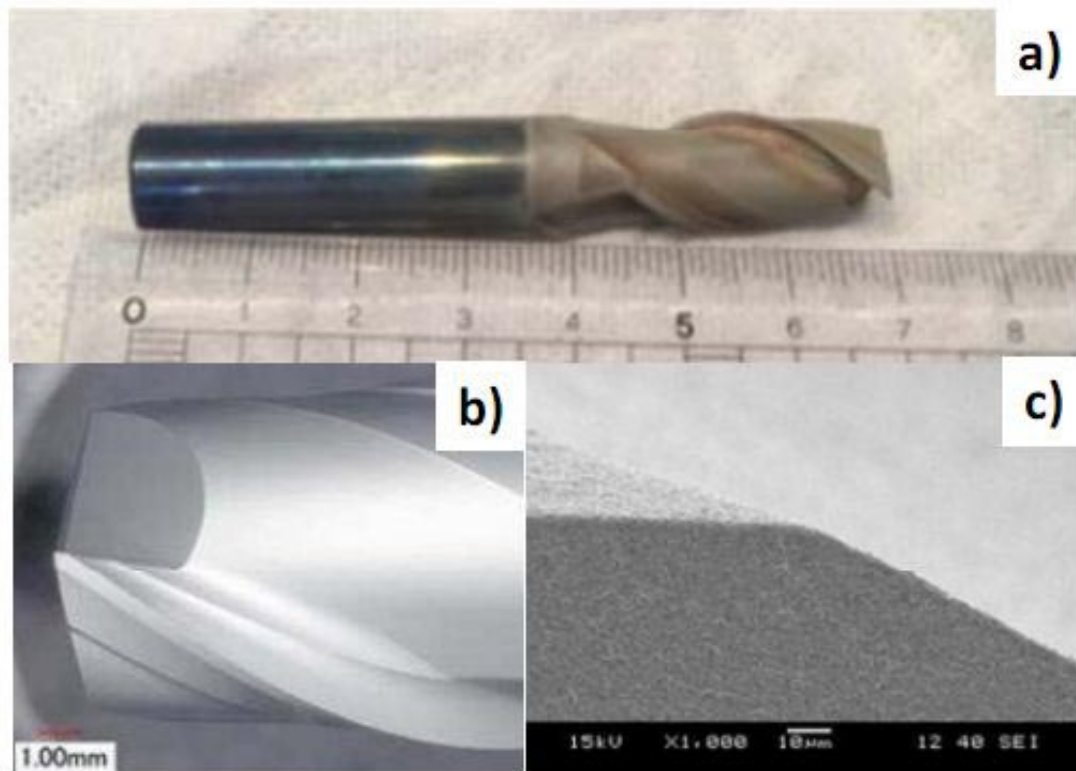
Figure 6.2 Ashed specimen by the present processing by the condition no 2 in the table 1. a) Outlook of ashed CVD-diamond coated tool, b) A top tooth of ashed tool after cleansing, and c)SEM image of tooth edge

The experiment condition no 2 was employed in the cutting tools and the ashing result as depicted in the Figure 6.2. Compare with the condition no 1, in this condition the DC-bias voltage value was decreased to -500 V and pressure was increased to 45 Pa. The figure 6.2 a) represents the cutting tools has different colour after ashing process compare with the condition no 1. In this result, the yellow and green colour becomes thinner than figure 6.1 a). It is indicated the oxidation in the condition no 2 becomes lower than condition no 1. Figure 6.2 b) shows the cleansing result by using ultrasound vibration

machine. The result has the same result with the condition no 1 and proves that no carbon dust and tints were present after cleansing. The figure 6.2 c) show the SEM image of the edge and tooth surface. The outer diameter (D_m) of top tooth after ashing was measured and compared to the calculated one (D_c) by subtracting the coating thickness from the outer diameter of coated top tooth. If D_m is much less than D_c, the tooth edge and surface are significantly removed to lower the tool substrate life in recycling. Hence, $D= D_c - D_m$ plays an important parameter to evaluate the microscopic damage of tool tooth. The experiment condition no 2 has result in D reach to 9.7µm. This value is prohibited to make recycling process because tolerance in reduction of tooth diameter by a single shot of ashing is 5µm.
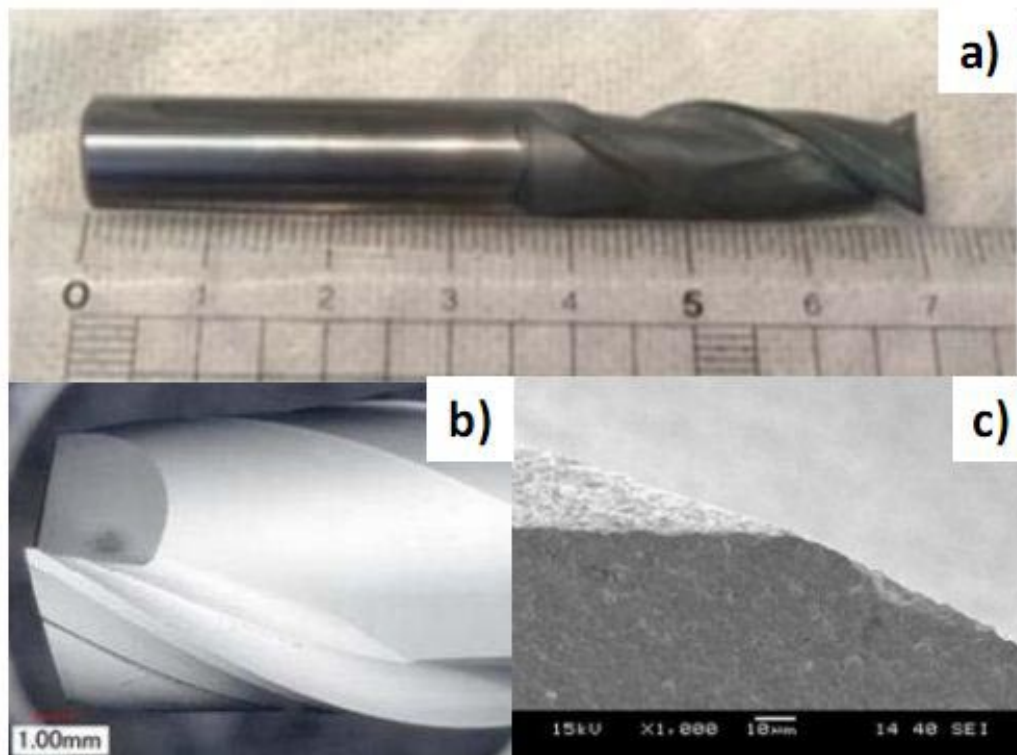

Figure 6.3 Ashed specimen by the present processing by the condition no 3 in the table 1. a) Outlook of ashed CVD-diamond coated tool, b) A top tooth of ashed tool after cleansing, and c)SEM image of tooth edge

The experiment condition was set in the condition no 3 and the result as depicted in the Figure 6.3. The experiment set-up was modified with the purposed to get the optimum condition and minimize the damage of the cutting tools. In this condition, the RF-voltage was reduced to 100 V and others parameter were keep with the same condition with the previous one. The figure 6.3 a) shows the surface colour after ashing is covered by thin grey-colored film. This colour is different compare with the previous ashing result. Figure 6.3 b) represent the same result with the previous result that there was no residual diamond coating after cleansing process. Figure 6.3 c) depics the microscopic image of top tooth edge. The original small holes were doted on the tooth surface; they were made by chemical treatment before diamond coating as a nucleation site of diamond films. By using this condition the D reach to 1.1 μm. This D value is allowed to make recycling and re coating of WC (Co) end milling tool.

6.3 RAMAN SPECTROSCOPY ANALYSIS

The Raman spectroscopy was utilized to check diamond coating in the CVD diamond coated end milling tool before and after plasma ashing process. Figure 6.4 represent Raman spectroscopy result peaks comparison from diamond peak before and after ashing process. The method to indentify diamond peak was same with plasma etching process. The Raman spectroscopy laser was directed to diamond coating in the cutting tool surface before etching. The diamond peaks was identified in the wavelength 1330 cm^{-1}. The same process was done for the end milling cutting tool after ashing process. The diamond peaks was plotted in one graph to get the differences before plasma ashing and after plasma ashing process.
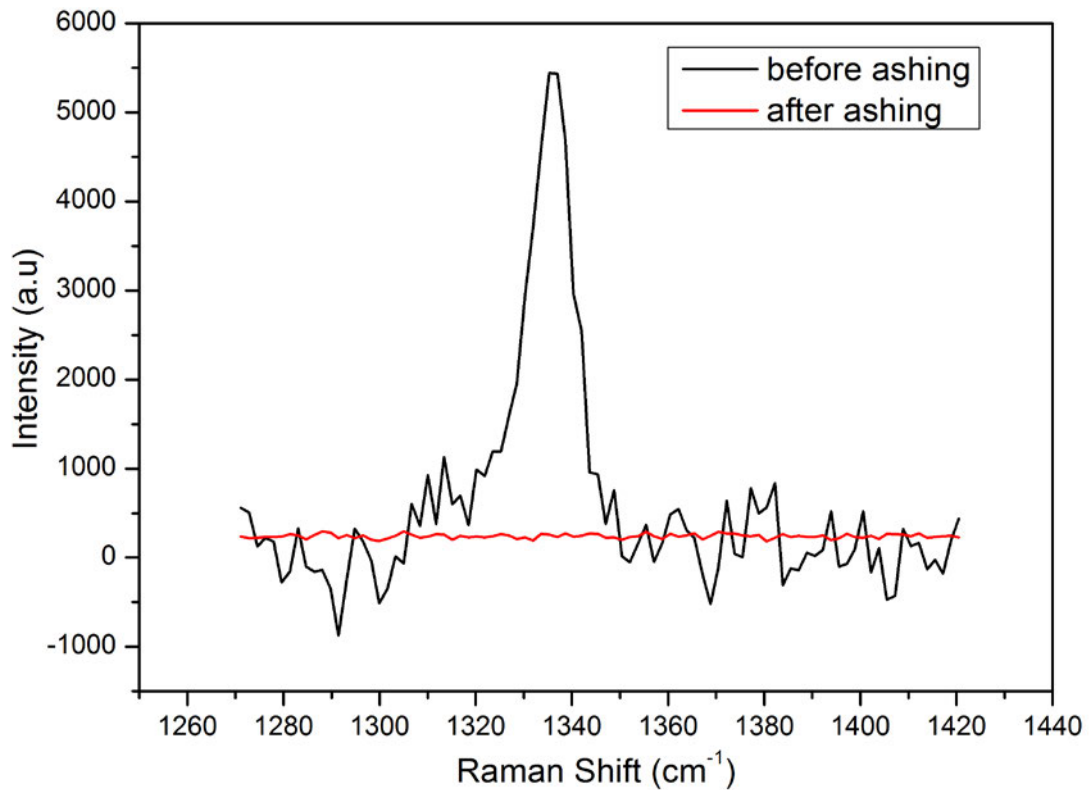
Figure 6.4 Comparison of Raman spectra on the mask area before and after ashing process

The black line indicates the diamond peak has identified in the cutting tools surface. The diamond peak has a intensity nearly 5000 a.u and detected in the wavelength 1330 cm^{-1}. The red line represents the diamond peaks has no intensity in the same wavelength with the black line. The comparison result show high intensity indicated diamond peak is stayed in the cutting tool surface. However, the red line indicated no diamond in the cutting tool surface. This result has proved diamond coating has completely removed by using hollow cathode oxygen plasma ashing.

6.4 SIMULTANEOUS ASHING PROCESS

The single coulomn of hollow cathode was effective to remove diamond coating in the cutting tools surface. For mass production, the simultaneous plasma ashing is effective to remove diamond coating in the cutting tools by

one process operation. The geometric design of single hollow device is expanded to a double-columned hollow cathode one, where each tool in the either hollow cathode is immerged into the oxygen plasma state. Both tools in the double-columned hollow are controlled to rotate with the DC-bias applied both to the hollows and tools.
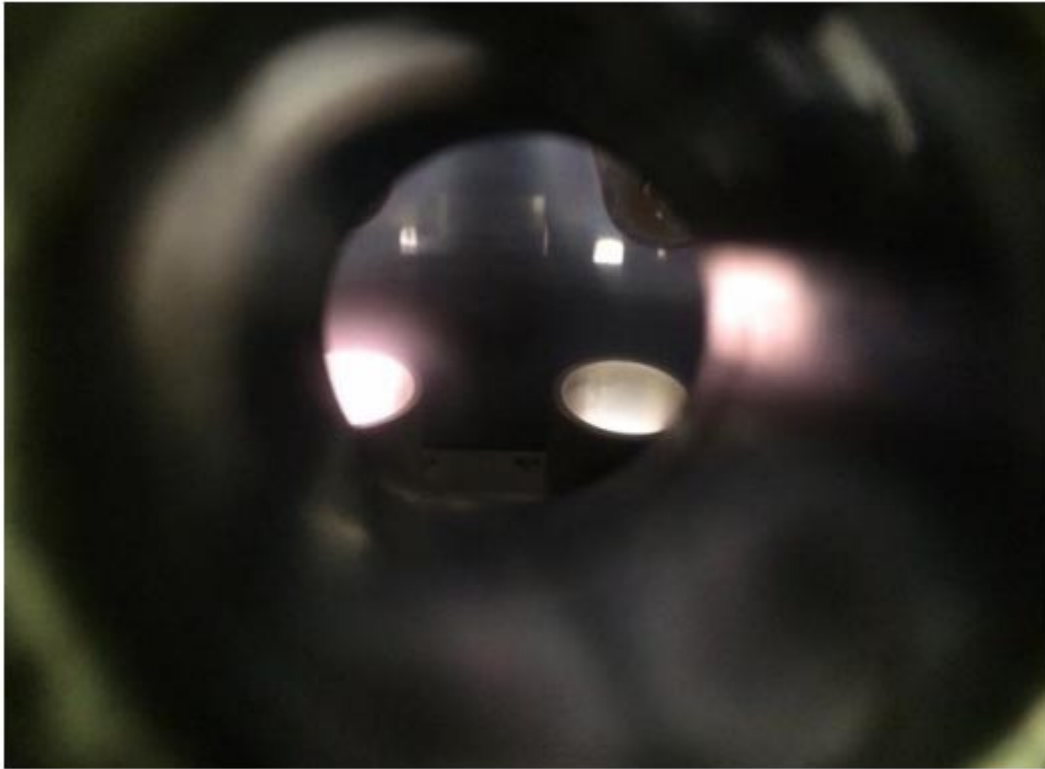
Figure 6.5 On-line observation on the plasma states which are independently confined in each hollow of the double-columned ashing systems

Figure 6.5 depicts the snap-shot of double-columned hollow during the ashing process. The ion and electron densities become lower outside of the hollows; while the oxygen plasma are confined in each hollow to have much higher electron and ion densities. During the ashing process by using this double-columned hollow cathode device, two diamond-coated tools are immerged into the above oxygen plasma sheath and rotated in the hollows.

The same plasma parameter condition was set to make double column hollow cathode plasma ashing. But in this case time processing was set for 7200 second. The ashing result from this measurement is depicted in the Figure 6.6.
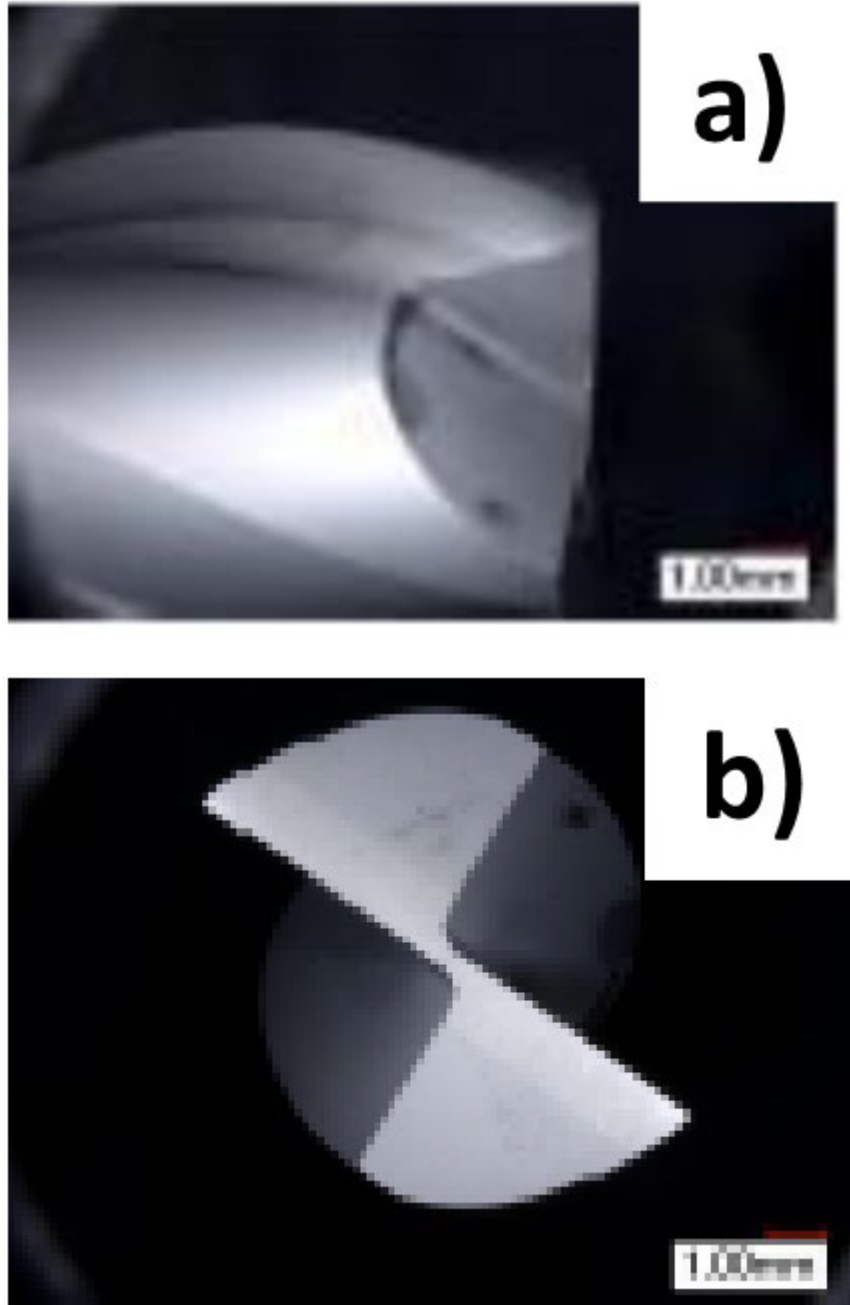
Figure 6.6 Tooth surface of ashed CVD-diamond coated tools by using double columned hollow cathode device

The single column of hollow cathode was effective to remove diamond coating in the cutting tools surface. For mass production, the simultaneous

plasma ashing is effective to remove diamond coating in the cutting tools. Figure 6.6 show the optical microscopic image of ashed tool for 7.2ks. Although the residual diamond dusts are slightly left as dot, the whole CVD-diamond film is removed away from the toot surface. Little residual are also seen even on the back surface of teeth; this demonstrate that the rotating tools surface should be homogeneously subjected tothe oxygen plasma flux in the confined plasma sheath in the hollows. Figure 6.6 b) shows the top view of ashed teeth. Little or nearly zero loss of teeth is detected in this ashing experiment. This suggests that the multi-columned hollow cathode device is possible for simultaneous ashing to remove the used CVD-diamond films in the mass of tens of tools at the same time.

6. 5 DISCUSSION

The hollow cathode plasma ashing has utilized to remove CVD diamond coated end milling tool from the tool surface. The plasma parameter has given influence for the ashing result. Three cutting tools has ashed away by using hollow cathode plasma system and has deferent result as depicted in the Figure 6.7. The ashing result indicates the oxidation has taken place in the cutting tools. The oxidation occurs due to the high bombardment of ion and electron density on the cutting tool surface. In the hollow cathode oxygen plasma, the RF-voltage is the main influence factor to generate oxidation. The RF-voltage has a role to control plasma density population inside the hollow cathode. High value of RF-voltage effects in high ionization process in the hollow cathode plasma and as result high population plasma density inside the hollow tube. In the experiment set up no 1, high RF-voltages accompany with high DC bias. This combination produces high population plasma density

and high speed of plasma density bombardment. The plasma density attack to the cutting tools surface rapidly and as a result high oxidation was take place in the cutting tools after ashing process.
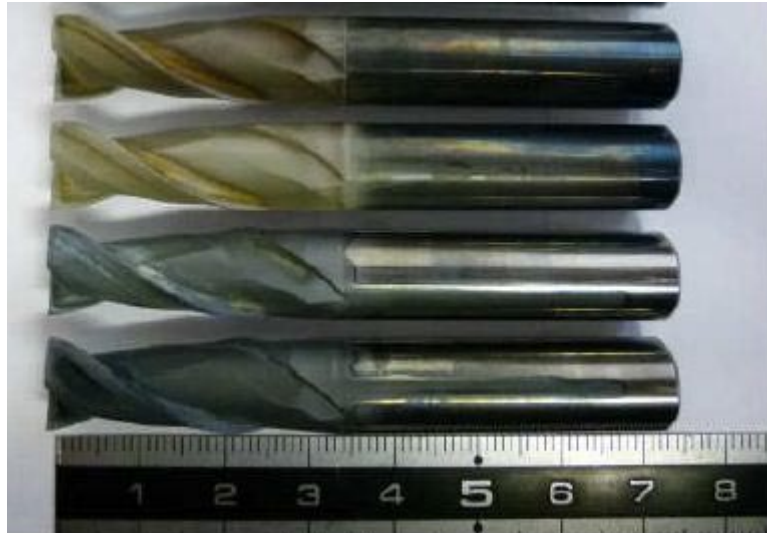
Figure 6.7 The end milling cutting tools after ashing process

In the experiment set up no 3, the RF-voltage was lowered to 100 V. The population of plasma density was decreased significantly. However, this condition was combined with low pressure and high DC-bias. Low pressure results in high plasma density and high DC-bias result in high speed of plasma bombardment. By this combination, the bombardment of plasma density was controlled during the ashing process. The bombardment was not damage to the cutting tools surface and produce low oxidation result.

The SEM result has compared the surface profile before and after hollow cathode plasma ashing in the CVD diamond cutting tools. The comparison result from this measurement was depicted in the Figure 6.8. The figure represent the crystal structure of diamond coating and WC(Co) cutting tool before and after plasma ashing process.
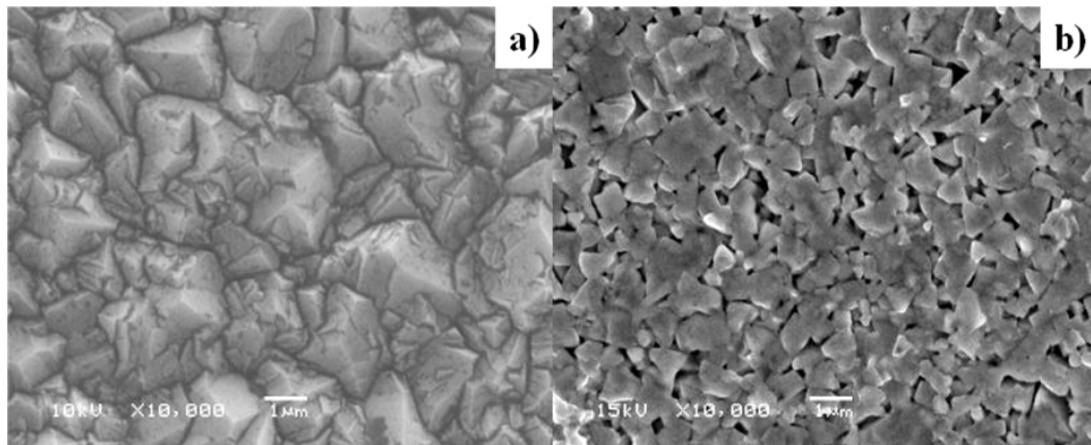
Figure 6.8 The surface comparison result of cutting tools a) before ashing, b) after ashing process

The figure a represents the diamond crystal has stayed in the cutting tools. The diamond crystal structure has a big size and uneven surface. After ashing process, the diamond crystals have attacked by oxygen ion bombardment. The crystal diamonds has removed from the cutting tool surface. The figure 6.8 b) represent the original WC (Co) crystal surface. Compare with figure a) the crystal in the figure b) is smaller and far in distance. By this comparison result, hollow cathode oxygen plasma ashing is effective to remove hard coating material without damage to the original tool substrate.

6. 6 SUMMARY

The hollow cathode plasma system has employed to remove diamond coating from the substrate. Homogeneous plasma ashing and low damage to the end milling tools substrate have achieved by using hollow cathode plasma. The RF-voltage, DC-bias voltage, and pressure have varied to get the optimum condition for ashing process. Three condition of plasma ashing have utilized to remove diamond coating from the substrate. High RF-voltage, High DC-bias, and low pressure as set in condition one has a result in high oxidation after ashing process. The second condition has set with lowering the

DC-bias voltage. The oxidation occurs less than the first condition, but the surface damage reach to 9.7μm. The third condition has set in low RF-voltage during ashing process. The result indicates a good result; no oxidation is taken place after ashing process. The surface damage after ashing reaches to 1.1μm. By this result, the recoating of end milling tool can be done after ashing process. In the ashing process, RF voltage has a big role to supply energy for ionization and generated the ion population for ashing. The Raman spectroscopy has employed to check the diamond has removed from the surface. The graph comparison indicates the diamond peak does not appear after ashing process. The result prove hollow cathode plasma ashing is effective to remove diamond coating from the substrate. The SEM has also indicated the original surface profile of WC (Co) end milling after ashing process. The simultaneous ashing system has employed toward to industrial application.

REFERENCES

[1] T. Aizawa, T. Fukuda, Oxygen plasma etching of diamond-like carbon coated mold-die for micro-texturin, Surface and coating technology, 215, 2013, 364-368.

[2] S. Yoo, T. Lho, et al, Large area ashing process using an atmospheric pressure plasma, Thin solid films, 519, 2011, 6746-6749.

[3] B.J. Jung, H. J. Kong, et al, Fabrication of 15 nm curvature radius polymer tip probe on an optical fiber via two-photon polymerization and O_2 plasma ashing , Current applied physics. 13, 2013, 2064-2069.

[4] T.J.Kang, J.G. Kim, et al, Deformation characteristic of electroplated MEMS cantilever beams released by plasma ashing, Sensors and actuators a: physical. 148, 2008, 407-415.

[5] B. R. Rogers and T.S Cale, Plasma processing in microelectronic device manufacturing, Vacuum, 65, 2002, 267-279.

[6] K. Yamauchi, E. E. Yunata, T. Aizawa, High density oxygen plasma ashing of used CVD diamond coating for recycling of WC(Co) Tools, The international forum on micro manufacturing and biofabrication, 2015.

[7] R. Hasegawa, Cutting tools for aircraft and application, Journal of japan society for precision engineering, 75, 8, 2009, 953-957.

[8] T.Aizawa, Y. Sugita, High-density plasma technology for etching and ashing of carbon material, Res. Rep. SIT 55-2, 2011, 13-22.

[9] T. Aizawa, E. Masaki, Y. Sugita, Oxygen plasma ashing of used DLC coating for reuse of milling and cutting tools, Proc. Int. Conf. Mater. Process.(MAPT-2013), 15-20.

[10] T. Aizawa, E. Masaki, Y. Sugita, Complete ashing of used DLC coating for reuse of the end-milling tools, Manufacturing Letters, 2, 2014, 1-3.

[11] T.Aizawa, E. Masaki, E. Moromoto, Y. Sugita, Recycling of DLC-coated tools for dry machining of aluminium alloys via oxygen plasma ashing, Mechanical engineering research, 4, 1,2014, 52-62.

[12] P. Agrwal, A. Manoria, et al, J.Mech, Engineering and robotic. 1, 2012, 121-128

[13] L. Loghina, K. Palka, et al, Selective wet etching of amorphous As_2Se_3 thin films, Journal of non-crystalline solids, 430, 2015, 21-24.

[14] M. P. Jahan, K. R. Virwani, et al, A comparative study of the dry and wet nano-scale electro machining, Procedia CIRP, 6, 2013, 626-631.

[15] R. Ji, Y. Yonghong Liu, et al, Machining performance of silicon carbide ceramic in end electric discharge milling, International journal of refractory metal and hard material, 29, 2011, 117-122.

7. DISCUSSION

7.1 INTRODUCTION

The present study has two fundamental aims, first is to characterize and develop hollow cathode plasma system. Second, the developed hollow cathode plasma system is applied for plasma technology sector event for small scale (laboratory) or big scale (manufacturing). The hollow cathode plasma system is a new developed method to generate high plasma density inside the hollow tube. The high plasma densities are obtained by setting plasma system parameter, respectively. Pressure, DC-bias, RF-voltage, time, gas flows are kind of plasma system parameter are need to be controlled to obtain high plasma density.

Langmuir probe and optical emission spectroscopy have utilized to make quantitative plasma diagnosis in the hollow cathode plasma. The measurement result indicates the high plasma densities are obtained by using hollow cathode system. The high plasma density is obtained in the one location inside the hollow tube. The other location inlet and outlet of hollow cathode are needed to characterize more detail. This process has proposed to discover the plasma density distribution measurement inlet and outlet of the hollow cathode. The quantitative diagnosis result is used to determine the highest concentration location of plasma density.

The optical emission spectroscopy is effective to describe the atomic, molecule, activated molecule, and radical during plasma process. In the plasma application process, the optical emission spectroscopy is utilized to predict the end of ashing or etching process. The time evolution method is online method during plasma processing. The method is done by focusing to

the influence peak from this process. The influence peak is the peak from the plasma generation which reactive with the coating material.

7.2 THE ROLE OF PLASMA PARAMETER IN THE HOLLOW CATHODE PLASMA

The hollow cathode plasma system has succeeded to generate high plasma density. The hollow cathode plasma system also effective to remove coating material from the substrate and has proven from plasma etching and ashing process. The plasma parameter has a role in influence the plasma density during the plasma generation. The RF-voltage has role in the ionization process from hollow cathode plasma. Low RF voltage value has a low percentage of ionization process. In this condition, electrons do not have sufficient energy to ionize the gas molecule inside the chamber. As a result, electron density is increase and ion density is decrease. However, high RF voltage values supply more energy to make ionization. The electrons have sufficient energy to ionize the gas molecule inside the chamber. The percentage of ionization is increase and as a result high ion density and low electron density.

Pressure has a role in control population of plasma density inside the chamber. In the low pressure, a few gas molecules are introduced inside the chamber. The electron with sufficient energy collides with the gas molecule and makes ionization process. Much more electron collides with gas molecule than itself. High percentage of ionization are taken place occur in the low pressure. As a result, high ion density and low electron density are happen in the low pressure. In other hand, by increasing the gas pressure supply much more gas molecules inside the chamber. And also, electric field barrier in the

hollow cathode plasma makes electron inside hollow tube difficult to leave the hollow tube. In the same time, huge amount of gas molecules is introduced inside the hollow tube.   With this condition, the percentage of electron collide itself is higher than collide with gas molecule. This condition produce low percentage of ionization process and as a result high electron density accompany by low ion density

The DC-bias has effect in enhance the ionization process in the hollow cathode plasma. Both of ion and electron densities increase by increasing the DC-bias. Since the DC-bias is directly applied to the hollow cathode, the confinement of free electron is significantly dependent on the DC-bias. In case of low DC bias, both electron and ion penetrate easily into hollow tube. Low electron and ion density is resulted by this condition. Increasing the DC-bias, both electron and ion are difficult to leave from hollow tube by strong electric field barrier. The the electron and ion density increase by increasing the DC-bias.

7.3 THE PLASMA DENSITY DISTRIBUTION INSIDE THE HOLLOW CATHODE PLASMA

The characterization of plasma density in the hollow cathode plasma system has done by varying plasma parameter respectively. Langmuir probe has utilized to measured plasma density from each condition and variation. However, the measurement process has done in one point spot or un-movable location. Plasma density distribution measurement from inlet to outlet of the hollow cathode has done by using Langmuir probe. Langmuir probe has controlled in stepwise motion from inlet to outlet of hollow cathode. The plasma density measurement result is depicted in the Figure 7.1
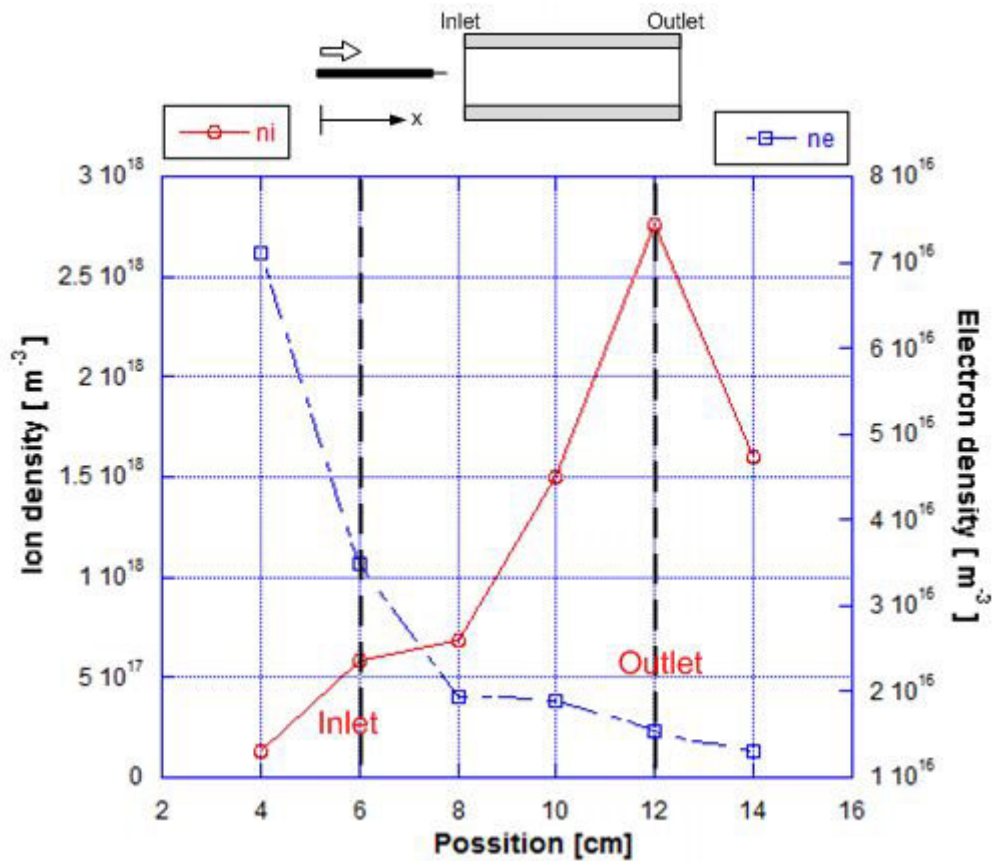
**Figure 7.1 Ion and electron density distribution in the hollow cathode plasma from inlet to outlet**

The Langmuir probe has utilized to measure plasma density distribution in the hollow cathode plasma from inlet to outlet. Since the origin x=0 is away from the inlet of hollow by 4 cm and the length of hollow is 8 cm, the probe detects the variation of electron and ion density distribution in the inside of hollow cathode tube from x = 4 to 12 cm. At the inlet position, $n_i = 1.28 \times 10^{17}$ m^{-3} and $n_e = n_i = 7.11 \times 10^{16}$ m^{-3}. Move to central of hollow cathode, ion density is increase but electron density is decrease. And in the outlet position, $n_i = 2.76 \times 10^{18}$ m^{-3} and $n_e = n_e = 1.6 \times 10^{18}$ m^{-3}. The decreasing of electron density is effected by ionization process. Most of electron recombined with the O$^+$ species to form the high oxygen atom flux at the hot spot with ionization. Otherwise, the ion density is increase from the

inlet to the outlet position. It describes the ionization is enhanced in the hollow cathode device, especially at the hot spot, the oxygen ion density increase exponentially from the inlet to the outlet of the hollow. The ion density is decrease after outlet position. It is caused by there is no electric field barrier to hold ion density stay in limited area. So the ion density is free to move to all direction in the chamber. Compare with the inlet spot, this spot has higher ion and electron density. The plasma density distribution characterization describe inside hollow cathode plasma produce high ion density, the maximum ion density reaches to 3×10^{18} m^{-3} at the vicinity of outlet. This spot with high ion density is suitable to make complete ashing of CVD diamond coating on the tool substrate.

7.4 TIME EVOLUTION OF SPECIES DURING PLASMA ETCHING AND ASHING PROCESS

The optical emission spectroscopy (OES) is also utilized to monitor the reactive peaks during plasma process. The reactive peak comes from the reaction from plasma and the coating material. In this case, the oxygen plasma has reacted with the carbon in the CVD diamond coating to produce CO peak. The CO peak has detected in the wavelength 287.79 nm. The online monitoring has done by plotting the intensity of CO peaks again the time. Figure 7.2 represent the time evolution of the CO-peaks and O peak again the time. The oxygen peaks with the same wavelength has plotted in the same graph to make easily understanding about time evolution process. The red line represents the oxygen atomic peak at the wavelength 287.79 nm without any specimen in the chamber. The intensity of O-peak is constant by 1145 count irrespective of time. The black line shows the time evolution of

the CO peak at the same wavelength as the O peak. The black line trend shows different trend with the O peak. It is indicated there is some reaction in this wavelength during plasma etching or ashing process.
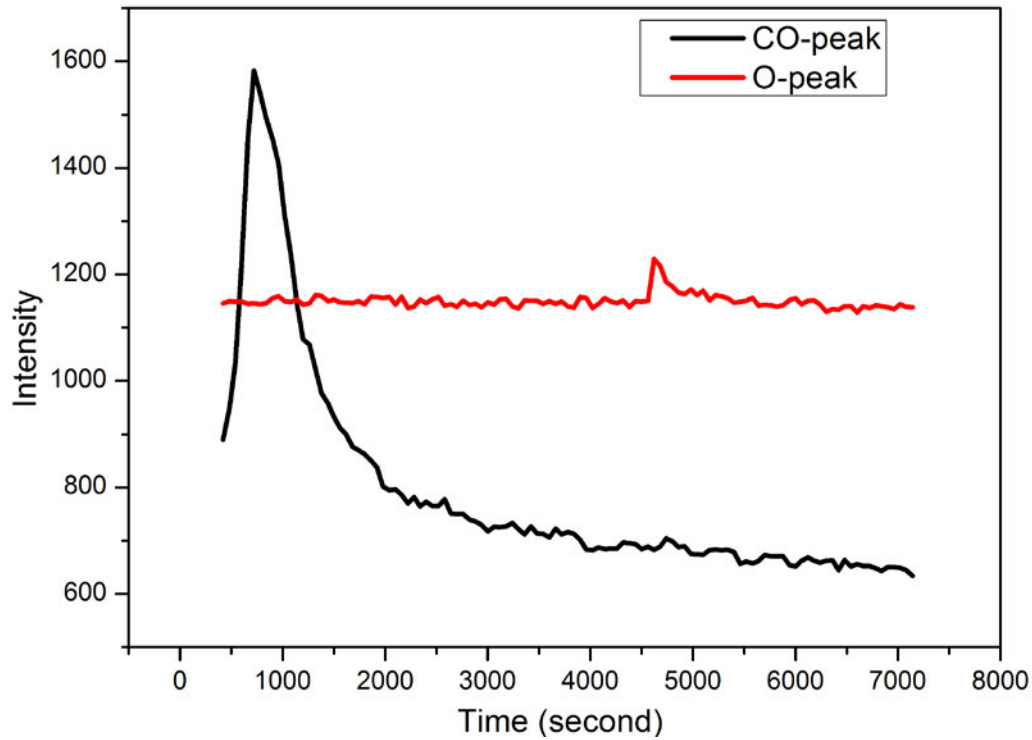
Figure 7.2 The comparison from CO-peak and oxygen peaks at the wavelength 287.79 nm

The CO peak has high intensity in the beginning plasma processing. Its intensity keep to be high until 1000 s. In this condition the diamond react with the activated oxygen atom inside the hollow cathode to form more carbon monoxide. After 1000 s, the peak intensity gradually decreases. The residual diamond layer becomes thinner through etching or ashing by the chemical reaction of C (in the diamond) and O $\rightarrow$ CO and ion bombardment. The CO peak reduction intensity becomes saturates nearly 7.2ks. This termination condition is employed to stop the etching process to protect from over etching

or ashing. This method is effective not only to describe the etching behaviour with the time but also to predict the termination of etching process.

8. CONCLUSION

The following conclusions can be drawn from the present study:

1. The hollow cathode oxygen plasma behaviour was described by varying RF-voltage, DC-bias, and pressure. The ion density was increased by increasing RF-voltage and DC-bias. Low pressure in the hollow cathode plasma produces high ion density. The order value of ion and electron density from hollow cathode plasma system is higher than the common plasma systems. (e.g. $n_e = 10^{17}$ m^{-3} , $n_i = 10^{18}$ m^{-3} by using hollow cathode plasma, and $n_e = 10^{15}$ m^{-3} , $n_i = 10^{15}$ m^{-3} by using the common plasma systems).

2. The characterization of plasma density distribution inlet to outlet of hollow tube provides the different value from each spot. The inlet spot has a low ion density and high electron density. Move to outlet spot, the ion density is increased and accompany by decreasing of electron density. The electron inside hollow tube was trapped and difficult to leave the hollow tube due to the confinement electric field in the hollow tube. The electron attack to gas molecule and increase the ionization process.

3. The hollow cathode plasma etching provides high etching rate and anisotropic etching. The average etching rate is 10 μm/ H event for diamond coating. The micro-texturing has succeeded to imprint in the diamond coating surface with the metal mask and 7200 second etching process.

4. Perfect ashing of the used CVD diamond coating without any damage and defects onto the WC (Co) substrates was completed by using hollow cathode device. Short leading time by 3.6 ks or 1 hour in the present ashing process is also attractive to tooling companies which offer suffer from long ashing time over 20 hours.

5. The simultaneous plasma ashing was developed by using multi-columned of hollow cathode plasma in the one chamber. The ashing result of CVD diamond coating has the same characteristic with the single hollow tube. Completed ashing of two diamond-coated tools by the present system proves that a mass of used CVD-diamond end-milling tools in the order of tens should be simultaneously ashed away by the present method.

Research Publications

Publication

1: E. E. Yunata and T. Aizawa, K. Yamauchi, "High density oxygen plasma ashing of CVD- diamond coating with minimum damage to WC (CO) tool substrates", Mechanical engineering, 2016, Vol. 3, No. 2 (In Press)

Hollow cathode plasma was employed to make ashing of CVD diamond coatings on the WC (CO) tool substrate. Perfect ashing and low damage to the cutting tool were achieved by using the hollow cathode plasma systems.

2: E. E. Yunata and T. Aizawa, "Micro-texturing into DLC/diamond coated mold and dies via high density oxygen plasma etching", Manufacturing Review, 2015, Vol. 2, No. 13, pp.1-7.

High plasma density was utilized to make micro-textures into the DLC and diamond films. The homogeneous and anisotropic etchings of diamond film tool place, resulting in imprinting of micro-textures into the films. The high etching rate reached to 9.2 μm/h by using hollow cathode system.

3: E. E. Yunata, T. Aizawa,"Micro-grooving into thick CVD diamond films via hollow-cathode oxygen plasma etching", J. Manufacturing Letters, 2016 (In Press)

Hollow cathode plasma system was utilized to make micro-grooving into diamond coated WC (Co) disk specimen. The metal mask was utilized for patterning. Within the short duration for 7200 second homogeneous and anisotropic etching took place.

Refereed proceedings

4: E. E. Yunata, T. Aizawa, "Plasma oxidation printing onto carbon-based coating for micro-texturing", Proc. 10th SEATUC Symposium, 2016, Toyosu, Japan. (In Press)

The platinum mask was imprinted in the diamond like carbon coating film as a mask for etching process. The homogeneous micro texture was imprinted in the substrate by using the messo-pressure and short time etching process.

5: E. E. Yunata, T. Aizawa, K. Yamauchi, Y. Sugita, "Simultaneous oxygen plasma ashing of CVD diamond coated WC(Co) tools", Proc. 9th SEATUC Symposium, 2015, Nakhon Ratchasima, Thailand.

Hollow cathode plasma ashing was successfully applied to remove coating material with low damage to substrate. The simultaneous plasma ashing was employed to make ashing process for mass scale process.

6: K. Yamauchi, E. E. Yunata, T. Aizawa,"High density oxygen plasma ashing of used CVD diamond coating for recycling of WC (Co) Tools", The International Forum on Micro Manufacturing and Biofabrication, 2015, Toyama, Japan.

High Plasma density of hollow cathode plasma was employed to make ashing of diamond coatings on the WC (CO) tool substrate. Low damage and short time ashing process on the cutting tool were achieved by using hollow cathode plasma systems.

7: E. E. Yunata, T. Aizawa, D. J. H. Djoko Santyojo, "Characterization of hollow cathode plasma for etching and ashing processes", Pro. 8th SEATUC Symposium, 2014, Johor Baru, Malaysia, D1-02, pp. 86.
Characterization of hollow cathode plasma was done by varying pressure, DC bias, and RF voltage respectively. Low pressure, high RF voltage and high DC bias result in high densification of plasmas in the hollow cathode plasma.

8: E. E. Yunata, R. Suenaga, T. Aizawa, D. J. H. Djoko Santyojo, "Quantitative argon plasma characterization by Langmuir-probe method", Pro. 7th SEATUC Symposium, 2013, Bandung, Indonesia, pp. 105.
Characterization of argon plasma was done by using the Langmuir probe and optical emission spectroscopy. RF and pressure were found to be main factors to influence ion and electron densities in the argon plasma. The optical emission spectroscopy exhibited that the argon plasma mainly consisted in its atomic peaks in the range 600-900nm

ACKNOWLEDGEMENTS